

1
2
3
4
5
6
7
8
9
10
11
12
13
14
15
16
17
18
19
20
21
22
23

U.S. Climate Change Science Program

Synthesis and Assessment Product 3.2

**Climate Projections Based on Emissions
Scenarios for Long-Lived Radiatively
Active Trace Gases**

and

**Future Climate Impacts of Short-Lived Radiatively Active
Gases and Aerosols**

Lead Agency:

National Oceanic and Atmospheric Administration

Contributing Agencies:

Department of Energy

National Aeronautics and Space Administration

National Science Foundation

Table of Contents

24		
25		
26	PREFACE.....	5
27	EXECUTIVE SUMMARY	14
28	ABSTRACT	14
29	1. Key Results and Findings	16
30	2. Recommendations for Future Research	19
31	3. Guide to Readers	20
32	CHAPTER 1 INTRODUCTION	22
33	PREAMBLE	22
34	1.1 Historical Overview.....	24
35	1.2 Goals and Rationale	27
36	1.3 Limitations	29
37	1.4 Methodology.....	30
38	1.5 Terms and Definitions.....	33
39	CHAPTER 2 CLIMATE PROJECTIONS FROM WELL-MIXED GREENHOUSE	
40	GAS STABILIZATION SCENARIOS.....	38
41	KEY FINDINGS.....	38
42	2.1 Introduction	41
43	2.2 Well-Mixed Greenhouse Gas Emission Scenarios From SAP 2.1a	45
44	2.3 Simplified Global Climate Model (MAGICC)	49
45	2.4 Long-Lived Greenhouse Gas Concentrations and Radiative Forcings.....	50
46	2.5 Short-Lived Species and Total Radiative Forcing	52
47	2.6 Surface Temperature: MAGICC AND IPCC Comparisons	55
48	2.7 Climate Projections for SAP 2.1a Scenarios	57

49	Appendix 2.1 IPCC 4th Assessment Climate Projections	66
50	A.2.1.1 Mean Temperature	66
51	A.2.1.2 Temperature Extremes.....	67
52	A.2.1.3 Mean Precipitation.....	68
53	A.2.1.4 Precipitation Extremes and Droughts.....	68
54	A.2.1.5 Snow and Ice.....	68
55	A.2.1.6 Carbon Cycle.....	69
56	A.2.1.7 Ocean Acidification.....	69
57	A.2.1.8 Sea Level	70
58	A.2.1.9 Ocean Circulation	71
59	A.2.1.10 Monsoons.....	71
60	A.2.1.11 Tropical Cyclones (Hurricanes and Typhoons).....	72
61	A.2.1.12 Midlatitude Storms	72
62	A.2.1.13 Radiative Forcing.....	72
63	A.2.1.14 Climate Change Commitment (Temperature and Sea Level).....	73
64	Appendix 2.2 MAGICC Model Description.....	74
65	CHAPTER 3 CLIMATE CHANGE FROM SHORT-LIVED EMISSIONS DUE TO	
66	HUMAN ACTIVITIES	78
67	3.1 Introduction	80
68	3.2 Emission Scenarios and Composition Model Descriptions	82
69	3.2.1 Emission Scenarios	82
70	3.2.2 Composition Models	86
71	3.2.3 Tropospheric Burden	89
72	3.2.4 Aerosol Optical Depth	94
73	3.3 Climate Studies	99
74	3.3.1 Experimental Design.....	99
75	3.3.2 Climate Models	100
76	3.3.3 Radiative Forcing Calculations	102
77	3.3.4 Climate Model Simulations 2000 – 2050	116
78	3.3.5 Climate Simulations Extended to 2100	132
79	3.4 Regional Emission Sector Perturbations and Regional Models	136
80	3.4.4 Regional Downscaling Climate Simulations	145
81	Appendix 3.1 Composition Models	155
82	A.3.1.1 Geophysical Fluid Dynamics Laboratory	155
83	A.3.1.2 Goddard Institute for Space Studies	158
84	A.3.1.3 National Center for Atmospheric Research.....	162
85	Appendix 3.2 Climate Models.....	165
86	A.3.2.1 Geophysical Fluid Dynamics Laboratory	165
87	A.3.2.2 Goddard Institute for Space Studies	166
88	A.3.2.3 National Center for Atmospheric Research.....	167
89	CHAPTER 4 FINDINGS, ISSUES, OPPORTUNITIES, AND	
90	RECOMMENDATIONS.....	172

91 4.1 Introduction 172

92 4.2 Major Findings 172

93 4.3 Issues Raised 175

94 4.3.1 Emission Projections..... 175

95 4.3.2 Aerosols (Indirect Effect, Direct Effect, Mixing, Water Uptake) 178

96 4.3.3 Climate and Air Quality Policy Interdependence 179

97 4.4 Research Opportunities and Recommendations..... 181

98 4.4.1 Emission Scenario Development..... 182

99 4.4.2 Aerosol Studies (Direct Effect, Indirect Effect, Mixing, Water Uptake) 183

100 4.4.3 Improvements in Transport, Deposition, and Chemistry 184

101 4.4.4 Recommendations for Regional Downscaling 185

102 4.4.5 Expanded Analysis and Sensitivity Studies 186

103 4.5 In Conclusion 187

104 APPENDIX A 190

105 ACRONYMS 193

106 GLOSSARY..... 196

107

108 **Preface**

109

110 **Motivation and Guidance for Using Synthesis and Assessment Product 3.2**

111

112 **Authors:** Hiram Levy II, GFDL/NOAA; Drew T. Shindell, GISS/NASA; Alice
113 Gilliland, ARL/NOAA; M. Daniel Schwarzkopf, GFDL/NOAA; Larry W. Horowitz,
114 GFDL/NOAA

115

116 **Contributing Author:** Anne Waple, STG, Inc. at NCDC/NOAA

117

118 **Introduction**

119 The U.S. Climate Change Science Program (CCSP) was established in 2002 to coordinate
120 climate and global change research conducted in the United States. Building upon and
121 incorporating the U.S. Global Change Research Program of the previous decade, the
122 program integrates federal research on climate and global change, as sponsored by 13
123 federal agencies and overseen by the Office of Science and Technology Policy, the
124 Council on Environmental Quality, the National Economic Council, and the Office of
125 Management and Budget.

126

127 “A primary objective of the U. S. Climate Change Science Program (CCSP) is to provide
128 the best possible scientific information to support public discussion and government and
129 private sector decision-making on key climate-related issues. To help meet this objective,
130 the CCSP has identified an initial set of 21 synthesis and assessment products that
131 address its highest priority research, observation, and decision-support needs.”

132

133 The CCSP is conducting 21 such activities, covering topics such as the North American
134 carbon budget and implications for the global carbon cycle, coastal elevation and
135 sensitivity to sea-level rise, trends in emissions of ozone-depleting substances and ozone
136 recovery and implications for ultraviolet radiation exposure, and use of observational and
137 model data in decision support and decision making. The stated purpose for this report,
138 Synthesis and Assessment Product (SAP) 3.2, is to provide information to those who use
139 climate model outputs to assess the potential effects of human activities on climate, air
140 quality and ecosystem behavior.

141

142 In an examination of the U.S. CCSP Strategic Plan, the National Research Council
143 (NRC) recommended that synthesis and assessment products should be produced with
144 independent oversight and review from the wider scientific and stakeholder communities.
145 To meet this goal, NOAA requested an independent review of SAP 3.2 by the NRC. The
146 NRC appointed an ad hoc committee composed of eight members who provided their
147 review findings, and recommendations, suggestions, and options for the authors to
148 consider in revising the first draft SAP 3.2. This second draft is in response to that
149 review.

150

151 **Background and Goals**

152 The initial mandate for Synthesis and Assessment Product 3.2 (SAP 3.2), which is still
153 listed on the official CCSP website [[http://www.climate-science.gov/Library/sap/sap-](http://www.climate-science.gov/Library/sap/sap-summary.php)
154 [summary.php](http://www.climate-science.gov/Library/sap/sap-summary.php)], was to provide “*Climate Projections for Research and Assessment Based*
155 *on Emissions Scenarios Developed Through the Climate Change Technology Program*”.

156 With the development of long-lived greenhouse gas scenarios by another Synthesis and
157 Assessment Product (SAP 2.1a) our mandate evolved to “*Climate Projections for SAP*
158 *2.1a Emissions Scenarios of Greenhouse Gases*”. These emission scenarios¹ were for the
159 long-lived² and therefore globally well-mixed greenhouse gases and were constrained by
160 the requirement that their atmospheric concentrations stabilize within 100 – 200 years at
161 specified levels more-or-less equivalent to 450, 550, 650, and 750 parts per million (ppm)
162 of carbon dioxide. See the Box for additional details.

¹ Emission scenarios represent the future emissions based on a coherent and internally consistent set of assumptions about the driving forces (*e.g.* population change, socio-economic development, technological change) and their key relationships.

² Long-lived radiative species of interest have atmospheric lifetimes that range from 10 years for methane to more than 100 years for nitrous oxide. While carbon dioxide’s lifetime is more complex, we think of it as being more than 100 years in the climate system. Due to their long atmospheric lifetime, they are well-mixed and evenly distributed throughout. Global atmospheric lifetime is the mass of a species in the atmosphere divided by the mass that is removed from the atmosphere each year.

Box P1: Stabilization Scenarios and Background from CCSP SAP 2.1a

Synthesis and Assessment Product 2.1 is an important precursor to this report. It explores different scenarios that lead to greenhouse gas emissions stabilizing at different (higher) levels in the future. Scenario analysis is a widely used tool for decision making in complex and uncertain situations. Scenarios are “what ifs”—sketches of future conditions (or alternative sets of future conditions), used as inputs to exercises of decision making or analysis. Scenarios have been applied extensively in the climate change context. Examples include greenhouse gas emissions scenarios, climate scenarios, and technology scenarios.

The scenarios in SAP 2.1a are called “stabilization emission scenarios” because they are constrained so that the atmospheric concentrations of the long-lived greenhouse gases level off, or stabilize, at pre-determined levels by the end of the 21st century. They explicitly treat the economic and technological drivers needed to generate each level of greenhouse gases.

Pre-industrial levels of carbon dioxide were approximately 280 part per million (ppm), and are currently around 380 ppm – a third higher than prior to the industrial era and higher than at any other time in at least the last 420,000 years (CCSP SAP 2.2). The four stabilization levels for 2.1a were constructed so that the carbon dioxide concentrations resulting from stabilization are roughly 450, 550, 650, and 750 ppm. While the Intergovernmental Panel on Climate Change (IPCC) has also examined greenhouse gas emission scenarios and those provided by SAP 2.1a are generally within the envelope of the IPCC scenarios, 2.1a is an alternative approach to developing a consistent set of long-lived greenhouse gas concentrations.

This report (3.2) explores the climate implications of such greenhouse gas “stabilization scenarios” via several different computer simulations. The results of these projections are presented in Chapter 2 of this report.

164 The SAP 2.1a scenarios did not explicitly address the direct influence of short-lived³
165 drivers of climate: carbon and sulfate particles and lower atmospheric ozone. Therefore
166 we expanded our mandate to include “*Future Climate Impacts of Short-lived Radiatively*
167 *Active⁴ Gases and Aerosols*”. These short-lived species are largely of human-caused
168 origin, important contributors to large-scale changes in atmospheric temperature and
169 climate in general and primarily controlled for reasons of local and regional air quality.
170 Therefore, this added portion of the report is a critical first step in examining the climate
171 impact of future actions taken to reduce air pollution.

172

173 The Prospectus for Synthesis and Assessment Product 3.2 contained two charges to the
174 authors of this report:

175

176 1. Develop climate projections for a series of emission scenarios for long-lived
177 greenhouse gases provided by Synthesis and Assessment Product 2.1 “Scenarios
178 of Greenhouse Gas Emissions and Atmospheric Concentrations and Review of
179 Integrated Scenario Development and Application“;

180

181 2. Investigates the contributions of four short-lived pollutants in the lower
182 atmosphere – ozone and three types of particles (soot/elemental carbon, organic
183 carbon and sulfate) usually identified in scientific terms as aerosols⁵.

³ Short-lived radiative species of interest have atmospheric lifetimes that range in the lower atmosphere from a day for nitrogen oxides, from a day to a week for most particles, and from a week to a month for ozone. Their concentrations are highly variable and concentrated in the lowest part of the atmosphere, primarily near their sources.

⁴ Radiatively active species absorb and re-emit energy, thus changing the temperature of the atmosphere.

⁵ Aerosols are very small airborne solid or liquid particles that reside in the atmosphere for at least several hour with the smallest remaining airborne for days.

184

185 Short-lived greenhouse gases and particles have received less attention than long-lived
186 greenhouse gases in previous international assessments and were not explicitly treated in
187 Synthesis and Assessment Product 2.1, but, as this report describes, they may affect the
188 future climate in a substantial manner. Although sources of these pollutants tend to be
189 localized, their impact is felt globally. This is of direct relevance to policy decisions
190 regarding pollution, air quality and climate change.

191

192 **Readers Guide to Synthesis and Assessment Product 3.2**

193 The report includes an Executive Summary and four Chapters.

194

195 **Executive Summary** presents the key results and findings and recommends four critical
196 areas of future research. It is written in non-technical language and is intended to be
197 accessible to all audiences.

198

199 **Chapter 1** provides an Introduction to this study and is intended to provide all audiences
200 with a general overview. It is written in non-technical language, which should be
201 accessible to all readers with an interest in climate change. It includes background
202 material, discusses the scope of and motivation for this study, addresses its goals and
203 objectives, and identifies the issues that are not addressed. It also contains two Boxes,
204 one providing non-technical definitions of important terms and the other containing a
205 clear concise description of the computer models employed in this study.

206

207 **Chapter 2** focuses on the long-lived greenhouse gases and a set of emission scenarios
208 provided by Synthesis and Assessment Product 2.1. The Statement of Findings and the
209 Introductory section 2.1 are written in non-technical language and intended for the
210 general reader. The remainder of the Chapter 2 provides detailed technical information
211 about specific computer models, the resulting climate simulations and a detailed
212 interpretation of the results. It is intended primarily for the scientific community.

213

214 A simplified global climate model, MAGICC⁶, is used to simulate globally-averaged
215 surface temperature increases for the stabilization scenarios and the results are assessed in
216 the context of the most recent Intergovernmental Panel on Climate Change (IPCC) report
217 (4th Assessment Report, Working Group 1). These comparisons are used to answer the
218 first four questions posed in our Prospectus:

219

- 220 1. Do SAP 2.1a emission scenarios differ significantly from IPCC emission
221 scenarios?
- 222 2. If the SAP 2.1a emission scenarios do fall within the envelope of emission
223 scenarios previously considered by the IPCC, can the existing IPCC climate
224 simulations be used to estimate 50 -100 year climate responses for the CCSP 2.1
225 carbon dioxide emission scenarios?
- 226 3. What would be the changes to the climate system under the scenarios being put
227 forward by SAP 2.1a?

⁶ MAGICC is a two component numerical model consisting of a highly simplified representation of a climate model coupled to an equally simplified representation of the atmospheric composition of radiatively active species. This model is adjusted, based on the results of more complex climate models, to make representative predictions of global mean surface temperature and sea-level rise.

228 4. For the next 50 to 100 years can the climate projections using the emissions from
229 SAP 2.1a be distinguished from one another or from the scenarios recently
230 studied by the IPCC?

231

232 **Chapter 3** attempts to assess the direction, magnitude and duration of future climate
233 impacts due to changing levels of short-lived radiative active species of human-caused
234 origin. This is an area of research that is still at the initial stages of exploration and which
235 4th Assessment Report, as well as previous IPCC reports, investigated only superficially.

236

237 First the stabilization emission scenarios and models used to generate them are discussed.
238 Next the chemical composition models⁷ used to produce the global distributions of short-
239 lived species that help to drive the climate models are introduced. 21st century climate is
240 then simulated with three state-of-the-art comprehensive climate models⁸, and the results
241 are then used to address the four questions raised in the second section of our Prospectus:

242

- 243 1. What are the impacts of the radiatively active short-lived species not explicitly the
244 subject of SAP 2.1a?
- 245 2. How do the impacts of short-lived species compare with those of the well-mixed
246 green house gases as a function of the time horizon examined?

⁷ Chemical composition models are state-of-the-art numerical models that use the emission of gases and particles as inputs and simulate their chemical interactions, global transport by the winds, and removal by rain, snow and deposition to the earth's surface. The resulting outputs are global three-dimensional distributions of the initial gases and particles and their products.

⁸ Comprehensive climate models are a numerical representation of the climate based on the physical properties of its components, their interactions and feedback processes. Coupled atmosphere/ocean/sea-ice General Circulation Models (AOGCMs) represent our current state-of-the-art.

247 3. How do the regional impacts of short-lived species compare with those of long-
248 lived gases in or near polluted areas?

249 4. What might be the climate impacts of mitigation actions taken to reduce the
250 atmospheric levels of short-lived species to address air quality issues?

251

252 The Statement of Findings and the Introductory section 3.1 are written in non-technical
253 language and intended for the general reader. The remainder of the chapter provides
254 detailed technical information about the models, the resulting climate simulations and our
255 interpretation of the results. It is intended primarily for the scientific community.

256

257 **Chapter 4** provides a summary of the major findings, identifies a number of scientific
258 issues and questions that arise from our study, and identifies new opportunities for future
259 research. The four most critical areas identified by this study are:

260

- 261 1. The projection of future human-caused emissions for the short-lived species;
- 262 2. The of indirect and direct effects of particulates and mixing between particulate
263 types;
- 264 3. Transport, deposition, and chemistry of the short lived species.
- 265 4. Regional climate forcing vs. regional climate response.

266

267 We have written Chapter 4, as much as is possible, in non-technical language and it is
268 intended for all audiences.

269 **Executive Summary**

270

271 **Lead Author(s):** Hiram Levy II, GFDL/NOAA; Drew T. Shindell, GISS/NASA; Alice
272 Gilliland, ARL/NOAA; M. Daniel Schwarzkopf, GFDL/NOAA; Larry W. Horowitz,
273 GFDL/NOAA

274

275 **Contributing Authors:** Tom Wigley, NCAR; Ron Stouffer, GFDL; Anne Waple, STG
276 Inc. at NCDC/NOAA

277

278 **ABSTRACT**

279 The influence of greenhouse gases and particles on our present and future climate has
280 been widely examined and most recently reported in the Intergovernmental Panel on
281 Climate Change (IPCC) Fourth Assessment Report. While both long-lived⁹ (*e.g.* carbon
282 dioxide) and short-lived¹⁰ (*e.g.* soot) species affect the climate, previous projections of
283 future climate, such as the IPCC reports, have focused largely on the long-lived gases.
284 This Climate Change Science Program Synthesis and Assessment Product provides a
285 different emphasis.

286

287 We first examine the effect of long-lived greenhouse gases on the global climate based on
288 updated emission scenarios produced by another CCSP Synthesis and Assessment
289 Product (2.1a). Unlike those used in the latest IPCC report, these scenarios were

⁹ Atmospheric lifetimes for the long-lived radiative species of interest range from 10 years for methane to more than 100 years for nitrous oxide. While carbon dioxide's lifetime is more complex, we can think of it as being more than 100 years in the climate system. As a result of their long atmospheric lifetime, they are well-mixed and evenly distributed throughout. Global atmospheric lifetime is the mass of a species in the atmosphere divided by the mass that is removed from the atmosphere each year.

¹⁰ Atmospheric lifetimes for the short-lived radiative species of interest range in the lower atmosphere from a day for nitrogen oxides, from a day to a week for most particles, and from a week to a month for ozone. As a result of their short lifetime their concentrations are highly variable and concentrated in the lowest part of the atmosphere, primarily near their sources.

290 constrained so that the atmospheric concentrations of the long-lived greenhouse gases
291 leveled off, or stabilized, at pre-determined levels by the end of the 21st century. However
292 the projected future temperature changes, based on these stabilization emission scenarios,
293 fall within the same range as those projected for the latest IPCC report. Therefore we are
294 able to use the very extensive analysis in the 4th Assessment Report of the IPCC to
295 summarize the key global and regional climate projections for the stabilization emission
296 scenarios produced by 2.1a. We confirm the robust future warming signature and other
297 associated changes in the climate.

298

299 We next explicitly assess the effects of short-lived gases and particulates. Their influence
300 is found to be global in nature, substantial when compared with long-lived greenhouse
301 gases and potentially extending to the end of this century. They can significantly change
302 the regional surface temperature (for example over the summertime continental US). It is
303 noteworthy that the location of the simulated climate response is not local to the forcing.
304 This has implications for regional air quality control strategies and also reveals the
305 necessity for explicit and consistent inclusion of these pollutants in further assessments of
306 future climate.

307 **1. Key Results and Findings**

308 These results constitute important improvements in our understanding of the influence of
309 both long-lived gases and short-lived gases and particulates. The Fourth Assessment
310 Report of the IPCC recognized that most of the global-scale warming since the middle of
311 last century was very likely due to the increase in greenhouse gas concentrations, and
312 also that the warming has been partially damped by increasing levels of short-lived
313 particles. However, while the IPCC models were coordinated in using identical
314 greenhouse gas emission scenarios, the short-lived radiatively active pollutants were
315 widely varying in the emission scenarios used, and their future impacts were not isolated
316 from the long-lived gases

317

318 This Synthesis and Assessment Product is able to provide a more comprehensive and
319 updated assessment of the relative future contributions of long and short-lived gases and
320 particulates, with special, explicit focus on the short-lived component. This study
321 encompasses a realistic time frame over which available technological solutions can be
322 employed, and this study in particular, focuses on those gas and aerosol species whose
323 future atmospheric levels are also subject to reduction due to air pollution control.

324

325 1. Climate projections from CCSP 2.1a stabilization emission scenarios¹¹ generally
326 fall within the IPCC range of projections for their standard storyline scenarios.

327 The most extreme stabilization scenarios, which are equivalent to a carbon

¹¹ Stabilization scenarios are a representation of the future emissions of a substance based on a coherent and internally consistent set of assumptions about the driving forces (such as population, socio-economic development, technological change) and their key relationships. These emissions are constrained so that the resulting atmospheric concentrations of the substance level-off at a pre-determined value in the future.

328 dioxide stabilization level of 450 ppm, result in global surface temperatures below
329 those calculated for the most moderate IPCC scenario, particularly beyond 2050.
330 Nonetheless, all of them unequivocally cause warming across the range of
331 possible emission scenarios.

332 2. By 2050, changes in short-lived pollutant concentrations in two of the three
333 studies contribute 20-25% of their simulated global-mean annual average
334 warming. Further, our results suggest that the short-lived species significantly
335 influence climate out to 2100. The presence of radiatively active¹² short-lived
336 species can significantly change the regional surface temperature response (for
337 example over the summertime continental US).

338 3. The range of plausible short-lived emissions projections is very large, even for a
339 single well-defined global socio-economic development scenario. This currently
340 limits our ability to provide definitive statements on their contribution to future
341 climate change. The three comprehensive climate models¹³ and their associated
342 chemical composition models¹⁴ participating in this report produced differing
343 outcomes. Each model represents a thoughtful, but incomplete characterization of
344 the driving forces and processes that are believed to be important to the climate or
345 to the global distributions of the short-lived species. Much work remains to be
346 done.

¹² Radiatively active indicates the ability of a substance to absorb and re-emit radiation, thus changing the temperature of the lower atmosphere.

¹³ A comprehensive climate model is a state-of-the-art numerical representation of the climate based on the physical, chemical and biological properties of its components, their interactions and feedback processes that accounts for many of climate's known properties. Coupled atmosphere/ocean/sea-ice General Circulation Models (AOGCMs) provide a comprehensive representation of the physical climate system.

¹⁴ Chemical composition models are state-of-the-art numerical models that use the emission of gases and particles as inputs and simulate their chemical interactions, global transport by the winds, and removal by rain, snow and deposition to the earth's surface. The resulting outputs are global three-dimensional distributions of the initial gases and particles and their products.

- 347 4. We find that the geographic (spatial) distribution of forcing is less important than
348 the spatial distribution of climate response. Thus, both short-lived and long-lived
349 species appear to cause enhanced climate responses in the same regions rather
350 than short-lived species having an enhanced effect primarily in or near polluted
351 areas. This means that regional emission control strategies for short-lived
352 pollutants will have large-scale climate impacts.
- 353 5. The two most important uncertainties in characterizing the potential climate
354 impact of short-lived species are found to be the projection of their future
355 emissions and the determination of the indirect effect¹⁵ of particles on climate.
356 The fundamental difference between uncertainties in future emissions and
357 uncertainties in processes, such as the indirect effect of particles, is discussed in
358 section 4.3.
- 359 6. Natural particles such as dust and sea salt also play an important role and their
360 emissions and interactions differed significantly among the models, with
361 consequences to the role of short-lived pollutants. This inconsistency among
362 models should be reconciled in future studies.
- 363 7. Emissions reductions of soot in the domestic energy/power sector in Asia appear
364 to offer the greatest potential for substantial, simultaneous improvement in local
365 air quality and reduction of global climate change.

¹⁵ The indirect effects of particles lead to an indirect forcing of the climate system through their acting as cloud condensation nuclei or modifying the optical properties and lifetime of clouds.

366 **2. Recommendations for Future Research**

367 The four most critical areas for future research identified in this Report are:

- 368 1. The projection of future human-caused emissions for the short-lived species;
- 369 2. The of indirect and direct effects of particulates and mixing between particulate
- 370 types;
- 371 3. Transport, deposition, and chemistry of the short lived species.
- 372 4. Regional climate forcing vs. regional climate response.

373

374 1. Plausible emission scenarios for the second half of the 21st century show significant

375 climate impacts, yet the range of plausible scenarios is currently large and some increase

376 in confidence in these scenarios is necessary. Short-lived species, unlike the well mixed

377 greenhouse gases, do not accumulate in the atmosphere. Therefore, combined with a

378 large range of possible emission scenarios, the climate impact of the short-lived species is

379 currently extremely difficult to predict. Improvements in our ability to predict social,

380 economic and technological developments affecting future emissions are needed.

381 However, uncertainties in future emissions will always be with us. What we can do is

382 develop a set of internally consistent emission scenarios that include all of the important

383 radiative species and bracket the full range of possible future outcomes.

384

385 2. The aerosol indirect effect, which is very poorly known, is probably the process in

386 most critical need of research. The modeling community as a whole cannot yet produce a

387 credible characterization of the climate response to aerosol/cloud interactions. All models

388 (including those participating in this study) are currently either ignoring it, or strongly
389 constraining the model response.

390

391 3. The three global composition models in this study all employed different treatments of
392 mixing in the lowest layers of the atmosphere, transport and mixing by turbulence and
393 clouds, removal of gases and particles by rain, snow and contact with the earth's surface,
394 and different approximate treatments of the very large collection of chemical reaction that
395 we do not yet fully understand. Further research is needed in all of these processes.

396

397 4. The major unfinished analysis question in this study is the relative contribution of a
398 model's regional climate response, as opposed to the contribution from the regional
399 pattern of radiative forcing¹⁶, to the observed regional change in seasonal surface
400 temperature. Is there a model independent regional climate response? What are the actual
401 physical mechanisms driving the region temperature patterns that we observe? This
402 appears to be a very important area of study, particularly given the apparently strong
403 climate response in the summertime central US.

404

405 **3. Guide to Readers**

406 For those readers who would like to learn more about the research behind the Key
407 Results and Findings and the Recommendations for Future Research, we provide the

¹⁶ Radiative forcing is a measure of how the energy balance of the Earth-atmosphere system is influenced when factors that affect climate, such as atmospheric composition or surface reflectivity, are altered. When radiative forcing is positive, the energy of the Earth-atmosphere system will ultimately increase, leading to a warming of the system. In contrast, for a negative radiative forcing, the energy will ultimately decrease, leading to a cooling of the system. For technical details see Box 3.2

408 following guide to reading the four chapters. Chapter 1 provides an introduction to this
409 study and relevant findings from previous climate research, introduces the goals and
410 methodology, and provides Box 1.1 and Box 1.2 with relatively non-technical
411 descriptions of the modeling tools and definitions of terms. It is written in a non-technical
412 manner and is intended to provide all audiences with a general overview. Chapters 2 and
413 3 provide detailed technical information about specific models, model runs and trends
414 and are intended primarily for the scientific community, though the key findings and the
415 introduction to each chapter are written in non-technical language and intended for all
416 audiences. Chapter 4 is intended for all audiences. It provides a summary of the major
417 findings and identifies new opportunities for future research.

418 Chapter 1 Introduction

419

420 **Lead Author(s):** Hiram Levy II, GFDL/NOAA; Drew T. Shindell, GISS/NASA; Alice

421 Gilliland, ARL/NOAA

422

423 **Contributing Authors:** Tom Wigley, NCAR,; Ron Stouffer, GFDL; Anne Waple, STG

424 Inc. at NCDC/NOAA

425

426 PREAMBLE

427 Comprehensive climate models¹⁷ have become the essential tool for understanding past

428 climates and making projections of future climate resulting from changes in radiative

429 forcing¹⁸, both natural and anthropogenic. Projections of future climate require estimates430 (*e.g.* scenarios) of future emissions of long-lived¹⁹ greenhouse gases and short-lived²⁰431 radiatively active²¹ gases and particles. A number of standard emission scenarios²² have

432 been developed for the Intergovernmental Panel on Climate Change (IPCC) assessment

¹⁷ Comprehensive climate models are a numerical representation of the climate based on the physical properties of its components, their interactions and feedback processes. Coupled atmosphere/ocean/sea-ice General Circulation Models (AOGCMs) represent our current state-of-the-art.

¹⁸ Radiative forcing is a measure of how the energy balance of the Earth-atmosphere system is influenced when factors that affect climate, such as atmospheric composition or surface reflectivity, are altered. When radiative forcing is positive, the energy of the Earth-atmosphere system will ultimately increase, leading to a warming of the system. In contrast, for a negative radiative forcing, the energy will ultimately decrease, leading to a cooling of the system. For technical details see Box 3.2

¹⁹ Long-lived species of interest have atmospheric lifetimes that range from 10 years for methane to more than 100 years for nitrous oxide and carbon dioxide. Due to their long atmospheric lifetimes, they are well-mixed and evenly distributed throughout. Global atmospheric lifetime is the mass of a species in the atmosphere divided by the mass that is removed from the atmosphere each year.

²⁰ Short-lived radiative species have atmospheric lifetimes that range in the lower atmosphere from a day for nitrogen oxides, from a day to a week for most particles, and from a week to a month for ozone. Their concentrations are highly variable and concentrated in the lowest part of the atmosphere, primarily near their sources.

²¹ Radiatively active gases and particles absorb and re-emit energy, thus changing the temperature of the atmosphere. They are commonly called greenhouse gases and particles

²² Emission scenarios represent the future emissions based on a coherent and internally consistent set of assumptions about the driving forces (*e.g.* population change, socio-economic development, technological change) and their key relationships.

433 process, and the future impacts of these have been discussed extensively in the 4th
434 Assessment Report.
435
436 As part of the Climate Change Science Program process, scenarios of long-lived
437 greenhouse gas emissions, with the added requirement that their resulting atmospheric
438 concentrations level-off at specified values sometime after 2100 (*e.g.* stabilization), were
439 developed by the Synthesis and Assessment Product 2.1 team and served as the basis for
440 SAP 3.2, for which the National Oceanic and Atmospheric Administration (NOAA) is the
441 lead agency. NOAA's stated purpose for Synthesis and Assessment Product 3.2 is to
442 provide information to those who use climate model outputs to assess the potential effects
443 of human activities on climate, air quality and ecosystem behavior. 3.2 is comprised of
444 two components that first assess the climate projections resulting from SAP 2.1a
445 scenarios in the context of existing IPCC climate projections and then isolate and assess
446 the future climate impacts resulting from future emissions of short-lived species.
447
448 This second component explores the impact of short-lived radiatively active species on
449 future climate, a critical issue that has recently become an active area of research in the
450 reviewed literature (*e.g.* Hansen *et al.*, 2000; Brasseur and Roekner, 2005; Delworth *et*
451 *al.*, 2005). The existing state-of-the-art models used in this study represent incomplete
452 characterizations of the driving forces and processes that are believed to be important to
453 the climate responses and global distributions of the short-lived species. Moreover, these
454 incomplete treatments are not consistent across the models. However, despite these

455 challenges, this report shows that short lived species have a significant impact on climate,
456 potentially throughout the 21st century.

457

458 **1.1 Historical Overview**

459 The climate models and the representation of the agents driving climate change used for
460 projections of the future have both evolved substantially during the past several decades.

461 In 1967 Manabe and Wetherald published the first model-based projection of future
462 climate change. Using a simple model representing the global atmosphere as a single
463 column, they projected a 2°C global surface air temperature change for a doubling of the
464 atmospheric concentration of carbon dioxide. Model development continued on a wide
465 range of numerical models, especially in the increasing sophistication of the ocean model.

466

467 In 1979, Manabe and Stouffer developed a global model at NOAA's Geophysical Fluid
468 Dynamics Laboratory (GFDL) useful for estimating the climate sensitivity. They called
469 this model an atmosphere-mixed layer ocean model which is some times called a slab
470 model. A slab model consists of global atmospheric, land and sea ice component models,
471 coupled to a static 50 m deep layer of seawater. By construction, this type of model
472 assumes no changes in the oceanic heat transports as the climate changes. It is used to
473 estimate only equilibrium climate changes. In 1984, Hansen *et al.* used the NASA
474 Goddard Institute of Space Studies (GISS) model in the first climate studies in which
475 ocean heat transports were included in the climate calculation, although these were
476 prescribed (fixed).

477

478 The two models discussed above, as well as one developed at the National Center for
479 Atmospheric Research (NCAR), all played an important part in the first
480 Intergovernmental Panel on Climate Change (IPCC) Assessment Report in 1990. It
481 should be noted that the IPCC does not directly perform any research. Rather, its reports
482 are intended to be reviews of current research. However, it must also be noted that the
483 IPCC is, in fact, a very powerful driver of research and setter of research agendas in
484 climate science. It is very far from a passive player. Moreover, only the latest report
485 strictly enforced the requirement that all results discussed in it be previously published in
486 the reviewed literature.

487

488 In the late 1980's, Washington and Meehl (1989) at NCAR and Stouffer *et al.* (1989) at
489 GFDL developed the first comprehensive climate models (Atmosphere-Ocean General
490 Circulation Models - AOGCMs) useful for investigating climate change over multi-
491 decadal and longer time periods. These models consisted of global atmosphere, ocean,
492 land surface and sea ice components. Both groups used an idealized radiative forcing to
493 drive their models. Stouffer *et al.* used a 1% per year increase in the carbon dioxide
494 concentration (compounded), where its atmospheric concentration doubles in 70 years.

495

496 By the time of the IPCC Second Assessment Report in 1995, all three U.S. modeling
497 centers were running comprehensive climate models. In addition, representation of the
498 climate forcing was improving. Mitchell *et al.* (1995) in the United Kingdom (U.K.)
499 developed a scheme for crudely incorporating the impact of sulfate particles on climate.
500 Similarly, actual concentrations of long-lived greenhouse gases were used for the past,

501 allowing more realistic climate simulations of the historical time period (1860 to present
502 day). Using emission scenarios²³ developed by the IPCC in 1992, the U.K. group also
503 made future projections of climate change out to the year 2100. Their results were very
504 important in the Second Assessment Report of the IPCC

505

506 By the time of the Third IPCC Assessment Report in 2001 about 12 comprehensive
507 climate models were used to project climate out to year 2100. They used the emission
508 scenarios produced by the Special Report on Emission Scenarios (Nakićenović, N., *et al.*;
509 2000) with most groups using a high (A2) and low (B2) emission scenario. Some of the
510 models included components to predict atmospheric particle concentrations, but most of
511 the 12 models used variants of the Mitchell *et al.*(1995) method to include their impact on
512 climate. While particle changes were included in the historical simulations, most of the
513 future projections did not include any changes in them or tropospheric ozone.

514

515 In the most recent IPCC report, the Fourth Assessment Report (AR4, 2007), about 24
516 comprehensive climate models participated. The component models continue to become
517 more sophisticated and include more physical processes. The new components allowed
518 the inclusion of more radiatively active agents such as dust, black carbon and organic
519 carbon particles and land use in the scenarios. Again, most models included all or nearly
520 all these climate forcing agents in their historical simulations, but many did not do so for
521 the future. Most groups used the three standard IPCC scenarios (B1, A1B and A2) to

²³ Scenarios are a representation of the future development of emissions of a substance based on a coherent and internally consistent set of assumptions about the driving forces (such as population, socio-economic development, and technological change) and their key relationships.

522 make their future projections. These are the same three IPCC scenarios represented in
523 Figures 2.1-4 in Chapter 2.

524

525 **1.2 Goals and Rationale**

526 As described in the Prospectus outlining the purpose of this report, Synthesis and
527 Assessment Product 3.2 has two primary goals:

528

529 1. Produce climate projections for research and assessment based on the stabilization
530 scenarios of long-lived greenhouse gas emissions developed by Synthesis and
531 Assessment Product 2.1.

532 2. Assess the sign, magnitude, and duration of future climate impacts due to
533 changing levels of short-lived gaseous and particulate species that are radiatively
534 active and that may be subject to future mitigation actions to address air quality
535 issues.

536

537 The 8 key questions which address the above goals and were also listed in the Prospectus
538 for this report are:

539 1. Do SAP 2.1a emissions scenarios differ significantly from IPCC emissions
540 scenarios?

541 2. If the SAP 2.1a emissions scenarios do fall within the envelope of emissions
542 scenarios previously considered by the IPCC, can the existing IPCC climate
543 simulations be used to estimate 50-to 100-year climate responses for the CCSP
544 2.1 CO₂ emissions scenarios?

- 545 3. What would be the changes to the climate system under the scenarios being put
546 forward by SAP 2.1a?
- 547 4. For the next 50 to 100 years, can the time-varying behavior of the climate
548 projections using the emissions scenarios from SAP 2.1a be distinguished from
549 one another or from the scenarios currently being studied by the IPCC?
- 550 5. What are the impacts of the radiatively active short-lived species not being
551 reported in SAP 2.1?
- 552 6. How do the impacts of short-lived species compare with those of the well-mixed
553 green house gases as a function of the time horizon examined?
- 554 7. How do the regional impacts of short-lived species compare with those of long-
555 lived gases in or near polluted areas?
- 556 8. What might be the climate impacts of mitigation actions taken to reduce the
557 atmospheric levels of short-lived species to address air quality issues?

558

559 The answers to these questions are summarized in the Key Findings of the Executive
560 Summary and discussed in more technical detail in Chapters 3 and 4.

561

562 Synthesis and Assessment Product 3.2 is intended to provide information to those who
563 use climate model outputs to assess the potential effects of human activities on climate,
564 air quality, and ecosystem behavior. Since neither the IPCC nor SAP 2.1 explicitly
565 addressed the direct influence of changing emissions of short-lived pollutants (carbon and
566 sulfate particles and lower atmospheric ozone) on climate change, their impact became a
567 major focus of this report.

568

569 This study encompasses a realistic time frame over which available technological
570 solutions can be employed, and focuses on those gases and particles whose future
571 atmospheric levels are also subject to mitigation via air pollution control. Thus Synthesis
572 and Assessment Product 3.2 can be very beneficial to all stakeholders of climate change
573 science. The intended audiences include those engaged in scientific research, the media,
574 policymakers, and members of the public. Policy and decision-makers in the public sector
575 (e.g., congressional staff) need to understand the implications of these scenarios and the
576 climates that they force, in contrast to the research science community, who may be more
577 interested in the physical basis for the behavior.

578

579 **1.3 Limitations**

580 The 1st goal, assessing the climate impacts of the SAP 2.1 stabilization emission
581 scenarios for long-lived greenhouse gases, is relatively narrowly defined and so treated.

582 While the 2nd goal, assessing the climate impact of changing emissions of short-lived
583 radiatively active gases and particles, could be viewed much more broadly, we do not.

584 Our focus is primarily on the direct effect²⁴ of these short-lived pollutants on climate.

585 Only in the case of methane do we explore any of the potential interactions of chemical
586 sources, reactions and removal with a changing climate.

587

588 We do not examine any of the indirect effects²⁵ of pollutant particles on climate, nor do
589 we address other potentially important impacts such as land use change, reactive nitrogen

²⁴ The direct effect refers to the influence of aerosols on climate through scattering and absorbing radiation.

²⁵ Particles may lead to an indirect radiative forcing of the climate system through acting as cloud condensation nuclei or modifying the optical properties and lifetime of clouds.

590 deposition and ecosystem responses, changing natural hydrocarbon emissions, changing
591 oxidant levels and changing particle formation or a wide range of other processes that can
592 interact with climate such as ice clouds and changes in vegetation burning. The resources
593 were also not available for extensive sensitivity studies that might help explore more
594 deeply the causes and mechanisms behind the potentially significant impact of short-lived
595 pollutant levels on future climate. The above and many others are potential topics for
596 future research, but were beyond the scope of this study. We will only address the climate
597 impacts due to direct radiative forcing by long and short-lived greenhouse gases and
598 particles.

599

600 **1.4 Methodology**

601 In addressing the questions posed above, we rely on several different types of computer
602 models to project the climate changes that would result from the scenarios of emissions
603 of greenhouse gases and particles. Projections of future climate first require estimates
604 (*e.g.* scenarios) of future emissions of long-lived greenhouse gases and radiatively active
605 short-lived gases and particles (technically called aerosols²⁶). Next, global composition
606 models, computer models of atmospheric transport and chemistry, employ the emission
607 scenarios to generate global distributions of the concentrations of short-lived radiatively
608 active species. Then comprehensive climate models (computer models of the coupled
609 atmosphere, land-surface, ocean, sea-ice system) employ global distributions of both the
610 long-lived and short-lived radiatively active species to simulate past climates and make

²⁶ Aerosols are very small airborne solid or liquid particles, that reside in the atmosphere for at least several hour with the smallest remaining airborne for days.

611 projections of future climates resulting from natural and anthropogenic changes affecting
612 the climate system. This whole modeling process is discussed in more detail in Box 1.1.

613

614 A number of standard scenarios have been developed for the Intergovernmental Panel on
615 Climate Change (IPCC) assessment process, and the future impacts of these have been
616 explored. As part of the Climate Change Science Program (CCSP) process, updated
617 scenarios of long-lived greenhouse gases and their atmospheric concentrations were
618 developed by the Synthesis and Assessment Product 2.1 team and served as a basis for
619 this Product. In addressing the first four questions, we examine the 12 scenarios for long-
620 lived greenhouse gases developed by SAP 2.1a. We use simulate the global surface
621 temperature increases and sea-level rise (due only to thermal expansion of water, not
622 melting ice caps) resulting from these scenarios using a simplified global climate
623 computer model, MAGICC.

624

625 In addressing the latter four questions listed in 1.2, we focus on the effects of short-lived
626 radiative species, and use three different state-of-the-art complex climate models.
627 Intercomparison studies including the latest IPCC assessment have shown that the
628 performance of these models is comparable to other state-of-the-art comprehensive
629 climate models (AOGCMs). Each of the three models was used to simulate future climate
630 under two different scenarios, one in which human-caused short-lived species were
631 allowed to change in the future, and one in which these species were held constant at
632 present-day concentrations. The differences between the simulated climates for the two
633 scenarios is attributed to the impact of short-lived species.

Box 1.1: Model Descriptions (modified from latest IPCC Report)

Integrated Assessment Models combine key elements of physical, chemical, biological and economic systems into a decision-making framework with various levels of detail for the different components. These models differ in their use of monetary values, their integration of uncertainty, and in their formulation of the policy with regard to optimization, evaluation and projections. For our study, their product was a set of stabilization emission scenarios.

An **Emission Scenario** is a plausible representation of the future development of emissions of substances (in our case, greenhouse gases, aerosols and precursors) that is based on a coherent and internally consistent set of assumptions about the driving forces (*e.g.* demographic and socioeconomic development, technological change) and their key relationships.

Chemical composition models are used to estimate the concentrations and distributions of trace species in the atmosphere that result from a given emission scenario. These models, known technically as chemical transport models, are driven by winds, temperatures, and other meteorological properties that are either compiled from observations or supplied by climate models. Once the gas and particle emissions from human-induced and natural sources are supplied to the chemical composition model, they can be transported through the atmosphere, converted to other species by chemical reactions, and removed from the atmosphere by rain, snow and contact with the surface. These models provide concentrations of radiatively active species that vary in space and time, for use in climate models.

A **climate model** is a numerical representation of the climate system based on the physical, chemical and biological properties of its components, their interactions and their feedback processes. The climate system can be represented by models of varying complexity. For any one component or combination of components a hierarchy of models can be identified, differing in the number of spatial dimensions represented, the extent to which physical, chemical or biological processes are explicitly represented, or the level at which empirical parameterizations are involved.

Simple Climate Models estimate the change in global mean temperature and sea level rise due to thermal expansion. They represent the ocean-atmosphere system as a set of global or hemispheric boxes, and predict global surface temperature using an energy balance equation, a prescribed value of climate sensitivity and a basic representation of ocean heat uptake. Such models can also be coupled to simplified models of biogeochemical cycles and allow rapid estimation of the climate response to a wide range of emission scenarios. MAGICC (for details see Appendix 2.2) is such a coupled model

State-of-the-art **comprehensive climate models** (generally referred to as AOGCMs) include interacting components describing atmospheric, oceanic and land surface processes, as well as sea ice. Although the large-scale dynamics of these models are treated exactly, approximations are still used to represent smaller, but critical, processes such as the formation of clouds and precipitation, ocean mixing due to waves and the mixing of air, heat and moisture near the earth's surface. Uncertainties in these approximations are the primary reason for climate projections differing among different comprehensive climate models. Furthermore, the global models are generally unable to capture the small-scale features of climate in many regions. In such cases, the output from the global models can be used to drive regional climate models that have the same comprehensive treatment of interacting components, but, being only applied to part of the globe, are able to representation a region's climate in much greater detail.

635 **1.5 Terms and Definitions**

636 A number of technical terms are defined and briefly discussed for the benefit of those
637 non-technical readers who wish to proceed to Chapters 2 and 3. The definitions are
638 collected in Box 1.2.

639

640 Emission scenario and stabilization emission scenario are two different approaches to
641 estimating future emissions. The standard emission scenarios used to provide the climate
642 projections for the last two IPCC assessments (Third and Fourth) were storyline
643 scenarios. A set of economic development paths and rates of technological innovation,
644 population growth and social-political development were specified and integrated
645 assessment models (see Box 1.1) were asked to solve for the greenhouse gas and particle
646 emissions that were consistent with the specified conditions.

647

648 Synthesis and Assessment Product 2.1 took quite a different approach. They effectively
649 established a set of targets for long-lived greenhouse gas concentration and then had their
650 three integrated assessment models determine emission pathways to those targets by
651 applying economic principles to the relationships existing among economic development
652 paths and rates of technological innovation, population growth and social-political
653 development. Each group used somewhat different approaches to determine the economic
654 pathway to stabilization. Technically, only one of the models used the “least cost”
655 approach in its strictest economic sense. However, as we show in Chapter 2, the resulting
656 emissions and concentrations of the long-lived greenhouse gases over the 21st century are
657 similar among models for a given target. Furthermore, all of the stabilization scenarios,
658 with the exception of those for most extreme target (only 18% increase in carbon dioxide

659 over the next 100 years), fall within the range of the principal storyline scenarios used for
660 the last two IPCC assessments. While the two approaches to constructing the emission
661 scenarios are different, the resulting concentrations of greenhouse gases and their impacts
662 on climate are not.

663

664 An important quantity that is frequently used when discussing the impact of radiatively
665 active gases and particles is radiative forcing. A technical definition is provided in
666 Chapter 3, Box 3.2. We provide a relatively non-technical explanation in the Box 1.2. It
667 will be useful in the following discussion of long and short-lived gases and particles.

668

669 The long-lived greenhouse gases have atmospheric lifetimes ranging from a decade to
670 more than a century. As a result, they are uniformly mixed and their radiative forcing is
671 also relatively uniformly distributed, both in space and time, throughout the lower
672 atmosphere. On the other hand, the short-lived gases and particles have atmospheric
673 lifetimes ranging from a day to weeks. Their concentrations are highly variable in space
674 and time, and they are concentrated in the lowest part of the atmosphere, primarily near
675 their sources. As a result their radiative forcing is also highly localized and can vary
676 significantly in time. However, one of our Key Findings is that, while radiative forcing
677 patterns for long and short-term species are quite different, the regional patterns of
678 climate change due to long and short-lived radiatively active gases are similar.

Box 1.2: Useful Definitions

Emission scenarios represent future emissions based on a coherent and internally consistent set of assumptions about the driving forces (*e.g.* population change, socio-economic development, technological change) and their key relationships.

Stabilization scenarios represent future emissions based on a coherent and internally consistent set of assumptions where, additionally, these emissions are constrained so that the resulting **atmospheric concentration** levels-off at a pre-determined value in the future.

Radiative forcing is a measure of how the energy balance of the Earth-atmosphere system is influenced when factors that affect climate are altered. The word radiative arises because these factors change the balance between incoming solar radiation and outgoing infrared radiation within the Earth's atmosphere. This radiative balance controls the Earth's surface temperature. The term forcing is used to indicate that Earth's radiative balance is being pushed away from its normal state. When radiative forcing from a factor or group of factors is evaluated as positive, the energy of the Earth-atmosphere system will ultimately increase, leading to a warming of the system. In contrast, for a negative radiative forcing, the energy will ultimately decrease, leading to a cooling of the system.

Global Atmospheric Lifetime is the mass of a species in the atmosphere divided by the mass that is removed from the atmosphere each year.

Long-lived species of interest to climate have atmospheric lifetimes that range from 10 years for methane to more than 100 years for nitrous oxide. While carbon dioxide's lifetime is more complex, we can think of it as being more than 100 years in the climate system. As a result of their long atmospheric lifetime, long-lived gases are well-mixed and evenly distributed throughout the lower atmosphere. Their concentrations also change slowly with time.

Short-lived species of interest to climate have atmospheric lifetimes in the lower atmosphere that range from a day for nitrogen oxides, from a day to a week for most particles, and from a week to a month for ozone. As a result of their short lifetime their concentrations are highly variable in space and time and concentrated in the lowest part of the atmosphere, primarily near their sources

For those wishing to read further, we provide a brief reader's guide. Chapters 2 and 3 provide detailed technical information about specific models, model runs and trends and are intended primarily for the scientific community, though the key findings and the introduction to each chapter are written in non-technical language and intended for all audiences. Chapter 4 is intended for all audiences. It provides a summary of the major findings and identifies new opportunities for future research.

718 **Chapter 1 References**

719

720 **Brasseur, G. P.**, and E. Roeckner (2005), Impact of improved air quality on the future
721 evolution of climate, *Geophys. Res. Lett.*, *32*, L23704,
722 doi:10.1029/2005GL023902.

723

724 **Delworth, T. L.**, V. Ramaswamy, and G. L. Stenchikov, 2005: The impact of aerosols on
725 simulated ocean temperature and heat content in the 20th century. *Geophysical*
726 *Research Letters*, *32*, L24709, doi:10.1029/2005GL024457.

727

728 **Hansen, J.**, A. Lacis, D. Rind, G. Russell, P. Stone, I. Fung, R. Ruedy, and J. Lerner,
729 1984: Climate sensitivity: Analysis of feedback mechanisms. In *Climate*
730 *Processes and Climate Sensitivity*, AGU Geophysical Monograph 29, Maurice
731 Ewing Vol. 5. J.E. Hansen and T. Takahashi, Eds. American Geophysical Union,
732 pp. 130-163.

733

734 **Hansen, J.**, Mki. Sato, R. Ruedy, A. Lacis, and V. Oinas (2000), Global warming in the
735 twenty-first century: An alternative scenario, *Proc. Natl. Acad. Sci.*, *97*, 9875-
736 9880, doi:10.1073/pnas.170278997.

737

738 **IPCC, 1990:** Climate Change, The IPCC Scientific Assessment, (J. T. Houghton, G. J.
739 Jenkins, and J. J. Ephraums, eds.), Cambridge University Press, 365 pp. (the
740 FAR).

741

742 **IPCC, 1992:** Climate Change 1992: The Supplementary Report to the IPCC Scientific
743 Assessment. (J. T. Houghton, B. A. Callander, and S. K. Varney, eds.),
744 Cambridge University Press, 200 pp.

745

746 **IPCC, 1996:** Climate Change 1995: The Science of Climate Change. (J. T. Houghton *et*
747 *al.*, eds), Cambridge University Press, 572 pp. (the SAR).

748

749 **IPCC, 2001:** Climate Change 2001: The Scientific Basis, J.T. Houghton *et al.*, eds.,
750 Cambridge U. Press, 881 pp. (the TAR).

751

752 **IPCC, 2007:** Climate Change 2007: The Cambridge U. Press, 881 pp. AR4...

753

754 **Manabe, S.**, and R. J. Stouffer, 1979: A CO₂-climate sensitivity study with a
755 mathematical model of the global climate. *Nature*, **282** (5738), 491-493.

756

757 **Manabe, S.**, and R. T. Wetherald, 1967: Thermal equilibrium of the atmosphere with a
758 given distribution of relative humidity. *Journal of the Atmospheric Sciences*, **24**
759 (3), 241-259.

760

761 **Mitchell, J. F. B.**, T. C. Johns, J. M. Gregory, and S. F. B. Tett, 1995: Climate response
762 to increasing levels of greenhouse gases and sulphate aerosols. *Nature*, **376**, 501-
763 504.

764

765 **Nakićenović, N., et al.**, 2000: Emissions scenarios: A special report of Working Group
766 III of the Intergovernmental Panel on Climate Change, 599 pp., Cambridge
767 University Press, New York.

768

769 **Stouffer, R. J., S. Manabe, and K. Bryan**, 1989: Interhemispheric asymmetry in climate
770 response to a gradual increase of atmospheric CO₂. *Nature*, **342**, 660-662.

771

772 **Washington, W. M., and G. A Meehl**, 1989: Climate sensitivity due to increased CO₂:
773 experiments with a coupled atmosphere and ocean general circulation model,
774 *Geophysical Research Letters*, **4** (1), 1-38, doi:10.1007/BF00207397.

775

776 **Chapter 2 Climate Projections From Well-Mixed**
777 **Greenhouse Gas Stabilization Scenarios**

778

779 **Lead Author(s):** Hiram Levy II, GFDL/NOAA; Drew T. Shindell, GISS/NASA; Alice
780 Gilliland, ARL/NOAA

781

782 **Contributing Authors:** Tom Wigley, NCAR; Anne Waple, NCDC/NOAA

783

784 **KEY FINDINGS**

785 This chapter focuses on climate projections for the long-lived greenhouse gas
786 stabilization scenarios for the time period 2000–2100 that were produced under the U.S.
787 Climate Change Science Program by an earlier Synthesis and Assessment Product, 2.1a.
788 Those scenarios²⁷ are called “stabilization scenarios” because they are constrained so that
789 the atmospheric concentrations of the long-lived greenhouse gases level off, or stabilize,
790 at pre-determined levels by the end of the 21st century. Our overall goal in this Chapter is
791 to assess these “stabilization scenarios” and the climates they would project for the 21st
792 century in the context of the most recent Intergovernmental Panel on Climate Change
793 (IPCC) report (4th Assessment Report, Working Group 1). The major conclusions are
794 summarized below as the answers to the first four questions in our Prospectus, and then
795 receive more detailed attention in the remainder of the Chapter:

796

²⁷ Scenarios are representations of the future development of emissions of a substance based on a coherent and internally consistent set of assumptions about the driving forces (such as population, socio-economic development, technological change) and their key relationships.

- 797 • **Do the stabilization¹ emission scenarios produced by Synthesis and**
798 **Assessment Product (SAP) 2.1a differ significantly from those used in the 4th**
799 **Assessment Report of the IPCC?**

800 While different in concept and method of derivation (stabilization vs. "storyline" –
801 see Box in Preface for detail) the long-lived greenhouse gas stabilization scenarios
802 outlined in Synthesis and Assessment Product 2.1 fall among the principle storyline
803 emission scenarios studied in the 4th Assessment Report of the IPCC. While each
804 individual stabilization scenario differs somewhat from the individual IPCC
805 scenarios, they are encompassed by the IPCC envelope of estimated future emissions.

806

- 807 • **If the Synthesis and Assessment Product 2.1a emission scenarios do fall**
808 **within the envelope of emission scenarios previously considered by the IPCC,**
809 **can the existing IPCC climate simulations be used to estimate 50 - 100 year**
810 **climate responses for the CCSP 2.1 carbon dioxide emission scenarios?**

811 Given the close agreement between the ranges of emission scenarios, time evolution
812 of global concentrations and associated radiative forcings²⁸, and global mean
813 temperature responses in the two assessments, we conclude that the key global and
814 regional climate features noted in the IPCC reports can indeed be used to estimate the
815 50 - 100 year climate responses for the CCSP 2.1 scenarios.

816

²⁸ Radiative forcing is a measure of how the energy balance of the Earth-atmosphere system is influenced when factors that affect climate, such as atmospheric composition or surface reflectivity, are altered. When radiative forcing is positive, the energy of the Earth-atmosphere system will ultimately increase, leading to a warming of the system. In contrast, for a negative radiative forcing, the energy will ultimately decrease, leading to a cooling of the system. For technical details see Box 3.2

- 817 • **What would be the changes to the climate system under the scenarios being**
818 **put forward by SAP 2.1a?**

819 The key climate changes resulting from the “stabilization scenarios” should be quite
820 similar to the key findings from Chapters 10 and 11 of the 4th Assessment Report of
821 the IPCC, which are listed in the Box in Section 2.7 and discussed in more detail in
822 Appendix 2.1. The simulations by the simple climate model used in this Chapter, as
823 well as the comprehensive climate model²⁹ simulations in Chapter 10 of the 4th
824 Assessment Report of the IPCC all find increases in global-average surface air
825 temperature throughout the 21st century; with the warming increasing roughly
826 proportional to the increasing concentrations of long-lived greenhouse gases.

827

- 828 • **For the next 50 to 100 years, can the climate projections using the emission**
829 **scenarios from SAP 2.1a be distinguished from one another or from the**
830 **scenarios recently studied by the IPCC?**

831 For the first 30 years there is little difference in the predicted global-average climate
832 among either the principal IPCC scenarios or the SAP 2.1 stabilization scenarios for
833 the long-lived greenhouse gases. For the second half of the 21st century, global mean
834 and certain robust regional properties predicted for the different IPCC scenarios and
835 applicable to the SAP 2.1a scenarios are distinguishable from each other in magnitude
836 (the greater the concentration of long-lived greenhouse gases, the greater the
837 magnitude) though not in their qualitative features.

²⁹ Comprehensive climate model is a numerical representation of the climate based on the physical, chemical, and biological properties of its components, their interactions and feedback processes, which account for many of its known properties. Coupled atmosphere/ocean/sea-ice General Circulation Models (AOGCMs) provide the current state-of-the-art representation of the physical climate system.

838

839 **2.1 Introduction**

840 Chapter 2 is focused on climate projections for the four long-lived greenhouse gas
841 scenarios developed by an earlier report, Synthesis and Assessment Product 2.1a (SAP
842 2.1a). Our work in this chapter involves two different types of models:

843

844 1) Three integrated assessment models³⁰ that were used in Synthesis and Assessment
845 Product 2.1a to produce stabilization scenarios for long-lived greenhouse gases;

846

847 2) A simplified global climate model, Model for the Assessment of Greenhouse-gas
848 Induced Climate Change (MAGICC)³¹ that was used to simulate global levels of carbon
849 dioxide, global-average radiative forcings for a variety of radiatively active³² species,
850 global-average surface temperature increases and global-average sea-level rise (due only
851 to thermal expansion of water, not melting ice caps) for the four stabilization scenarios.

852

853 The second section, 2.2, introduces the stabilization scenarios and the models that were
854 used to generate them in Synthesis and Assessment Product 2.1a. The stabilization levels
855 were defined in terms of the combined radiative forcing for carbon dioxide (CO₂) and the
856 other long-lived greenhouse gases that are potentially controlled under the Kyoto

³⁰ Integrated assessment models are a framework of models, currently quite simplified, from the physical, biological, economic and social sciences that interact among themselves in a consistent manner and can evaluate the status and the consequences of environmental change and the policy responses to it.

³¹ MAGICC is a two component numerical model consisting of a highly simplified representation of a climate model coupled with an equally simplified representation of the atmospheric composition of radiatively active species. This model is adjusted, based on the results of more complex climate models, to make representative predictions of global mean surface temperature and sea-level rise.

³² Radiatively active indicates the ability of a substance to either absorb or emit sunlight or infrared radiation, thus changing the temperature of the atmosphere.

857 Protocol (methane, nitrous oxide, a suite of halocarbons, and sulfur hexafluoride (SF₆)).
858 These levels were chosen to be more or less equivalent to 450, 550, 650, and 750 parts
859 per million (ppm) of carbon dioxide, and attainment was required within 100 – 200 years.
860 For reference, pre-industrial levels of carbon dioxide were approximately 280 ppm, and
861 are currently around 380 ppm of carbon dioxide.

862

863 Each integrated assessment model produced its own reference scenario, which is
864 considered a "business as usual" or no-climate-policy scenario, as well as four
865 stabilization scenarios for long-lived greenhouse gas emissions that required a range of
866 policy choices. The scenarios generated by each integrated assessment model were
867 internally consistent, and each modeling group made independent choices in determining
868 both their reference emissions, and their multi-gas policies required to achieve the
869 specified stabilization levels. "All of the groups developed pathways to stabilization
870 targets designed around economic principles. However, each group used somewhat
871 different approaches to stabilization scenario construction."

872

873 The third section, 2.3, introduces the simplified global climate model, MAGICC, which
874 is used to generate the projections of carbon dioxide concentrations, radiative forcings
875 due to the long-lived greenhouse gases, and global surface temperature increases for the
876 four stabilization scenarios introduced in the previous section 2.2. While the three
877 integrated assessment models used in Synthesis and Assessment Product 2.1a each
878 treated the cycling of carbon dioxide between the land, ocean and atmosphere in their
879 own ways, in this study we use the carbon cycling treatment employed by MAGICC for

880 all of the stabilization emission scenarios. This provides a level playing field for all of
881 the scenarios (see Wigley *et al.*, 2007b for a detailed discussion of this issue). We find
882 that there is little difference between the two approaches.

883

884 MAGICC has four atmosphere boxes, one each over land and sea in each hemisphere,
885 and two ocean boxes, one for each hemisphere. It consists of two highly simplified
886 components: a climate component that has been adjusted to produce a global-average
887 temperature change when the carbon dioxide concentration is doubled that is similar to
888 the complex climate models used in the latest IPCC Report, and a greenhouse gas and
889 particle component that has also been adjusted to reproduce the global-average surface
890 temperature and sea-level rise simulated by the same set of complex climate models for
891 the various storyline emission scenarios analyzed in the 4th Assessment Report of the
892 IPCC. A more detailed description of MAGICC is provided for the technical audience in
893 Appendix 2.2.

894

895 In the fourth section, 2.4, we show that the concentrations of carbon dioxide projected by
896 MAGICC for the twelve stabilization emission scenarios (three models, four stabilization
897 levels each) from Synthesis and Assessment Product 2.1a fall among earlier projections
898 of carbon dioxide concentrations for the three primary storyline scenarios employed in
899 the 4th Assessment Report of the IPCC. We next show that the radiative forcings for the
900 long-lived greenhouse gases potentially regulated by the Kyoto Protocol, again calculated
901 by MAGICC, fall among the radiative forcings time series for the 21st century previously

902 calculated with the same gases for the three principle storyline emission scenarios used in
903 the 4th IPCC report.

904

905 In the fifth section, 2.5, we deal with the contribution of the short-lived pollutants
906 (ozone, elemental and organic carbon particles and sulfate particles) to radiative forcing
907 calculations by MAGICC for the stabilization scenarios. While short-lived pollutants
908 were not explicitly included in determining the stabilization scenarios for the long-lived
909 greenhouse gases, two of the three integrated assessment models did produce emission
910 scenarios for the short-lived pollutants that were consistent with the energy and policy
911 decisions required for stabilization of the long-lived greenhouse gas concentrations. To
912 assign a full radiative forcing to the scenarios calculated by the third model, an
913 intermediate IPCC emission scenario was used for the short-lived pollutants. Again we
914 find that the total radiative forcing (short-lived and long-lived radiatively active species)
915 calculated by MAGICC for the 12 stabilization scenarios fall among the total radiative
916 forcings calculated by MAGICC for the principle storyline emission scenarios employed
917 in the 4th Assessment Report of the IPCC.

918

919 In the sixth section, 2.6, we compare two sets of global-average surface temperature time
920 series: an average of those calculated by a broad collection of complex global climate
921 models for the three principle IPCC scenarios and reported in Chapter 10 of the IPCC's
922 4th Assessment Report, and those calculated by MAGICC for the twelve SAP 2.1a
923 stabilization scenarios and reported here. As we found for the carbon dioxide
924 concentration and radiative forcing time series discussed previously, the global-average

925 surface temperatures calculated for the twelve stabilization scenarios by MAGICC are
926 generally contained within those calculated for the three IPCC scenarios by complex
927 global climate models. The exceptions are for the most extreme stabilization scenario
928 that would require carbon dioxide not to exceed 450 ppm by year 2100 (remember that
929 current levels of carbon dioxide already exceed 380 ppm). The global-average surface
930 temperatures for this extreme stabilization scenario tend to fall below those for the
931 lowest IPCC scenario, particularly in the 2nd half of the 21st century.

932

933 In the seventh and final section, 2.7, we address the primary objective of Chapter 2,
934 “*Climate Projections for SAP 2.1a Emissions Scenarios of Greenhouse Gases.*” While
935 the stabilization scenarios were derived in a fundamentally different manner from the
936 storyline scenarios used in the most recent IPCC report, they are generally contained
937 within the storyline scenarios and show a similar evolution with time. Moreover, the
938 same is true for the resulting radiative forcings and global-average surface temperatures
939 that are calculated with a simple global climate model. Drawing on the conclusion from
940 the latest IPCC report that “Projected warming in the 21st century shows scenario-
941 independent geographical patterns”, we conclude that the robust conclusions arrived at in
942 the latest IPCC report apply equally well to the climate responses expected for the four
943 stabilization scenarios provided by Synthesis and Assessment Product 2.1a.

944

945 **2.2 Well-Mixed Greenhouse Gas Emission Scenarios From SAP 2.1a**

946 The three integrated assessment models used in SAP 2.1a were EPPA (Paltsev *et al.*,
947 2005), MiniCAM (Kim *et al.*, 2006) and MERGE (Richels *et al.*, 2007). These models

948 have different levels of complexity in their modeling of socioeconomic, energy, industry,
949 transport, and land-use systems. With respect to emissions, EPPA and MiniCAM are
950 similarly comprehensive, and produce output for emissions of the following: all the major
951 greenhouse gases (carbon dioxide (CO₂), methane (CH₄), nitrous oxide (N₂O), and a suite
952 of halocarbons and sulfur hexafluoride-SF₆); sulfur dioxide (SO₂); black carbon (BC) and
953 organic carbon (OC) aerosols and their precursors; and the reactive gases carbon
954 monoxide (CO), nitrogen oxides (NO_x) and volatile organic compounds (VOCs), which
955 are important determinants of tropospheric ozone change. MERGE produces emissions
956 output for the major greenhouse gases (carbon dioxide (CO₂), methane (CH₄) and nitrous
957 oxide (N₂O)) and idealized short-lived and long-lived halocarbons (characterized by
958 HFC134a and SF₆), but not for any other short-lived radiative species and their
959 precursors.

960

961 The stabilization levels were defined in terms of the combined radiative forcing for CO₂
962 and for the other gases that are potentially controlled under the Kyoto Protocol (CH₄,
963 N₂O, halocarbons, and SF₆). *“All of the groups developed pathways to stabilization
964 targets designed around economic principles. However, each group used somewhat
965 different approaches to stabilization scenario construction.”* (see, e.g., Reilly *et al.*,
966 1999; Manne and Richels, 2001; Sarofim *et al.*, 2005).

967

968 Consistent time series for the emissions of short-lived radiative species, carbon (both
969 elemental and organic) and the precursors of sulfate aerosols and tropospheric ozone,
970 were produced by the integrated assessment models to varying degrees, but the resulting

971 radiative forcings were not part of the scenario definitions, nor were they considered as
972 contributing to the radiative forcing targets. The stabilization levels for radiative forcing
973 were constructed by determining the CO₂-only forcing associated with concentrations of
974 450, 550, 650 and 750 ppm and then adding additional radiative forcing to account for
975 the other Kyoto gases (0.8, 1.0, 1.2 and 1.4 W/m² respectively). The four stabilization
976 levels are referred to as Level 1, Level 2, Level 3, and Level 4, where Level 1 requires
977 the largest reduction in radiative forcing and is associated with CO₂ stabilization at
978 roughly 450 ppm.

979

980 As SAP 2.1a notes, “The three models display essentially the same relationship between
981 greenhouse gas concentrations and radiative forcing, so the three reference scenarios also
982 all exhibit higher radiative forcing, growing from roughly 2.2 Wm⁻² above preindustrial
983 in 2000 for the Kyoto gases to between 6.4 Wm⁻² and 8.6 Wm⁻² in 2100.” These
984 differences arise primarily from differences in the assumptions underlying the reference
985 scenarios, which lead to different reference emissions across the models.

986

987 The three models incorporate carbon cycles of different complexity, ranging from
988 MERGE’s neutral biosphere assumption to EPPA’s coarse 3-D ocean. MiniCAM uses
989 MAGICC to represent its carbon cycle. However SAP 2.1a notes, “The concentration of
990 gases that reside in the atmosphere for long periods of time – decades to millennia – is
991 more closely related to cumulative emissions than to annual emissions. In particular, this
992 is true for CO₂, the gas responsible for the largest contribution to radiative forcing. This
993 relationship can be seen for CO₂ in Figure 3.21 in SAP 2.1a, where cumulative emissions

994 over the period 2000 to 2100, from the three reference scenarios and the twelve
995 stabilization scenarios, are plotted against the CO₂ concentration in the year 2100. The
996 plots for all three models lie on essentially the same line, indicating that despite
997 considerable differences in representation of the processes that govern CO₂ uptake, the
998 aggregate response to increased emissions is very similar. This basic linear relationship
999 also holds for other long-lived gases, such as N₂O, SF₆, and the halocarbons.”

1000

1001 In this Chapter we start with the emission scenarios generated by the three integrated
1002 assessment models in SAP 2.1a and examine their atmospheric composition, radiative
1003 forcing and global-mean temperature. In the raw SAP 2.1a results, differences arise due
1004 to inter-model differences in the emissions for any given scenario, and differences
1005 between the models in their gas-cycle and climate components. Here we eliminate the
1006 second factor by using a single coupled gas-cycle/climate model to assess the scenarios -
1007 the MAGICC model as used in the IPCC Third Assessment Report (Cubasch and Meehl,
1008 2001; Wigley and Raper, 2001). Many of the results given here have also been produced
1009 by the integrated assessment models, and some are described in SAP 2.1a. Using a single
1010 gas-cycle/climate model provides a level playing field that isolates differences arising
1011 from emissions scenario differences. Moreover, the MAGICC model was used previously
1012 to generate the carbon dioxide concentrations, Kyoto Gas radiative forcing, and Total
1013 radiative forcing associated with the IPCC scenarios B1, A1B, and A2 (described in
1014 Appendix A) that we compare with the current MAGICC calculations for the SAP 2.1a
1015 scenarios (Wigley *et al.*, 2007b).

1016

1017 **2.3 Simplified Global Climate Model (MAGICC)**

1018 MAGICC is a coupled gas-cycle/climate model that was used in the Third Assessment
1019 (Cubasch and Meehl, 2001; Wigley and Raper, 2001).

1020

1021 The climate component is an energy-balance model with a one-dimensional, upwelling-
1022 diffusion ocean. For further details of models of this type, see Hoffert *et al.* (1980) and
1023 Harvey *et al.* (1997). In MAGICC, the globe is divided into land and ocean “boxes” in
1024 both hemispheres in order to account for different thermal inertias and climate
1025 sensitivities over land and ocean, and hemispheric and land/ocean differences in forcing
1026 for short-lived species such as sulfate aerosols and tropospheric ozone.

1027

1028 The climate model is coupled interactively with a series of gas-cycle models for CO₂,
1029 CH₄, N₂O, a suite of halocarbons, and SF₆. The carbon cycle model includes both CO₂
1030 fertilization and temperature feedbacks, with model parameters tuned to give results
1031 consistent with the other carbon cycle models used in the Third Assessment Report
1032 (Kheshgi and Jain, 2003) and the Bern model (Joos *et al.*, 2001). For sulfate aerosols,
1033 both direct and indirect forcings are included using forcing/emissions relationships
1034 developed in Wigley (1989, 1991), with central estimates for 1990 forcing values.

1035

1036 The standard inputs to MAGICC are emissions of the various radiatively important gases
1037 and various climate model parameters. These parameters were tuned so that MAGICC
1038 was able to emulate results from a range of complex global climate models called
1039 Atmosphere Ocean General Circulation Models (AOGCMs) in the Third Assessment

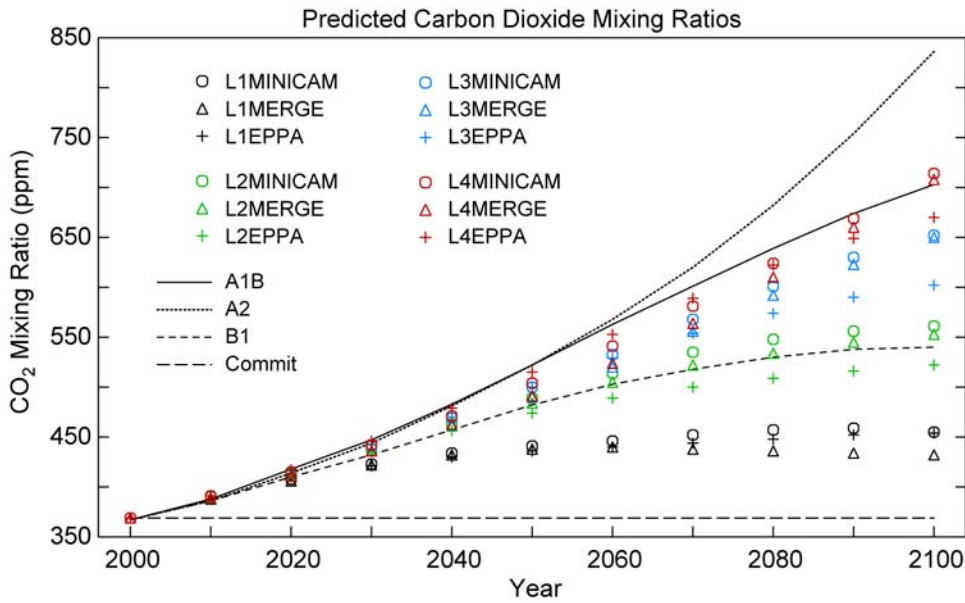
1040 Report (see Cubasch and Meehl, 2001). We use a value of 2.6C equilibrium global-mean
1041 warming for a CO₂ doubling, the median of values for the above set of AOGCMs. (see
1042 Appendix 2.2 for additional details).

1043

1044 **2.4 Long-Lived Greenhouse Gas Concentrations and Radiative Forcings**

1045 In Figure 2.1 we compare the concentrations of the primary greenhouse gas, CO₂,
1046 calculated by MAGICC for the 12 SAP 2.1a stabilization scenarios with earlier
1047 calculations of CO₂ concentrations for B1, A1B and A2, the principle storyline scenarios
1048 reported in Appendix II of the IPCC's Third Assessment Report (IPCC, 2001). For the
1049 first 20 years there is little difference among the 12 SAP 2.1a scenarios due to the long
1050 CO₂ lifetime, although the extreme Level 1 scenario starts to separate noticeably by 2030.
1051 By year 2100, CO₂ concentrations for the MiniCAM and EPPA Level 1 scenarios have
1052 converged on values close to 450 ppm. For MERGE, the 2100 value is lower. CO₂
1053 concentrations for Levels 2-4 start to spread in the second half of the 21st century but
1054 remain approximately bound between B1 and A1B all the way to 2100. EPPA now has
1055 the lowest CO₂ for Levels 2-4. The CO₂ levels for the extreme Level 1 scenario, which
1056 requires immediate reductions in CO₂ emissions followed by ever increasing reductions
1057 (see SAP 2.1a for details), remain substantially below those for B1.

1058



1059

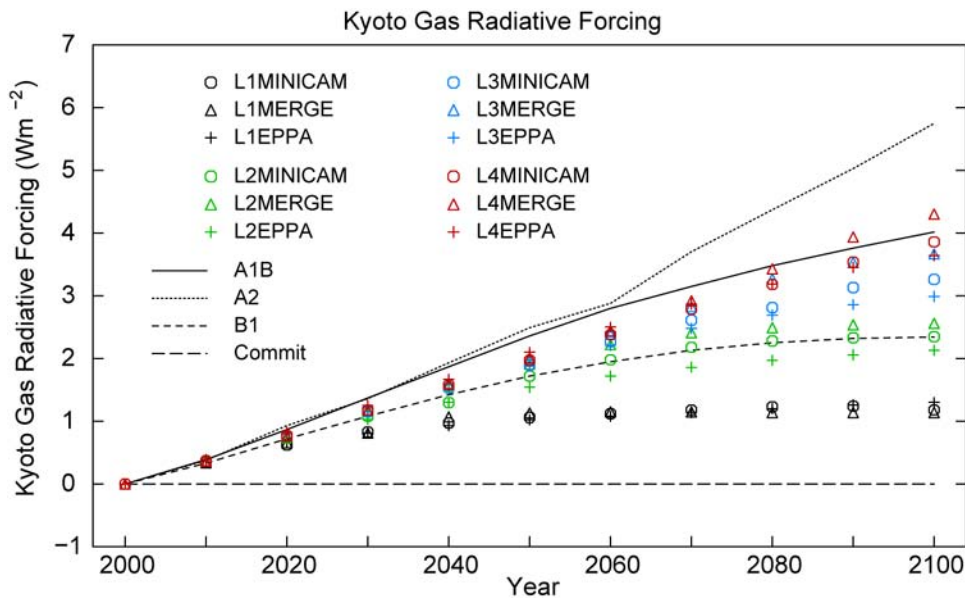
1060 **Figure 2.1** CO₂ concentrations (ppm) calculated by MAGICC for the 12 SAP 2.1a stabilization scenarios
 1061 plotted with calculations of CO₂ concentrations for the principle scenarios (B1, A1B and A2) reported in
 1062 Appendix II of the TAR (IPCC, 2001).
 1063

1064 We next consider Figure 2.2, where the radiative forcing due to increasing Kyoto
 1065 greenhouse gases in the 12 SAP 2.1a stabilization scenarios, again calculated by
 1066 MAGICC, are plotted with the Kyoto gas radiative forcing values taken from Appendix II
 1067 in the Third Assessment (IPCC, 2001) for the B1, A1B, and A2 storyline scenarios. The
 1068 evolution of the 12 radiative forcing time series over the 21st century is very similar to
 1069 that of CO₂, in Figure 2.1, which should not be surprising. However, there are some
 1070 differences. The EPPA values undershoot the stabilization target for Levels 2-4 because
 1071 they are on a trajectory where radiative forcing stabilizes some time after 2100, although
 1072 emissions were calculated only to 2100 (SAP 2.1a, 2007). For the Level 2, 3 and 4
 1073 stabilization cases, it is not possible to stabilize as early as 2100 (c.f. Wigley *et al.*, 1996).
 1074 As we saw for carbon dioxide, the Kyoto gas radiative forcing time series for
 1075 stabilization levels 2-4 are contained within the radiative forcings calculated for the IPCC
 1076 scenarios, A1B and B1.

1077

1078 It should be noted that in general the three integrated assessment models hit their
 1079 radiative forcing targets when they employed their own carbon cycle and atmosphere
 1080 models in SAP 2.1a. Thus, failure to hit these same radiative forcing targets when all
 1081 three long-lived gases are run in MAGICC would seem to reflect the underlying
 1082 uncertainty in the three integrated assessment models' carbon cycles, which is known to
 1083 be substantial.

1084



1085

1086 **Figure 2.2** Kyoto Gas Radiative Forcing (W/m²) for the SAP 2.1a scenarios, calculated by MAGICC,
 1087 plotted with the Kyoto Gas Radiative Forcing values taken from Appendix II in the TAR (IPCC, 2001) for
 1088 the B1, A1B, and A2 SRES scenarios.

1089

1090 **2.5 Short-Lived Species and Total Radiative Forcing**

1091 While EPPA and MiniCAM produce emissions of sulfur dioxide (SO₂), elemental or
 1092 black carbon and organic carbon aerosols³³ and their precursors, and the key precursors

³³ Very small airborne solid or liquid particles, that reside in the atmosphere for at least several hours with the smallest remaining airborne for days.

1093 of tropospheric ozone [CO), NO_x and VOCs] as part of their climate projections,
1094 MERGE does not. To complete the MERGE scenarios, all four of its stabilization Levels
1095 use the IPCC's B2 scenario of emissions for sulfur dioxide (Nakićenović and Swart,
1096 2000) and assume that ozone precursor emissions remain constant. For all of the models,
1097 rather than use emissions for the elemental and organic aerosols, it is assumed that the
1098 elemental and organic aerosol radiative forcings track the sulfur dioxide emissions in
1099 each integrated assessment model's 4 stabilization scenarios. Therefore, while carbon
1100 dioxide emissions tend to track the IPCC scenarios, the emissions of short-lived species
1101 may be different, with the exception of sulfur dioxide emissions in MERGE.

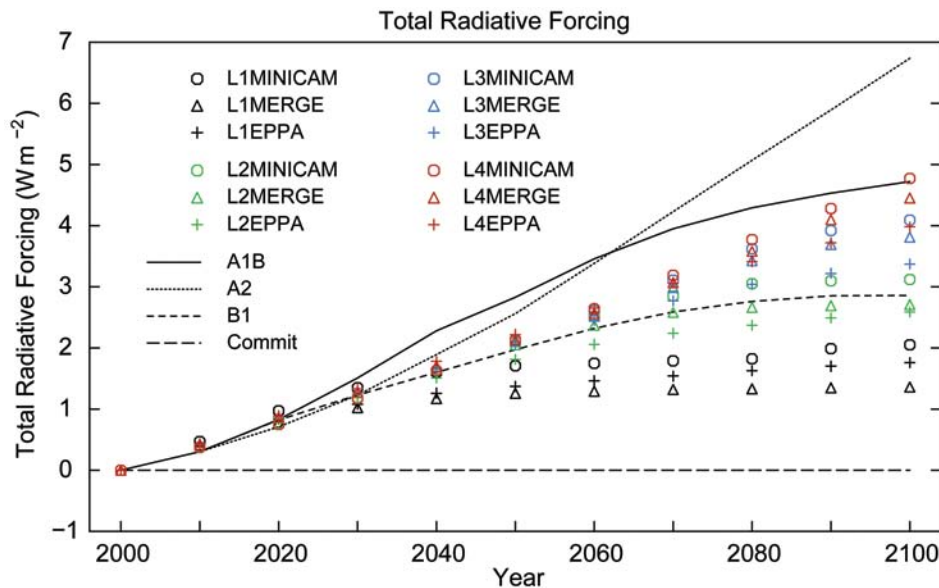
1102

1103 In Figure 2.3 we compare the Total radiative forcing calculated by MAGICC for the 12
1104 SAP 2.1a scenarios, *i.e.*, the sum of Kyoto-gas forcings (Fig. 2.2) plus forcings due to
1105 aerosols, tropospheric ozone, halocarbons controlled under the Montreal Protocol, and
1106 stratospheric ozone (Wigley *et al.*, 2007b and supplementary material referenced therein)
1107 with the Total radiative forcing calculated by MAGICC for the B1, A1B, and A2
1108 scenarios used in the latest IPCC report. Again, just as for CO₂ and Kyoto-gas radiative
1109 forcing, the 12 Total radiative forcing time series do not begin to separate noticeably
1110 before 2030.

1111

1112 Because of the assumptions made about the short-lived species, the MERGE Kyoto-gas
1113 and Total forcings differ least. MiniCAM shows the largest differences with Total
1114 forcings now significantly exceeding the stabilization targets for all 4 Levels, primarily
1115 due to sharp decreases in sulfur dioxide emissions, which produce significant increases in

1116 Total radiative forcing by 2100 ($\sim 1 \text{ Wm}^{-2}$). In the EPPA stabilization scenarios the
 1117 changes in sulfur dioxide emissions are small, and most of the non-Kyoto forcing comes
 1118 from increased nitrogen oxide emissions that drive increases in tropospheric ozone and its
 1119 positive radiative forcing (Wigley *et al.*, 2007b). Remember that in SAP 2.1, the
 1120 stabilization targets were met using only the long-lived greenhouse gases.
 1121



1122
 1123 **Figure 2.3** Total Radiative Forcing (W/m^2) calculated by MAGICC for the 12 SAP 2.1a scenarios plotted
 1124 with the Total calculated by MAGICC for the B1, A1B, and A2 scenarios (IPCC, 2001).
 1125
 1126 The spread of stabilization forcings is significantly less for the Kyoto-gas forcings (which
 1127 were used to define the stabilization targets) than for total forcing. Again the Level 1
 1128 Total radiative forcings are generally below those of the B1 scenario, while the other
 1129 Levels are bounded by B1 and A1B. However, in this case the Level 2-4 scenarios appear
 1130 to track the B1 Total radiative forcing out to 2060 - 2070 before the Level 3 and 4
 1131 scenarios start moving up to A1B. The differences between the radiative forcing time
 1132 evolution for the Kyoto gases in Figure 2.2 and for all radiative species in Figure 2.3 are

1133 the result of differences among treatments of short-lived species. The changes in global
1134 average surface temperatures that are driven by the Total radiative forcing in Figure 2.3
1135 are examined in the next section. We will continue to explore the potential impact of
1136 short-lived species on future global warming in considerable detail in Chapter 3.

1137

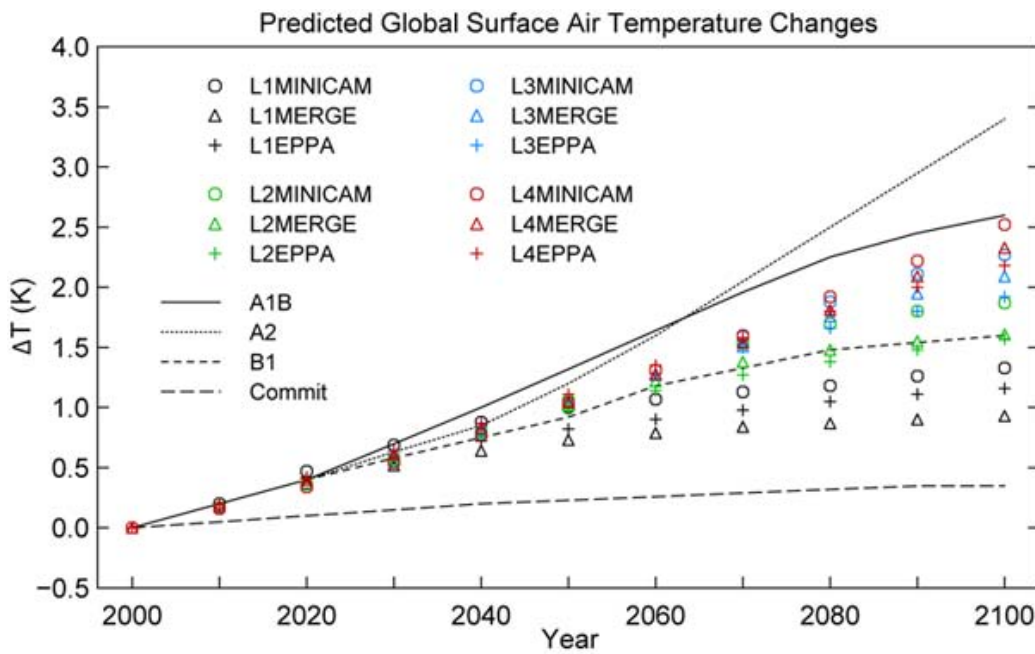
1138 **2.6 Surface Temperature: MAGICC AND IPCC Comparisons**

1139 Figure 2.4 compares multi-model global-mean surface temperature changes reported in
1140 Chapter 10 of the IPCC's 4th Assessment Report for the standard storyline scenarios, B1,
1141 A1B and A2, with global-mean surface temperature changes calculated by MAGICC for
1142 the twelve SAP 2.1a stabilization scenarios. As we might expect, the general behavior is
1143 quite similar to that observed for Total radiative forcing. All scenarios are close through
1144 2020. Levels 2-4 stay in close agreement out to around 2050. The Level 1 scenarios are
1145 lower than B1, except for MiniCAM, where there is enhanced warming out to 2050 due
1146 to the rapid reduction in SO₂ emissions (c.f., Wigley, 1991). The other three Levels
1147 follow B1 closely out to 2050 and then remain between B1 and A1B out to 2100.

1148

1149 For Level 1 and Level 2 temperatures, the rate of increase has begun to slow appreciably
1150 by 2100, which suggests that global-mean temperature could be stabilized if the
1151 emissions scenarios produced by the three integrated assessment models for these two
1152 most extreme stabilization cases (corresponding to 450 and 550 ppm CO₂ but also
1153 including the assumed or modeled levels of short-lived species) were followed. This in
1154 turn depends on the economic and technological feasibility of the Level 1 and 2 scenarios
1155 for both the long-lived greenhouse gases and the short-lived species. However, the

1156 temperatures for the less extreme Level 3 and 4 stabilization scenarios (corresponding to
 1157 650 and 750 ppm CO₂) are still growing, particularly Level 4 MiniCAM. It should also
 1158 be noted that their upper bound, the A1B model-mean surface temperature, is also still
 1159 growing at 2100. The global mean surface temperature projections for the twelve SAP
 1160 2.1a stabilization scenarios are well bounded by the complex climate model simulations
 1161 for the A1B scenario reported in Chapter 10 of the latest IPCC assessment.
 1162



1163

1164 **Figure 2.4** Multi-AOGCM global-mean surface temperature (deg C) changes reported in Chapter 10 of
 1165 AR4 (IPCC, 2007a) for the standard scenarios B1, A1B, and A2 plotted with global-mean surface
 1166 temperature changes calculated by MAGICC for the twelve SAP 2.1a stabilization scenarios.

1167 **Table 2.1 Year 2100 values from Figures 2.1, 2.2, 2.3 and 2.4.**

Scenario	CO2 (ppm)	Kyoto gases (W/m ²)	Total (W/m ²)	Temperature (deg C)
A2	836	5.75	6.74	3.40
A1B	703	4.02	4.72	2.60
B1	540	2.34	2.86	1.60
L1 MiniCAM	454	1.17	2.04	1.32
L1 Merge	432	1.14	1.36	0.93
L1 EPPA	453	1.28	1.75	1.16
L2 MiniCAM	559	2.33	3.10	1.83
L2 Merge	553	2.56	2.71	1.61
L2 EPPA	551	2.12	2.58	1.56
L3 MiniCAM	651	3.23	4.09	2.27
L3 Merge	650	3.67	3.81	2.09
L3 EPPA	601	2.98	3.36	1.92
L4 MiniCAM	712	3.83	4.73	2.50
L4 Merge	708	4.30	4.45	2.33
L4 EPPA	668	3.63	3.97	2.18

1168

1169 **2.7 Climate Projections for SAP 2.1a Scenarios**

1170 The 2.1a stabilization emission scenarios are derived in a fundamentally different manner
1171 from the development of the storyline emission scenarios used in 4th Assessment Report
1172 of the IPCC (IPCC, 2007a). However, we show in Section 2.4 that the twelve (three
1173 integrated assessment models, four stabilization scenarios each) stabilization scenarios
1174 reported in SAP 2.1a are contained within the principal emission scenarios used in the
1175 latest IPCC assessment and show a similar evolution with time. We also show that the
1176 Kyoto gases and Total radiative forcings for those 12 emission scenarios are generally
1177 constrained within the three principle scenarios used to make the climate projections
1178 discussed in Chapter 10 of the report (IPCC, 2007a).

1179

1180 In Section 2.6, we show that the global surface temperatures predicted for the 2.1a
1181 scenarios over the 21st century by a simple coupled gas-cycle/climate model, MAGICC,
1182 fall within the range of the multi-model mean temperatures calculated with state-of-the-
1183 art complex climate models for the three principle IPCC scenarios and reported in
1184 Chapter 10 (IPCC, 2007a). In fact, the global average surface temperatures for Levels 2-4
1185 scenarios all track the values reported by the IPCC for B1 out to 2050. The primary
1186 exceptions are all of the L1 scenarios beyond year 2050 which are significantly below
1187 B1. We also draw on the conclusion in the Summary for Policy Makers in the latest
1188 report (IPCC, 2007a): “Projected warming in the 21st century shows scenario-
1189 independent geographical patterns similar to those observed over the past 50 years.”
1190 Figure 10.8 in Chapter 10 of the 4th Assessment Report also clearly shows that the
1191 geographical pattern of the robust climate features are preserved across scenarios, while
1192 the magnitude of the warming increases with the magnitude of the radiative forcing and
1193 with increases in the concentration of the long-lived greenhouse gases.

1194

1195 We conclude that the robust conclusions arrived at in Chapter 10 of the 4th Assessment
1196 Report (IPCC, 2007a) regarding the predicted climate response to the three scenarios
1197 studied in most detail in that Report, B1, A1, and A1B, apply equally well to the climate
1198 responses expected for the four long-lived greenhouse gas stabilization scenarios (three
1199 realizations of each) provided by SAP 2.1a. These robust conclusions are highlighted in
1200 Box 2.1 below and summarized in Appendix 2.1.

1201

1202 At this time, we also introduce in Box 2.2 our general approach to treating uncertainty in
1203 this document. Since much of this report deals with ranges of projections of radiative
1204 forcing and surface temperature rather than explicit predictions, we do not generally
1205 assign uncertainty values. We do quote the IPCC explicit uncertainty values in Box 2.1.
1206 Later in Chapter 3 we will present a more technical Box 3.3 that addresses the
1207 determination of statistical significance and our use of it.

Box 2.1: Robust conclusions for global climate from Chapter 10 of the 4th Assessment Report (IPCC, 2007a):

- Surface Air Temperatures show their greatest increases over land (roughly twice the global average temperature increase), over wintertime high northern latitudes, and over the summertime US and southern Europe and show less warming over the southern oceans and North Atlantic. These patterns are similar across the B1, A1B, and A2 scenarios with increasing magnitude with increasing radiative forcing.
- It is **very likely** that heat waves will be more intense, more frequent and longer lasting in a future warmer climate.
- By 2100, global-mean sea level is projected across the 3 SRES scenarios to rise by 0.28m to 37m for the three multi-model averages with an overall 5-95% range of 0.19 to 0.50 m. Thermal expansion contributes 60-70% of the central estimate for all scenarios. There is, however, a large uncertainty in the contribution from ice sheet melt, which is poorly represented in current models.
- Globally averaged mean atmospheric water vapor content, evaporation rate and precipitation rate are projected to increase. While, in general, wet areas get wetter and dry areas get dryer, the geographical patterns of precipitation change during the 21st Century are not as consistent across the complex climate model simulations and across scenarios as they are for surface temperature.
- Multi-model projections based on SRES scenarios give reductions in ocean pH of between 0.14 and 0.35 units over the 21st century, adding to the present decrease of 0.1 units from pre-industrial times.
- There is **no** consistent change in El Niño-Southern Oscillation (ENSO) for those complex climate models that are able to reproduce ENSO-like processes.
- Those models with a realistic Atlantic Meridional Overturning Circulation (MOC) predict that it is **very likely** that the MOC will slow by 2100, but will **not** shut down.
- The AR4 Summary for Policymakers finds it “**Likely** that intense hurricanes and typhoons will increase through the 21st century”.

There are also important robust conclusions for North America from Chapter 11 of the 4th Assessment Report (IPCC, 2007b):

- “All of North America is **very likely** to warm during this century, and the annual mean warming is **likely** to exceed the global-mean warming in most areas.”
- “Annual-mean precipitation is **very likely** to increase in Canada and northeast USA, and **likely** to decrease in the southwest USA.”
- “Snow season length and snow depth are **very likely** to decrease in most of North America, except in the northernmost part of Canada where maximum snow depth is **likely** to increase.”

NOTE: The terms **very likely** and **likely** have specific statistical meanings defined by the IPCC.

Very likely	greater than 90% chance of occurring
Likely	greater than 67% chance of occurring

1209

Box 2.2: Uncertainty

In doing any assessment, it is helpful to precisely convey the degree of certainty of various findings and projections. There are numerous choices for categories of likelihood and appropriate wording to define these categories. In chapter 2 of this report, since many of the findings of this report are comparable to those discussed in the fourth assessment report of the IPCC, we have chosen to be consistent with the IPCC lexicon of uncertainty:

<i>Virtually certain</i>	> 99% probability of occurrence
<i>Extremely likely</i>	>95%
<i>Very likely</i>	> 90%
<i>Likely</i>	> 66%
<i>More likely than not</i>	> 50%
<i>Unlikely</i>	< 33%
<i>Very unlikely</i>	< 10%
<i>Extremely unlikely</i>	< 5%

Elsewhere in the report, we are projecting climate, based on model simulations that use, as a foundation, scenarios of short-lived gases and particulates, which are themselves, plausible, but highly uncertain. For this reason, we have largely avoided assigning uncertainty values. However, where they do occur, we have condensed the IPCC ranges of uncertainty to fewer categories because we are unable to be as precise as in the IPCC assessments, which consider primarily the long-lived greenhouse gases. This lexicon is also consistent with other CCSP reports, such as SAP 3.3, and SAP 4.1:



Figure P.1 Language in this Synthesis and Assessment Product (chapters 3 and 4) used to express the team’s expert judgment of likelihood, when such a judgment is appropriate.

1210 **Chapter 2 References**

- 1211 **Church, J. A., and J. M. Gregory, 2001: Changes in sea level. Climate Change 2001: The**
1212 **Scientific Basis, (J. T. Houghton, *et al.*, eds.), Cambridge University Press,**
1213 **Cambridge, U.K., 639–693.**
1214
- 1215 **Cubasch, U., and G. A. Meehl, 2001: Projections for future climate change. Climate**
1216 **Change 2001: The Scientific Basis, (J. T. Houghton, *et al.*, eds.), Cambridge**
1217 **University Press, Cambridge, U.K., 525–582.**
1218
- 1219 **Dai, A., G. A. Meehl, W. M. Washington, T. M. L. Wigley, and J. M. Arblaster, 2001a:**
1220 **Ensemble simulation of twenty-first century climate changes: Business As Usual**
1221 **vs. CO₂ stabilization. *Bulletin of the American Meteorological Society*, **82**, 2377–**
1222 **2388.**
1223
- 1224 **Dai, A., T. M. L. Wigley, G. A. Meehl, and W. M. Washington, 2001b: Effects of**
1225 **stabilizing atmospheric CO₂ on global climate in the next two centuries.**
1226 ***Geophysical Research Letters*, **82**, 4511–4514.**
1227
- 1228 **Efthimios, T., K. Manomaiphiboon, K.-J. Liao, L. R. Leung, J.-H. Woo, S. He, P. Amar,**
1229 **and A. G. Russell, 2007: Impacts of global climate change and emissions on**
1230 **regional ozone and fine particulate matter concentrations over North America, in**
1231 **press.**
1232
- 1233 **Gustafson, W. I., and L. R. Leung, 2007: Regional downscaling for air quality**
1234 **assessment: A reasonable proposition? *Bulletin of the American Meteorological***
1235 ***Society*, in press.**
1236
- 1237 **Harvey, L. D. D., J. Gregory, M. Hoffert, A. Jain, M. Lal, R. Leemans, S. B. C. Raper, T.**
1238 **M. L. Wigley, and J. de Wolde, 1997: An introduction to simple climate models**
1239 **used in the IPCC Second Assessment Report: IPCC Technical Paper 2 (J. T.**
1240 **Houghton, L. G. Meira Filho, D. J. Griggs, and M. Noguer, eds.),**
1241 **Intergovernmental Panel on Climate Change, Geneva, Switzerland, 50 pp.**
1242
- 1243 **Hoffert, M. L., A. J. Callegari, and C.-T. Hsieh, 1980: The role of deep sea heat storage**
1244 **in the secular response to climate forcing. *Journal of Geophysical Research*, **86**,**
1245 **6667– 6679.**
1246
- 1247 **Hogrefe C., B. Lynn, K. Civerolo, J.-Y. Ku, J. Rosenthal, C. Rosenzweig, R. Goldberg,**
1248 **S. Gaffin, K. Knowlton, and P. L. Kinney, 2004: Simulating changes in regional**
1249 **air pollution over the eastern United States due to changes in global and regional**
1250 **climate and emissions. *Journal of Geophysical Research-Atmospheres*, **109****
1251 **(D22), D22301, doi:10.1029/2004JD004690.**
1252
- 1253 **IPCC, 1990: *Climate Change, The IPCC Scientific Assessment* (J. T. Houghton, G. J.**
1254 **Jenkins, and J. J. Ephraums, (eds.)). Cambridge University Press, 365 pp.**

- 1255
1256 **IPCC**, 1992: *Climate Change 1992: The Supplementary Report to the IPCC Scientific*
1257 *Assessment* (J. T. Houghton, B. A. Callander, and S. K. Varney, (eds.)).
1258 Cambridge University Press, 200 pp.
1259
1260 **IPCC**, 1995: *Climate Change 1994: Radiative Forcing of Climate Change and An*
1261 *Evaluation of the IPCC IS92 Emission Scenarios* (J. T. Houghton *et al.*, eds.),
1262 Cambridge University Press, 339 pp.
1263
1264 **IPCC**, 1996: *Climate Change 1995: The Science of Climate Change* (J. T. Houghton, *et*
1265 *al.*, (eds.)), Cambridge University Press, 572 pp. (the SAR).
1266
1267 **IPCC**, 1999: *Special Report on Aviation and the Global Atmosphere* (J. E. Penner *et al.*,
1268 (eds.)). Cambridge University Press, Cambridge, UK, 373 pp.
1269
1270 **IPCC**, 2001a: *Climate Change 2001: The Scientific Basis* (J.T. Houghton *et al.*, (eds.)).
1271 Cambridge University Press, 881 pp.
1272
1273 **IPCC**, 2001b: *Climate Change 2001: Synthesis Report, A contribution of Working*
1274 *Groups I, II, and III to the Third Assessment Report of the Intergovernmental*
1275 *Panel on Climate Change* (R. T. Watson *et al.*, (eds.)). Cambridge University
1276 Press, New York, 398 pp.
1277
1278 **IPCC, 2007a**:... Chapter 10
1279
1280 **IPCC, 2007b**:... Chapter 11
1281
1282 **Joos, F.**, I. C. Prentice, S. Sitch, R. Meyer, G. Hooss, G.-K. Plattner, S. Gerber, and K.
1283 Hasselmann, 2001: Global warming feedbacks on terrestrial carbon uptake under
1284 the Intergovernmental Panel on Climate Change (IPCC) emissions scenarios.
1285 *Global Biogeochemical Cycles*, **15**, 891–908, doi:10.1029/2000GB001375.
1286
1287 **Kheshgi, H. S.**, and A. K. Jain, 2003: Projecting future climate change: implications of
1288 carbon cycle model intercomparisons. *Global Biogeochemical Cycles*, **17**, 1047,
1289 doi:10.1029/2001GB001842.
1290
1291 **Kim, S.H.**, Edmonds, J.A., Lurz, J., Smith, S.J. and Wise, M.A., 2006: The ObjECTS
1292 framework for integrated assessment: Hybrid modeling of transportation. *The*
1293 *Energy Journal, Special Issue No. 2 (2006)*, 51–80.
1294
1295 **Leung, L. R.**, and W. I. Gustafson, 2005: Potential regional climate change and
1296 implications to US air quality. *Geophysical Research Letters*, **32**, L16711,
1297 doi:10.1029/2005GL022911.
1298
1299 **Liang, X.Z. et al.**, 2006: Regional climate model downscaling of the U.S. summer
1300 climate and future change. *Journal Geophysical Research*, in press.

- 1301
1302 **Liang**, X. Z., L. Li, K. E. Kunkel, M. Ting, and J. X. L. Wang, 2004: Regional climate
1303 model simulation of U.S. precipitation during 1982–2002. Part I: Annual cycle.
1304 *Journal of Climate*, **17**(18), 3510–3529.
- 1305
1306 **Manne**, A. S., and R. G. Richels, 2001: An alternative approach to establishing trade-offs
1307 among greenhouse gases. *Nature*, **410**, 675–677.
- 1308
1309 **Mickley** L. J., D. J. Jacob, B. D. Field, D. H. Rind (2004), Climate response to the
1310 increase in tropospheric ozone since preindustrial times: A comparison between
1311 ozone and equivalent CO₂ forcings. *Journal Geophysical Research*, **109**,
1312 D05106, doi:10.1029/2003JD003653.
- 1313
1314 **Nolte**, C., A. B. Gilliland, and C. Hogrefe: Linking global to regional models to
1315 investigate future climate impacts on U.S. regional air quality 1. Surface ozone
1316 concentrations, submitted.
- 1317
1318 **Paltsev**, S., Reilly, J. M., Jacoby, H. D., Eckaus, R. S., McFarland, J., Sarofim, M.C.,
1319 Asadoorian, M. and Babiker, M., 2005: The MIT Emissions Prediction and Policy
1320 Analysis (EPPA) Model: Version 4.
- 1321
1322 **Prather**, M. and Ehhalt, D., 2001: Atmospheric chemistry and greenhouse gases. Climate
1323 Change 2001: The Scientific Basis, (J. T. Houghton, *et al.*, eds.), Cambridge
1324 University Press, Cambridge, U.K., 239–287.
- 1325
1326 **Reilly**, J.M., Prinn, R., Harnisch, J., Fitzmaurice, J., Jacoby, H., Kicklighter, D., Melillo,
1327 J., Stone, P., Sokolov, I. and Wang, C., 1999: Multi-gas assessment of the Kyoto
1328 Protocol. *Nature*, **401**, 549–555.
- 1329
1330 **Richels**, R., Manne, A.S. and Wigley, T.M.L., 2007: Moving beyond concentrations: The
1331 challenge of limiting temperature change. (In) *Human Induced Climate Change:
1332 An Interdisciplinary Assessment* (eds. Michael Schlesinger, Francisco C. de la
1333 Chesnaye, Haroon Kheshgi, Charles D. Kolstad, John Reilly, Joel B. Smith and
1334 Tom Wilson), Cambridge University Press (in press).
- 1335
1336 **Sarofim**, M. C., C. E. Forest, D. M. Reiner, and J. M. Reilly, 2005: Stabilization and
1337 global climate policy. *Global and Planetary Change*, **47** (2-4), 266–272.
- 1338
1339 **Wigley**, T. M. L., 1989: Possible climatic change due to SO₂-derived cloud condensation
1340 nuclei. *Nature* **339**, 365–367.
- 1341
1342 **Wigley**, T. M. L., 1991: Could reducing fossil-fuel emissions cause global warming?
1343 *Nature* **349**, 503–506.
- 1344
1345 **Wigley**, T. M. L., 1991: A simple inverse carbon cycle model. *Global Biogeochemical
1346 Cycles*, **5**, 373–382.

1347

1348 **Wigley, T. M. L., 1993: Balancing the carbon budget. Implications for projections of**
1349 **future carbon dioxide concentration changes. *Tellus*, **45B**, 409–425.**

1350

1351 **Wigley, T. M. L., 2000: Stabilization of CO₂ concentration levels. In *The Carbon Cycle*,**
1352 **(T.M.L. Wigley and D.S. Schimel, eds.). Cambridge University Press,**
1353 **Cambridge, U.K., 258–276.**

1354

1355 **Wigley, T. M. L., and S. C. B., Raper, 2001: Interpretation of high projections for global-**
1356 **mean warming. *Science*, **293**, 451–454.**

1357

1358 **Wigley, T. M. L., S. J. Smith, and M. J. Prather, 2002: Radiative forcing due to reactive**
1359 **gas emissions. *Journal of Climate*, **15**, 2690–2696.**

1360

1361 **Wigley, T. M. L., and S. C. B. Raper, 2005: Extended scenarios for glacier melt due to**
1362 **anthropogenic forcing. *Geophysical Research Letters*, **32**, L05704,**
1363 **doi:10.1029/2004GL021238.**

1364

1365 **Wigley, T. M. L., R. Richels, and J. A. Edmonds, 2007a: Overshoot pathways to CO₂**
1366 **stabilization in a multi-gas context. In *Human Induced Climate Change: An***
1367 ***Interdisciplinary Assessment* (Michael Schlesinger, Francisco C. de la Chesnaye,**
1368 **Haroon Kheshgi, Charles D. Kolstad, John Reilly, Joel B. Smith and Tom Wilson,**
1369 **eds.), Cambridge University Press, in press.**

1370

1371 **Wigley, T. M. L. *et al.*, 2007b: Uncertainties in climate stabilization (submitted)**

1372 **Appendix 2.1 IPCC 4th Assessment Climate Projections**

1373

1374 These robust conclusions, which we believe also apply to the climate projections from the
1375 SAP 2.1a scenarios, are taken primarily from the Executive Summary of Chapter 10 of
1376 the IPCC's 4th Assessment Report (IPCC, 2007a) as well as some details extracted from
1377 the body of Chapter 10, and are summarized below.

1378

1379 **A.2.1.1 Mean Temperature**

1380 All AOGCMs In Chapter 10 of the AR4 (IPCC, 2007a) project increases in global mean
1381 surface air temperature (SAT) throughout the 21st century, with the warming
1382 proportional to the associated radiative forcing. There is close agreement among globally
1383 averaged SAT multi-model mean warming for the early 21st century for the three SRES
1384 (B1, A1B and A2) scenarios as well as for SAP 2.1a Level 2-4 scenarios out to 2050. The
1385 warming rate over the next few decades in Chapter 10 (IPCC, 2007a) is affected little by
1386 different scenario assumptions or different model sensitivities, and is similar to that
1387 observed for the past few decades. By mid-century (2046 – 2065), the choice of SRES
1388 scenario becomes more important and they start to separate, though the range among the
1389 collection of AOGCMs is comparable. By the end of the 21st century, the SATs generated
1390 by MAGICC using the 12 SAP 2.1 scenarios as well as the full spread of all of the
1391 AOGCMs for the A2, B1 and Committed projections have completely separated, though
1392 A1B still has some overlap with A2 and B1.

1393

1394 In general, geographical patterns of projected SAT warming show greatest temperature
1395 increases over land (roughly twice the global average temperature increase) and at high
1396 northern latitudes, and show less warming over the southern oceans and North Atlantic,
1397 consistent with observations during the latter part of the 20th century. These patterns are
1398 similar across the B1, A1B, and A2 scenarios (see Figure 10.8 in Chapter 10 of the AR4;
1399 IPCC, 2007a) only increasing in magnitude with increasing radiative forcing. Results for
1400 the stabilization scenarios similar to those studied here should show the same pattern
1401 similarities at least out to 2100 (see, *e.g.*, Dai *et al.* 2001a, b). It should be noted that, in
1402 none of the cases considered here, has the climate stabilized by 2100 – for the higher
1403 stabilization levels this may take centuries. Temperature change patterns may differ as
1404 one approaches closer to a stable climate.

1405

1406 **A.2.1.2 Temperature Extremes**

1407 It is very likely that heat waves will be more intense, more frequent and longer lasting in
1408 a future warmer climate. Cold episodes are projected to decrease significantly in a future
1409 warmer climate. Almost everywhere, daily minimum temperatures are projected to
1410 increase faster than daily maximum temperatures, leading to a decrease in diurnal
1411 temperature range. Decreases in frost days are projected to occur almost everywhere in
1412 the mid and high latitudes, with a comparable increase in growing season length (IPCC,
1413 2007a).

1414

1415

1416

1417 A.2.1.3 Mean Precipitation

1418 Globally averaged mean atmospheric water vapor, evaporation and precipitation are
1419 projected to increase. By 2100, precipitation generally increases in the areas of regional
1420 tropical precipitation maxima (such as the monsoon regimes) and over the tropical Pacific
1421 in particular, with general decreases in the subtropics, and increases at high latitudes as a
1422 consequence of a general intensification of the global hydrological cycle. The
1423 geographical patterns of precipitation change during the 21st century are not as consistent
1424 across AOGCMs and across scenarios as they are for surface temperature (IPCC, 2007a).

1425

1426 A.2.1.4 Precipitation Extremes and Droughts

1427 Intensity of precipitation events is projected to increase, particularly in tropical and high
1428 latitude areas that experience increases in mean precipitation. There is a tendency for
1429 drying of the mid-continental areas during summer, indicating a greater risk of droughts
1430 in those regions. Precipitation extremes increase more than the mean in most tropical and
1431 mid- and high latitude areas (IPCC, 2007a).

1432

1433 A.2.1.5 Snow and Ice

1434 As the climate warms, snow cover and sea ice extent decrease; glaciers and ice caps lose
1435 mass owing to dominance of summer melting over winter precipitation increases. There
1436 is a projected reduction of sea ice in the 21st century both in the Arctic and Antarctic
1437 with a large range of model responses. Widespread increases in thaw depth over much of
1438 the permafrost regions are projected to occur in response to warming over the next
1439 century (IPCC, 2007a).

1440

1441 **Note:** All of the AR4 predictions for precipitations, snow cover and sea and land ice are
1442 less certain and more variable across the suite of AOGCMs than they are for both the
1443 global average and the more robust geographic patterns of temperature.

1444

1445 **A.2.1.6 Carbon Cycle**

1446 Under the SRES illustrative emissions scenarios, for central carbon-cycle model
1447 parameters, CO₂ concentrations are projected to increase from its present value of about
1448 380 ppm to 540–970 ppm by 2100. The SAP 2.1a Reference scenarios give 2100
1449 concentrations of 740–850 ppm. There is unanimous agreement amongst the simplified
1450 climate-carbon cycle models that future climate change would reduce the efficiency of
1451 the Earth system (land and ocean) to absorb anthropogenic carbon dioxide. The higher
1452 the stabilization scenario warming, the larger is the impact on the carbon cycle. Both
1453 MAGICC and two of the three integrated assessment models used in SAP 2.1a contain
1454 simplified carbon cycle models comparable to those in Chapter 10 of the AR4 (IPCC,
1455 2007a).

1456

1457 **A.2.1.7 Ocean Acidification**

1458 Increasing atmospheric CO₂ concentrations lead directly to increasing acidification of the
1459 surface ocean. Multi-model projections based on SRES scenarios give reductions in pH
1460 of between 0.14 and 0.35 units over the 21st century, adding to the present decrease of
1461 0.1 units from pre-industrial times. Southern Ocean surface waters are projected to
1462 exhibit undersaturation with regard to CaCO₃ for CO₂ atmospheric concentrations higher

1463 than 600 ppm. Low latitude regions and the deep ocean will be affected as well. While
1464 ocean acidification would lead to dissolution of shallow-water carbonate sediments and
1465 could affect marine calcifying organisms, the net effect on the biological cycling of
1466 carbon in the oceans is not well understood (IPCC, 2007a).

1467

1468 **A.2.1.8 Sea Level**

1469 “Sea level is projected to rise between the present (1980-1999) and the end of this
1470 century (2090-2099) under the SRES B1 scenario by 0.28 m for the multi-mode average
1471 (range 0.19 to 0.37 m), under A1B by 0.35 m (0.23 to 0.47 m), under A2 by 0.37 m (0.25
1472 to 0.50 m) and under A1FI by 0.43 m (0.28 to 0.58 m). These are central estimates with
1473 5-95% intervals based on AOGCM results, not including uncertainty in carbon-cycle
1474 feedbacks. In all scenarios, the average rate of rise during the 21st century very likely
1475 exceeds the 1961–2003 average rate ($1.8 \pm 0.5 \text{ mm yr}^{-1}$). During 2090 – 2099 under
1476 A1B, the central estimate of the rate of rise is 3.8 mm yr^{-1} . For an average model, the
1477 scenario spread in sea level rise is only 0.02 m by the middle of the century, and by the
1478 end of the century it is 0.15 m.”(IPCC, 2007a) The projections of sea-level rise for the 12
1479 SAP 2.1 scenarios by MAGICC are within the range reported by AR4 (Wigley *et al.*,
1480 2007b).

1481

1482 “Thermal expansion is the largest component, contributing 60-70% of the central
1483 estimate in these projections for all scenarios. Glaciers, ice caps and the Greenland ice
1484 sheet are also projected to contribute positively to sea level. GCMs indicate that the
1485 Antarctic ice sheet will receive increased snowfall without experiencing substantial

1486 surface melting, thus gaining mass and contributing negatively to sea level. Further
1487 accelerations in ice flow of the kind recently observed in some Greenland outlet glaciers
1488 and West Antarctic ice streams could substantially increase the contribution from the ice
1489 sheets. Current understanding of these effects is limited, so quantitative projections
1490 cannot be made with confidence” (IPCC, 2007a).

1491

1492 **A.2.1.9 Ocean Circulation**

- 1493 a. There is no consistent change in the ENSO for those AOGCMs with a quasi-
1494 realistic base state.
- 1495 b. Among those models with a realistic Atlantic Meridional Overturning Circulation
1496 (MOC),), while it is very likely that the MOC will slow by 2100, there is little
1497 agreement among models for the magnitude of the slow-down. Models agree that
1498 the MOC will not shut down completely (IPCC, 2007a).

1499

1500 **A.2.1.10 Monsoons**

1501 Current AOGCMs predict that, in a warmer climate, there will be an increase in
1502 precipitation in both the Asian monsoon (along with an increase in interannual
1503 variability) and the southern part of the west African monsoon with some decrease in the
1504 Sahel in northern summer, as well as an increase in the Australian monsoon in southern
1505 summer. The monsoonal precipitation in Mexico and Central America is projected to
1506 decrease in association with increasing precipitation over the eastern equatorial Pacific.
1507 However, the uncertain role of aerosols complicates the projections of monsoon
1508 precipitation, particularly in the Asian monsoon (IPCC, 2007a).

1509

1510 **A.2.1.11 Tropical Cyclones (Hurricanes and Typhoons)**

1511 The Summary for Policymakers finds it **likely** that intense hurricanes and typhoons will
1512 increase through the 21st century as it warms. Results from embedded high-resolution
1513 models and global models, ranging in grid spacing from 1 degree to 9 km, generally
1514 project increased peak wind intensities and notably, where analyzed, increased near-
1515 storm precipitation in future tropical cyclones (IPCC, 2007a). However, these questions
1516 of changes in frequency and intensity under global warming continue to be the subject of
1517 very active research.

1518

1519 **A.2.1.12 Midlatitude Storms**

1520 Model projections show fewer midlatitude storms averaged over each hemisphere,
1521 associated with the poleward shift of the storm tracks that is particularly notable in the
1522 Southern Hemisphere, with lower central pressures for these poleward-shifted storms.
1523 The increased wind speeds result in more extreme wave heights in those regions (IPCC,
1524 2007a).

1525

1526 **A.2.1.13 Radiative Forcing**

1527 “The radiative forcings by long-lived greenhouse gases computed with the radiative
1528 transfer codes in twenty of the AOGCMs used in the AR4 have been compared against
1529 results from benchmark line-by-line (LBL) models. The mean AOGCM forcing over the
1530 period 1860 to 2000 agrees with the mean LBL value to within 0.1 W m^{-2} at the
1531 tropopause. However, there is a range of 25% in longwave forcing due to doubling CO_2

1532 from its concentration in 1860 across the ensemble of AOGCM codes. There is a 47%
1533 relative range in longwave forcing at 2100 contributed by all greenhouse gases in the
1534 A1B scenario across the ensemble of AOGCM simulations. These results imply that the
1535 ranges in climate sensitivity and climate response from models discussed in this chapter
1536 may be due in part to differences in the formulation and treatment of radiative processes
1537 among the AOGCMs.”(IPCC, 2007a)

1538

1539 **A.2.1.14 Climate Change Commitment (Temperature and Sea Level)**

1540 “Results from the AOGCM multi-model climate change commitment experiments
1541 (concentrations stabilized for 100 years at year 2000 for 20th century commitment, and at
1542 2100 values for B1 and A1B commitment) indicate that if greenhouse gases were
1543 stabilized, then a further warming of 0.5°C would occur.”(IPCC, 2007a)

1544

1545 “If concentrations were stabilized at A1B levels in 2100, sea level rise due to thermal
1546 expansion in the 22nd century would be similar to in the 21st, and would amount to 0.3–
1547 0.8 m above present by 2300. The ranges of thermal expansion overlap substantially for
1548 stabilization at different levels, since model uncertainty is dominant; A1B is given here
1549 because most model results are available for that scenario. Thermal expansion would
1550 continue over many centuries at a gradually decreasing rate, reaching an eventual level of
1551 0.2–0.6 m per degree of global warming relative to present.”(IPCC, 2007a)

1552 **Appendix 2.2 MAGICC Model Description**

1553

1554 MAGICC (Model for the Assessment of Greenhouse-gas Induced Climate Change) is a
1555 coupled gas-cycle/climate model. Various versions of MAGICC have been used in all
1556 IPCC assessments. The version used here is the one that was used in the IPCC Third
1557 Assessment Report (TAR; Cubasch and Meehl, 2001; Wigley and Raper, 2001).

1558

1559 The climate component is an energy-balance model with a one-dimensional, upwelling-
1560 diffusion ocean (a “UDEBM”). For further details of models of this type, see Hoffert *et*
1561 *al.* (1980) and Harvey *et al.* (1997). In MAGICC, the globe is divided into land and ocean
1562 “boxes” in both hemispheres in order to account for different thermal inertias and climate
1563 sensitivities over land and ocean, and hemispheric and land/ocean differences in forcing
1564 for short-lived species such as sulfate aerosols and tropospheric ozone.

1565

1566 In order to allow inputs as emissions, the climate model is coupled interactively to a
1567 series of gas-cycle models for CO₂, CH₄, N₂O, a suite of halocarbons and SF₆. Details
1568 of the carbon cycle model are given in Wigley (1991, 1993, 2000). The carbon cycle
1569 model includes both CO₂ fertilization and temperature feedbacks, with model parameters
1570 tuned to give results consistent with the other two carbon cycle models used in the TAR;
1571 viz. ISAM (Kheshgi and Jain, 2003) and the Bern model (Joos *et al.*, 2001) over a wide
1572 range of emissions scenarios. Details are given in Wigley *et al.* (2007). The other gas
1573 cycle models are those used in the TAR (Prather and Ehhalt, 2001; Wigley *et al.*, 2002).
1574 Radiative forcings for the various gases are as used in the TAR. For sulfate aerosols, both

1575 direct and indirect forcings are included using forcing/emissions relationships developed
1576 in Wigley (1989, 1991), with central estimates for 1990 forcing values. Sea level rise
1577 estimates use thermal expansion values calculated directly from the climate model. Ice-
1578 melt and other contributions are derived using formulae given in the TAR (Church and
1579 Gregory, 2001), except for the glacier and small ice-cap contribution which employs an
1580 improved formulation that can be applied beyond 2100 (Wigley and Raper, 2005).

1581

1582 The standard inputs to MAGICC are emissions of the various radiatively important gases
1583 and various climate model parameters. For the TAR, these parameters were tuned so that
1584 MAGICC was able to emulate results from a range of AOGCMs (see Cubasch and
1585 Meehl, 2001; Raper *et al.*, 2001). For the present calculations, a central set of parameters
1586 has been used. The most important of these is the climate sensitivity, where we have used
1587 a value of 2.6C equilibrium global-mean warming for a CO₂ doubling, the median of
1588 values for AOGCMs used in the TAR.

1589 **Appendix 2.2 References**

- 1590 **Church, J.A.** and Gregory, J.M., 2001: Changes in sea level. *Climate Change 2001: The*
1591 *Scientific Basis*, (eds. J. T. Houghton, *et al.*), Cambridge University Press,
1592 Cambridge, U.K., 639–693.
1593
- 1594 **Cubasch, U.** and Meehl, G.A., 2001: Projections for future climate change. *Climate*
1595 *Change 2001: The Scientific Basis*, (eds. J. T. Houghton, *et al.*), Cambridge
1596 University Press, Cambridge, U.K., 525–582.
1597
- 1598 **Harvey, L.D.D.**, Gregory, J., Hoffert, M., Jain, A., Lal, M., Leemans, R., Raper, S.B.C.,
1599 Wigley, T.M.L. and de Wolde, J., 1997: *An introduction to simple climate models*
1600 *used in the IPCC Second Assessment Report: IPCC Technical Paper 2* (eds.
1601 J.T. Houghton, L.G. Meira Filho, D.J. Griggs and M. Noguer), Intergovernmental
1602 Panel on Climate Change, Geneva, Switzerland, 50 pp.
1603
- 1604 **Hoffert, M.L.**, Callegari, A.J. and Hsieh, C.-T., 1980: The role of deep sea heat storage
1605 in the secular response to climate forcing. *Journal of Geophysical Research* **86**,
1606 6667– 6679.
1607
- 1608 **Joos, F.**, Prentice, I.C., Sitch, S., Meyer, R., Hooss, G., Plattner, G.-K., Gerber, S. and
1609 Hasselmann, K., 2001: Global warming feedbacks on terrestrial carbon uptake
1610 under the Intergovernmental Panel on Climate Change (IPCC) emissions
1611 scenarios. *Global Biogeochemical Cycles* **15**, 891–908,
1612 doi:10.1029/2000GB001375.
1613
- 1614 **Kheshgi, H.S.** and Jain, A.K., 2003: Projecting future climate change: implications of
1615 carbon cycle model intercomparisons. *Global Biogeochemical Cycles* **17**, 1047,
1616 doi:10.1029/2001GB001842 (see also <http://frodo.atmos.uiuc.edu/isam>).
1617
- 1618 **Prather, M.** and Ehhalt, D., 2001: Atmospheric chemistry and greenhouse gases. *Climate*
1619 *Change 2001: The Scientific Basis*, (eds. J. T. Houghton, *et al.*), Cambridge
1620 University Press, Cambridge, U.K., 239–287.
1621
- 1622 **Raper, S.C.B.**, Gregory, J.M., and T.J. Osborn (2001), Use of an upwelling-diffusion
1623 energy balance climate model to simulate and diagnose A/OGCM results. *Climate*
1624 *Dynamics*, *17*, 601–613.
1625
- 1626 **Wigley, T.M.L.**, 1989: Possible climatic change due to SO₂-derived cloud condensation
1627 nuclei. *Nature* **339**, 365–367.
1628
- 1629 **Wigley, T.M.L.**, 1991: Could reducing fossil-fuel emissions cause global warming?
1630 *Nature* **349**, 503–506.
1631
- 1632 **Wigley, T.M.L.**, 1991: A simple inverse carbon cycle model. *Global Biogeochemical*
1633 *Cycles* **5**, 373–382.

- 1634
1635 **Wigley, T.M.L.**, 1993: Balancing the carbon budget. Implications for projections of
1636 future carbon dioxide concentration changes. *Tellus* **45B**, 409–425.
1637
- 1638 **Wigley, T.M.L.**, 2000: Stabilization of CO₂ concentration levels. (In) *The Carbon Cycle*,
1639 (eds. T.M.L. Wigley and D.S. Schimel). Cambridge University Press, Cambridge,
1640 U.K., 258–276.
1641
- 1642 **Wigley, T.M.L.** and Raper, S.C.B., 2001: Interpretation of high projections for global-
1643 mean warming. *Science* **293**, 451–454.
1644
- 1645 **Wigley, T.M.L.**, Smith, S.J. and Prather, M.J., 2002: Radiative forcing due to reactive
1646 gas emissions. *Journal of Climate* **15**, 2690–2696.
1647
- 1648 **Wigley, T.M.L.** and Raper, S.C.B., 2005: Extended scenarios for glacier melt due to
1649 anthropogenic forcing. *Geophysical Research Letters* **32**, L05704,
1650 doi:10.1029/2004GL021238.
1651
- 1652 **Wigley, T.M.L.**, Richels, R. and Edmonds, J.A., 2007: Overshoot pathways to CO₂
1653 stabilization in a multi-gas context. (In) *Human Induced Climate Change: An*
1654 *Interdisciplinary Assessment* (eds. Michael Schlesinger, Francisco C. de la
1655 Chesnaye, Haroon Kheshgi, Charles D. Kolstad, John Reilly, Joel B. Smith and
1656 Tom Wilson), Cambridge University Press, 84–92.

1657 **Chapter 3 Climate Change From Short-Lived**
1658 **Emissions Due to Human Activities**

1659

1660 **Lead Author(s):** Drew T. Shindell, GISS/NASA; Hiram Levy II, GFDL/NOAA; Alice
1661 Gilliland, ARL/NOAA; M. Daniel Schwarzkopf, GFDL/NOAA; Larry W. Horowitz,
1662 GFDL/NOAA

1663

1664 **Contributing Authors:** Jean-Francois Lamarque, NCAR; Anne Waple, NCDC/NOAA

1665

1666 This chapter addresses the four questions regarding short-lived species that were posed in
1667 the Prospectus for this Report:

1668

1669 **Question 1.** What are the impacts of the radiatively active short-lived species not
1670 explicitly the subject of prior CCSP assessments (SAP 2.1a: Scenarios of Greenhouse
1671 Gas Emissions and Atmospheric Concentrations)?

1672

1673 **Answer 1.** Uncertainties in emissions projections for short-lived species are very large,
1674 even for a particular storyline. For aerosols, these uncertainties are usually dominant,
1675 while for tropospheric ozone, uncertainties in physical processes are more important.
1676 Differences among modeled future atmospheric burdens and radiative forcing for
1677 aerosols are dominated by divergent assumptions about emissions from South and East
1678 Asia. Aerosol mixing, aerosol indirect effects, the influence of ecosystem-chemistry
1679 interactions on methane, and stratosphere-troposphere exchange all contribute to large
1680 uncertainties separate from the emissions projections.

1681

1682 **Question 2.** How do the impacts of short-lived species compare with those of the well-
1683 mixed greenhouse gases as a function of the time horizon examined?

1684

1685 **Answer 2.** By 2050, two of the three models show a global mean annual average
1686 enhancement of the warming due to long-lived greenhouse gases by 20-25% due to the
1687 radiatively active short-lived species (which are not being reported in SAP 2.1). One
1688 model shows virtually no effect from short-lived species. To a large extent, the inter-
1689 model differences are related to differences in emissions. Short-lived species may play a
1690 substantial role relative to well-mixed greenhouse gases out to 2100. One model finds
1691 that short-lived species can contribute 40% of the projected summertime warming in the
1692 central US.

1693

1694 **Question 3.** How do the regional impacts of short-lived species compare with those of
1695 long-lived gases in or near polluted areas?

1696

1697 **Answer 3.** The spatial distribution of radiative forcing is generally less important than the
1698 spatial distribution of climate sensitivity in predicting climate impact. Thus, both short-
1699 lived and long-lived species appear to cause enhanced climate responses in the same
1700 regions of high climate sensitivity rather than short-lived species having an enhanced
1701 effect primarily in or near polluted areas.

1702

1703 **Question 4.** What might be the climate impacts of mitigation actions taken to reduce the
1704 atmospheric levels of short-lived species to address air quality issues?

1705

1706 **Answer 4.** Regional air quality emission control strategies for short-lived pollutants have
1707 the potential to substantially affect climate globally. Emissions reductions in the domestic
1708 sector in developing Asia, and to a lesser extent in the surface transportation sector in
1709 North America, appear to offer the greatest potential for substantial, simultaneous
1710 improvement in local air quality and mitigation of global climate change.

1711

1712 **3.1 Introduction**

1713 In this chapter, we describe results from numerical simulations of 21st century climate,
1714 with a major focus on the effects of short-lived gases and particulates. The calculations
1715 incorporate results from three different types of models:

1716

- 1717 1. Integrated assessment models that produce emission scenarios for aerosols and for
1718 ozone and aerosol precursor species.
- 1719 2. Global chemical composition models, which employ these emission scenarios to
1720 generate concentrations for the short-lived radiatively active species.
- 1721 3. Global comprehensive climate models, which calculate the climate response to
1722 the projected concentrations of both the short-lived and long-lived species. Box
1723 1.1 outlines this sequence in detail.

1724

1725 The second part of Chapter 3, Section 3.2, is a discussion of the emission scenarios and
1726 the models used to generate them, and the chemical composition models (sometimes
1727 called chemical transport models) used to produce the global distributions of short-lived

1728 species that help to drive the comprehensive climate models. Section 3.2 shows that,
1729 beginning with a single socio-economic scenario for the time evolution of long-lived
1730 (well-mixed) greenhouse gases, different assumptions about the evolution of the aerosols
1731 and precursor species lead to very different estimates of aerosol and ozone concentrations
1732 for the 21st century. We conclude that uncertainties in emissions projections for short-
1733 lived species are very large, even for a particular storyline. For aerosols, these
1734 uncertainties are usually dominant, while for tropospheric ozone, uncertainties in physical
1735 processes are more important.

1736

1737 The third part of Chapter 3, Section 3.3, discusses the three global comprehensive climate
1738 models (Geophysical Fluid Dynamics Laboratory (GFDL); Goddard Institute for Space
1739 Studies (GISS); National Center for Atmospheric Research (NCAR)) that have been used
1740 used to calculate the impact of the short- and long-lived species³⁴ on the climate,
1741 focusing on the changes in surface temperature and precipitation. Supplementing the
1742 climate model results are calculations of the changes in radiative forcing³⁵ of the earth-
1743 atmosphere system. We find that by 2050, two of the three climate models show that
1744 radiatively active short-lived species enhance the global-mean annual-average warming
1745 due to long-lived greenhouse gases by 20-25%. One model shows virtually no effect from
1746 short-lived species. To a large extent, the inter-model differences are related to
1747 differences in emissions. One of the models has been extended to 2100. In that model,

³⁴ We distinguish here between short-lived species (which have atmospheric lifetimes less than one month and are non-uniformly distributed) and long-lived species (which have lifetimes of a decade or more and are generally well mixed in the atmosphere).

³⁵ Radiative forcing is defined in Section 3.3.3; briefly, it measures the net change in the energy balance of the earth-atmosphere system with space associated with a change in composition of any radiatively active species present in the atmosphere

1748 short-lived species play a substantial role, relative to the well-mixed greenhouse gases, in
1749 the surface temperature evolution out to 2100 and are responsible for 40% of the
1750 projected summertime warming in the central US.

1751

1752 The fourth part of Chapter 3, Section 3.4, discusses the effects of changes in regional
1753 aerosol and ozone and aerosol precursor emissions, using models that separate emissions
1754 by economic sector. The results show that regional air quality emission control strategies
1755 for short-lived pollutants have the potential to substantially affect climate at large-scales.
1756 Emission reductions from domestic sources in Asia, and to a lesser extent from surface
1757 transportation in North America, appear to offer the greatest potential for substantial,
1758 simultaneous improvement in local air quality and mitigation of global climate change.

1759

1760 **3.2 Emission Scenarios and Composition Model Descriptions**

1761 **3.2.1 Emission Scenarios**

1762 The long-lived (well-mixed) greenhouse gases included in this study were carbon dioxide
1763 (CO₂), nitrous oxide (N₂O), methane (CH₄), and the minor species (chlorofluorocarbons,
1764 sulfur hexafluoride). Projected global mean values were prescribed following the A1B
1765 ‘marker’ scenario for all three modeling groups. Emissions for anthropogenic sources of
1766 aerosols and precursor species for all 3 composition model calculations were based on an
1767 international emission inventory maintained in the Netherlands (Olivier and Berdowski,
1768 2001).

1769

1770 Though the three groups in this study all prescribed future emissions following a specific
1771 socio-economic scenario (A1B) that was highly studied in the latest report by the
1772 Intergovernmental Panel on Climate Change (IPCC), they used different emissions trends
1773 for the short-lived species. There are several reasons for the differences. For one, the
1774 A1B emissions projections only provide estimates of anthropogenic emissions, and each
1775 model used its own natural emissions (though these were largely held constant).
1776 Secondly, integrated assessment models, while using the same socio-economic storyline
1777 (A1B), provided a range of emission results (Nakicenovic *et al.*, 2000).
1778
1779 Two groups, GFDL and NCAR, used output from the AIM integrated assessment model
1780 (integrated assessment models are defined in Chapter 2, Section 2.1) while GISS used
1781 results from the IMAGE model. Though the emissions output generated from AIM was
1782 denoted the ‘marker’ scenario by the IPCC, it was noted that it did not represent the
1783 average, best, or median result, and that all integrated assessment model results should be
1784 treated equally. Finally, emissions for some species, such as carbonaceous aerosols, were
1785 not provided. This last issue motivated the GISS choice of the IMAGE model output, as
1786 it provided sufficient regional detail to allow carbonaceous aerosol emissions to be
1787 estimated consistently with the other species. Another complexity was the treatment of
1788 biomass burning emissions, which are partly natural and partly anthropogenic. In the
1789 GFDL model, biomass-burning emissions were assumed to be half-anthropogenic and
1790 half natural. The GISS model instead used biomass burning emissions projections from
1791 another inventory (Streets *et al.*, 2004).
1792

1793 The result is a substantial divergence in the projected trends among the three models
1794 (Figure 3.1, Table 3.1). For sulfur dioxide (SO₂), the precursor to sulfate aerosol, the
1795 emissions follow reasonably similar trajectories, with globally averaged increases until
1796 2030 followed by decreases to 2050 and even further decreases to 2100. However, the
1797 percentage increase is roughly double for GISS and NCAR as compared with GFDL.
1798 Thus even two composition models using anthropogenic emission projections from the
1799 same integrated assessment model show large differences in the evolution of their total
1800 emissions, presumably owing to differences in the present-day emission inventories . At
1801 2050, the GFDL model has substantially reduced emissions compared with 2000, while
1802 the other models show enhanced emissions relative to 2000. A similar divergence in
1803 projected sulfur-dioxide trends is present in the 2.1a stabilization emission scenarios
1804 discussed in Chapter 2, with emissions decreasing dramatically (~70%) by 2050 in one
1805 integrated assessment model (MINICAM) while decreasing only moderately (~20%) in
1806 the two others, and even beginning to increase again after about 2040 in one of those two.
1807
1808 Differences are even more striking for carbonaceous aerosols emissions, which were not
1809 provided by any of the integrated assessment models. We focus on black carbon (BC) as
1810 the more important radiative perturbation. For this aerosol (and for organic carbon(OC)),
1811 the GFDL composition model uses the IPCC recommendation to scale carbonaceous
1812 aerosol emissions to carbon monoxide emissions, leading to substantial increases with
1813 time (Figure 3.1, Table 3.1). However, many of the sources of carbon monoxide emission
1814 are different from those of carbonaceous aerosols. The NCAR group did not simulate the
1815 future composition of black and organic carbon based on emission projections, but

1816 instead scaled their present-day distribution by the global factors derived for sulfur
1817 dioxide. The time evolution of black and organic carbon emissions in the NCAR model
1818 thus follows the same trajectory as that of SO₂. On the other hand, the GISS group used
1819 emissions projections from (Streets *et al.*, 2004) based on energy and fuel usage trends
1820 from the IMAGE model (as for other species) and including expected changes in
1821 technology. This led to a substantial reduction in future emissions of carbonaceous
1822 aerosols.

1823

1824 For precursors of tropospheric ozone, there was again divergence among the models. The
1825 primary precursor in most regions, NO_x (nitrogen oxides = NO + NO₂), increased steadily
1826 in the projections used by GISS, while it peaked at 2030 and decreased slightly thereafter
1827 in the projections used at GFDL (Table 3.1). Hydrocarbons and carbon monoxide show
1828 analogous differences. Methane was prescribed according to the A1B “marker” scenario
1829 values for all three composition models. Thus ozone, in addition to the aerosols, was
1830 modeled in substantially different ways at the three centers.

1831

1832 The three models included projected changes in the same species, with the exception of
1833 nitrate, which only varied in the GISS model. As its contribution to total aerosol and total
1834 aerosol radiative forcing is small, at least in this GISS model, this particular difference
1835 was not significant in our results.

1836 **Table 3.1. Global Emissions. Emissions include both natural and anthropogenic sources. Values in**
 1837 **parentheses are changes relative to 2000.**

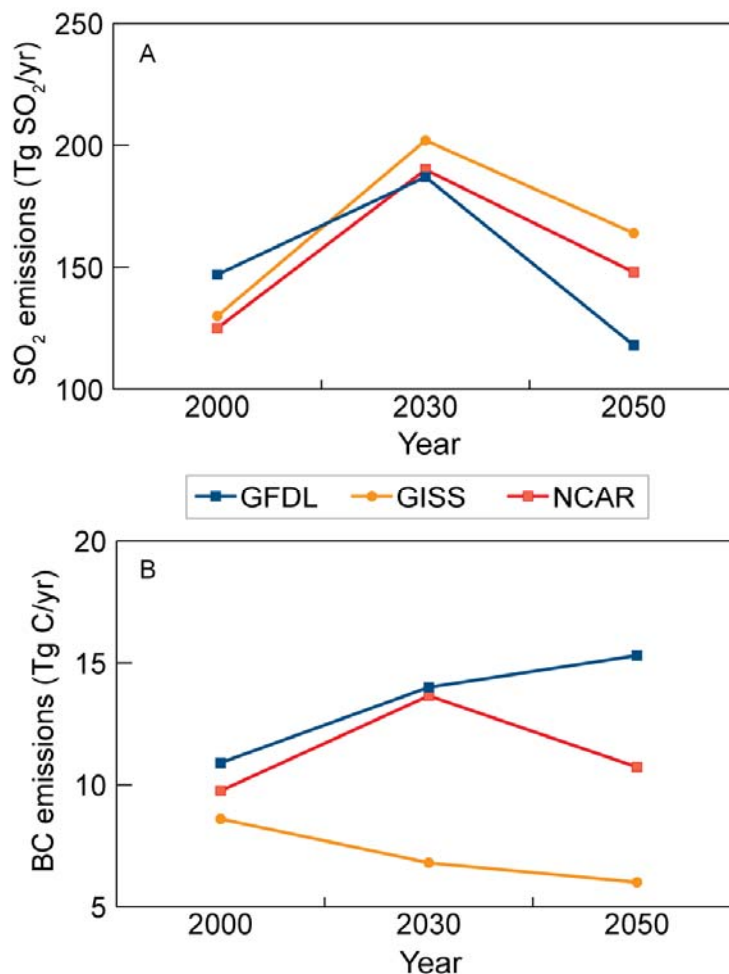
Species	Model	2000	2030	2050	2100
NO _x (Tg N/yr)	GFDL	40	57 (43%)	54 (35%)	48 (20%)
	GISS	50.5	67.0 (33%)	77.5 (53%)	NA
BC (Tg C/yr)	GFDL	10.9	14.0 (28%)	15.3 (40%)	19.9 (83%)
	GISS	8.6	6.8 (-21%)	6.0 (-30%)	NA
OC (Tg C/yr)	GFDL	51.5	61.9 (20%)	66.5 (29%)	84.3 (%)
	GISS	69.5	57.0 (-18%)	58.3 (-16%)	NA
SO ₂ (Tg SO ₂ /yr)	GFDL	147	187 (27%)	118 (-20%)	56 (-62%)
	GISS	130	202 (55%)	164 (26%)	NA
	NCAR	125	190 (52%)	148 (18%)	NA
Dust (Tg/yr)	GFDL	2471	2471	2471	2471
	GISS	1580	1580	1580	NA

1838

1839 3.2.2 Composition Models

1840 The chemical composition models used to produce short-lived species concentrations for
 1841 the GFDL, GISS, and NCAR climate models were driven by the emissions projections
 1842 discussed in Section 3.2.1. While the three models did not use identical present-day
 1843 emissions, their anthropogenic emissions were based on the same international inventory
 1844 (Olivier and Berdowski, 2001). The chemical composition simulations were run for one
 1845 or two years, with the three-dimensional monthly mean concentrations and optical
 1846 properties archived for use as off-line concentration fields to drive the climate model
 1847 simulations discussed in Section 3.3. These simulations were all performed with present-
 1848 day meteorology (values for temperature, moisture, and wind). Further details about the
 1849 chemical composition models are provided in Appendix 1.

1850



1851
1852
1853
1854
1855
1856
1857
1858

Figure 3.1 A1B emissions trends used in the three models for SO₂ (top) and BC (bottom). Note that in the NCAR model, the present day black carbon distribution was scaled in the future rather than calculated from BC emissions. Scaling was chosen to mimic the global sulfur dioxide emissions, a 40% increase over 2000 at 2030, and 10% at 2050. The NCAR 2000 black carbon global emission is set at the average of the GISS and GFDL 2000 values, and follows this scaling in the future, for illustrative purposes.

1859 3.2.2.1 Geophysical Fluid Dynamics Laboratory (GFDL)

1860 Composition changes for the short-lived species in the GFDL experiments were
1861 calculated using the global chemical transport model MOZART-2 (Model for OZone
1862 And Related chemical Tracers, version 2.4), which has been described in detail
1863 previously (Horowitz *et al.*, 2003; Horowitz, 2006; and references therein). This model
1864 was used to generate the monthly average distributions of tropospheric ozone, sulfate,
1865 and black and organic carbon as a function of latitude, longitude, altitude, and time for

1866 the emission scenarios discussed above. Simulated ozone concentrations agree well with
1867 present-day observations and recent trends (Horowitz, 2006). Overall, the predicted
1868 concentrations of aerosol are within a factor of two of the observed values and have a
1869 tendency to be overestimated (Ginoux *et al.*, 2006). Further details on the MOZART
1870 model are found in Appendix 3.1, in the section on Geophysical Fluid Dynamics
1871 Laboratory.

1872

1873 **3.2.2.2 Goddard Institute for Space Studies (GISS)**

1874 The configuration of the GISS composition model used here has been described in detail
1875 in (Shindell *et al.*, 2007). In brief, the composition model PUCINI (Physical
1876 Understanding of Composition-Climate INteractions and Impacts) includes ozone and
1877 oxidant photochemistry in both the troposphere and stratosphere (Shindell *et al.*, 2006b),
1878 sulfate, carbonaceous and sea-salt aerosols (Koch *et al.*, 2006, 2007), nitrate aerosols
1879 (Bauer *et al.*, 2006), and mineral dust (Miller *et al.*, 2006a). Present-day composition
1880 results in the model are generally similar to those in the underlying chemistry and aerosol
1881 models. Further details on the PUCINI model resolution, composition, and performance
1882 are found in Appendix 3.1, in the section on Goddard Institute for Space Studies.

1883

1884 **3.2.2.3 National Center for Atmospheric Research (NCAR)**

1885 For the climate simulations described in this section, present-day tropospheric ozone was
1886 taken from (Lamarque *et al.*, 2005a); beyond 2000, tropospheric ozone was calculated by
1887 T. Wigley using the MAGICC composition model
1888 (<http://www.cru.uea.ac.uk/~mikeh/software/magicc.htm>) forced by the time-varying

1889 emissions of NO_x, methane and volatile organic compounds (VOCs) and these average
1890 global values were used to scale the present-day distribution. Future carbonaceous
1891 aerosols are scaled from their present-day distribution (Collins *et al.*, 2001) by a globally
1892 uniform factor whose time evolution follows the global evolution of SO₂ emissions.
1893 Stratospheric ozone changes are prescribed following the study by (Kiehl *et al.*, 1999).
1894 Further details on the composition models used by NCAR are found in Appendix 3.1 in
1895 the section on National Center for Atmospheric Research.

1896

1897 **3.2.3 Tropospheric Burden**

1898 The composition models each calculate time-varying three-dimensional distributions of
1899 the short-lived species (except for NCAR where 2030 and 2050 ozone, black carbon, and
1900 organic carbon were scaled based on their 2000 distributions). We compare these using
1901 the simple metric of the global mean annual average tropospheric burden (*i.e.* the total
1902 mass in the troposphere). As was the case with emissions, the differences between the
1903 outputs of the composition models are substantial (Table 3.2). The GFDL model has a
1904 67% greater present-day burden of sulfate than the GISS model, for example. As the
1905 GFDL sulfur dioxide emissions were only 13% greater, this suggests that either sulfate
1906 stays in the air longer in the GFDL model than in the GISS model or sulfur dioxide is
1907 converted more efficiently to sulfate in the GFDL model.

1908 **Table 3.2 Global Burdens.** Values in parentheses are changes relative to 2000.

Species	Model	2000	2030	2050	2100
BC (Tg C)	GFDL	0.28	0.36 (29%)	0.39 (39%)	0.51
	GISS	0.26	0.19 (-27%)	0.15 (-42%)	NA
	NCAR		(40%)	(10%)	
OC* (Tg C)	GFDL	1.35	1.59 (18%)	1.70 (26%)	2.15
	GISS	1.65	1.33 (-19%)	1.27 (-23%)	NA
	NCAR		(40%)	(10%)	
Sulfate (Tg SO ₄ ⁻)	GFDL	2.52	3.21 (27%)	2.48 (-2%)	1.50 (-40%)
	GISS**	1.51	2.01 (33%)	1.76 (17%)	NA
	NCAR				
Dust (Tg)	GFDL	22.31	22.31	22.31	22.31
	GISS	34.84	34.84	34.84	NA
	NCAR				
Tropospheric Ozone (DU)	GFDL	34.0	38.4 (+13%)	39.3 (+16%)	38.2 (+12%)
	GISS	31.6	41.5 (31%)	47.8 (51%)	NA
	NCAR	28.0	41.5 (48%)	43.0 (54%)	NA

1909 *The organic carbon (OC) burdens include primary OC aerosols (with emissions as in above table) plus
 1910 secondary OC aerosols (SOA). In the GFDL model, the global burden of SOA is 0.07 Tg C in this
 1911 inventory. In the GISS model, organic carbon from SOA makes up ~24% of present-day OC emissions.

1912 **GISS sulfate burdens include sulfate on dust surfaces, which makes up as much as ½ the total burden.
 1913

1914 This can be tested by analyzing the atmospheric residence times of the respective models
 1915 (Table 3.3). The residence time of sulfate is within ~10% in the two models, and in fact is
 1916 slightly less in the GFDL model. This indicates that the conversion of sulfur dioxide
 1917 (SO₂) to sulfate must be much more efficient in the GFDL model for it to have a sulfate
 1918 burden so much larger than the GISS model. This is clearly seen in the ratio between
 1919 sulfate burden and SO₂ emissions (Table 3.4). This ratio can be analyzed in terms of the
 1920 total sulfur dioxide burden (in Tg) per SO₂ emission (in Tg/yr); the change in SO₂ burden
 1921 per SO₂ emission change, or alternatively in the percentage change in each. The latter is
 1922 probably the most useful evaluation, as the fractional change will reduce differences
 1923 between the starting points of the two models. We note that this metric is affected by both
 1924 production and removal rates in the models. Table 3.4 shows clearly that the production
 1925 of sulfate per Tg of sulfur emitted is much greater in the GFDL model than in the GISS

1926 model, either because of differences in other sources of sulfate (*e.g.*, from dimethyl
 1927 sulfate (DMS)) or difference in the chemical conversion efficiency of SO₂ to sulfate
 1928 (versus physical removal of SO₂ by deposition).

1929
 1930

Table 3.3 Global mean annual average aerosol residence times (days)

Species	Model	2000	2030	2050
BC	GFDL	9.4	9.4	9.3
	GISS	11.0	10.2	9.1
OC	GFDL	9.6	9.4	9.3
	GISS	8.7	8.5	8.0
Sulfate	GFDL	8.0	8.2	8.1
	GISS	8.8	8.8	9.0

1931

1932 The residence times of black and organic carbon (BC and OC) are also fairly similar in
 1933 these two models (Table 3.3). While the concentrations of sulfate and carbonaceous
 1934 aerosols are all influenced by differences in how the models simulate removal by the
 1935 hydrologic cycle, accounting for at least some of the 10-15% difference in residence
 1936 times, sulfate production can vary even more from model to model, as its production
 1937 from the emitted sulfur dioxide involves chemical oxidation, which can differ
 1938 substantially between models. Removal of sulfur dioxide prior to conversion to sulfate
 1939 may also be more efficient in the GISS model. In contrast, BC and OC are emitted
 1940 directly, and hence any differences in how these are represented in the models would be
 1941 apparent in their residence times.

1942 **Table 3.4 Ratio of sulfate and ozone burdens to precursor emissions, global mean annual average**

Species	Model	2000 Tg burden/ Tg emission	2030 vs. 2000 Tg burden/ Tg emission	2030 vs. 2000 % burden/ % emission	2050 vs. 2000 % burden/ % emission
Sulfate	GFDL	0.017	0.017	1.00	0.08*
	GISS	0.012	0.007	0.60	0.65
Ozone	GFDL	7.19	2.24	0.32	0.44
	GISS	6.82	6.54	0.94	0.96

1943 Ratios for sulfate are in Tg sulfate per Tg S/yr SO₂ emitted. Ozone ratios are in Tg ozone per Tg N/yr NO_x
 1944 emitted. Ozone values in Table 3.2 are converted to burden assuming 1 DU globally averaged = 10.9 Tg
 1945 ozone.

1946 *The burden change was only 2% in this case, making the calculation unreliable.

1947

1948 The aerosol residence times are relatively stable in time in the GISS and GFDL models.

1949 The carbonaceous aerosol residence times do decrease with time in the GISS model (and

1950 to a lesser extent in the GFDL model for OC), probably owing to the shift with time from

1951 mid to tropical latitudes, where wet and dry removal rates are different (more rapid net

1952 removal). The sulfate residence time is fairly stable over the 2000 to 2050 period. The

1953 ratio of sulfate burden to SO₂ emissions is the same for the present-day and the 2030 to

1954 2000 changes in the GFDL model. For the 2100 to 2000 change in that model (not

1955 shown), the ratio drops from 1.00 to 0.65. As the total emissions of SO₂ decrease, a larger

1956 fraction of the sulfate production comes from DMS oxidation rather than from emitted

1957 SO₂. The conversion efficiency from SO₂ to sulfate also varies over time in the GISS

1958 model, decreasing to 2030 and increasing thereafter (inversely related to total sulfur

1959 dioxide emissions). This may reflect both non-linearities in production (via oxidation

1960 chemistry) and the changing spatial pattern of emissions.

1961

1962 After comparison of the inter-model variations in aerosol residence times and chemical

1963 conversion efficiencies with the variations in emissions trends, it is clear that the

1964 differences in the projected changes in aerosol burdens in the GISS and GFDL

1965 simulations are primarily attributable to the underlying differences in emissions. This is
1966 especially true for carbonaceous aerosols, for which the residence times are quite similar
1967 in the models. Even though there is a greater difference in sulfate burdens due to the
1968 variations in chemical conversion efficiency between the models, the emissions trends at
1969 2050 relative to 2000 are of opposite sign in the two models and thus dominate the
1970 difference in the burden change. Thus, the GISS model projects a greater sulfate burden
1971 at 2050 than at 2000, but substantially reduced burdens of carbonaceous aerosols, while
1972 the GFDL model projects the opposite, both because of the underlying emissions
1973 projections.

1974

1975 The results for tropospheric ozone tell a different story. The ozone burden increases in
1976 the future in all three models, but the percentage increase relative to 2000 differs by more
1977 than a factor of three at 2030 (Table 3.2). Examining the ozone changes relative to the
1978 NO_x emissions changes, there are very large differences between the GFDL and GISS
1979 models (Table 3.4). This may reflect the influence of processes such as stratospheric
1980 ozone influx which are independent of NO_x emissions, as well as the roles of precursors
1981 such as carbon monoxide (CO) and hydrocarbons that also influence tropospheric ozone.
1982 In particular, the GISS model computed a large increase in the flux of ozone into the
1983 troposphere as the stratospheric ozone layer recovered, while the composition model used
1984 at GFDL to calculate ozone held stratospheric ozone fixed and hence did not simulate
1985 similar large increases. In addition, there are well-known non-linearities in O₃-NO_x
1986 chemistry (Stewart *et al.*, 1977), and it has been shown that the ozone production
1987 efficiency can vary substantially with time (Lamarque *et al.*, 2005a; Shindell *et al.*,

1988 2006a). Thus for tropospheric ozone, the differences in modeled changes of nearly a
1989 factor of three (13 vs. 33% increase) are much larger than the differences in the NO_x
1990 precursor emissions (33 vs. 43% increase).

1991

1992 **3.2.4 Aerosol Optical Depth**

1993 The global mean present-day all-sky aerosol optical depth (AOD)³⁶ in the three models
1994 ranges from 0.12-0.20 (Table 3.5). This difference of almost a factor of 2 suggests that
1995 aerosols are contributing quite differently to the Earth's energy balance with space in
1996 these models. Observational constraints on the all-sky value are not readily available, as
1997 most of the extant measurement techniques are reliable only in clear-sky (cloud-free)
1998 conditions. Sampling clear-sky areas only, the GISS model's global total aerosol optical
1999 depth is 0.12 for 2000 (0.13 Northern Hemisphere, 0.10 Southern Hemisphere). This
2000 includes contributions from sulfate, carbonaceous, nitrate, dust, and sea-salt aerosols. The
2001 clear-sky observations give global mean values of ~0.135 (ground-based AERONET) or
2002 ~0.15 (satellite composites, including AVHRR or MODIS observations), though these
2003 have substantial limitations in their spatial and temporal coverage. The NCAR and GFDL
2004 models did not calculate clear-sky aerosol optical depth. Given that the all-sky values are
2005 larger, and substantially so in the GISS model (though this will depend upon the water
2006 uptake of aerosols), it seems clear that the values for NCAR would be too small
2007 compared with observations since even their all-sky values are lower than the estimate
2008 from observations. This may be related to NCAR's use of AVHRR data in assimilation of

³⁶ Aerosol optical depth is a measure of the fraction of radiation at a given wavelength absorbed or scattered by aerosols while passing through the atmosphere.

2009 aerosol optical depth to create the NCAR climatology (Collins *et al.*, 2001, 2006), as that
2010 data appears to be low relative to MODIS observations, for example.
2011
2012 For all three models, there are large differences in the contributions of the various aerosol
2013 species (Figure 3.2, Table 3.5). This is true even for GFDL and GISS models, with
2014 relatively similar all-sky global mean aerosol optical depths. More than half the aerosol
2015 optical depth in the GFDL model comes from sulfate, while this species contributes only
2016 about 1/8th the aerosol optical depth in the GISS model. Instead, the GISS model's
2017 aerosol optical depth is dominated by the largely natural sea-salt and dust aerosols, which
2018 together contribute 0.14 to the aerosol optical depth. These two species contribute a much
2019 smaller aerosol optical depth in the NCAR and GFDL models, ~0.06 or less, with the
2020 differences with respect to GISS predominantly due to sea-salt. The relative contribution
2021 from sulfate in the NCAR model looks similar to the GFDL model, with nearly half its
2022 aerosol optical depth coming from sulfate, but the magnitude is much smaller. It seems
2023 clear that the GFDL model's direct sulfate contribution is biased high (Ginoux *et al.*,
2024 2006), while the GISS model's sulfate is biased low in this model version (Shindell *et al.*,
2025 2007). However, the relative importance of the different aerosols species is not well
2026 understood at present (Kinne *et al.*, 2006).
2027

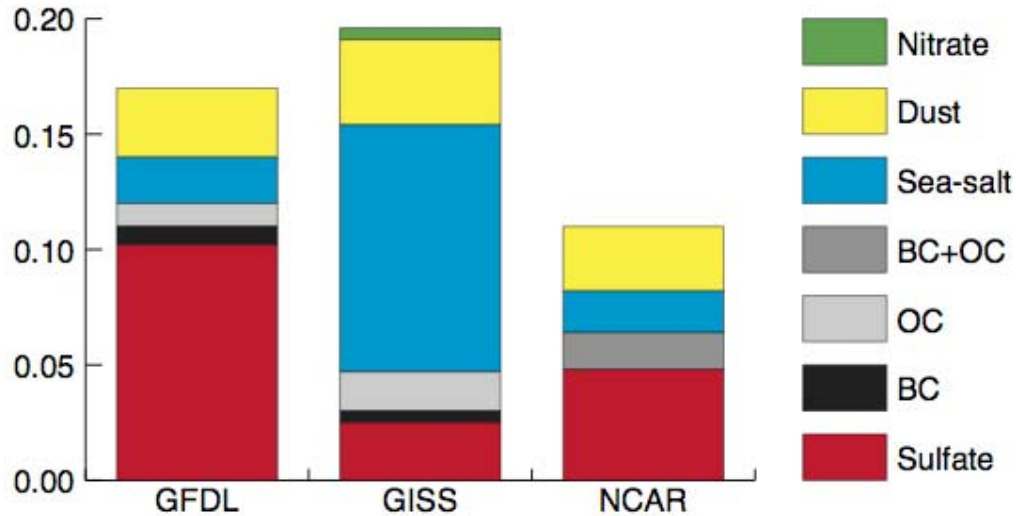


Figure 3.2 Present-day contributions from individual aerosol species to global mean all-sky aerosol optical depth (550 nm extinction). Neither GFDL nor NCAR include nitrate.

2028
2029
2030
2031

2032 Large differences in the relative aerosol optical depth in the Northern Hemisphere and
2033 Southern Hemisphere are also apparent in the models (Table 3.5). The ratios of the
2034 present-day Northern Hemisphere to Southern Hemisphere total aerosol optical depths in
2035 the three models differ widely, with values of 2.43, 1.97, and 0.96 in the GFDL, NCAR,
2036 and GISS models, respectively. This clearly reflects the dominant contribution of sulfate
2037 to optical depth in the GFDL and NCAR models, as this species has large anthropogenic
2038 Northern Hemisphere sources, and the dominance of sea-salt in the GISS model, with its
2039 largest source being the Southern Ocean. While composite satellite data shows clearly
2040 greater aerosol optical depths in the Northern Hemisphere than the Southern Hemisphere,
2041 most satellite instruments lose coverage near the northern edge of the Southern Ocean
2042 (Kinne *et al.*, 2006). Unfortunately, quality-controlled networks such as AERONET
2043 provide virtually no ground-based data poleward of 45°S. Thus while it seems unlikely
2044 that the aerosol optical depth is larger in the Southern Hemisphere than the Northern
2045 Hemisphere, as in the GISS model, presently available data are not adequate to fully

2046 characterize this ratio, as aerosol optical depths over the Southern Ocean are poorly
2047 known.

2048

Table 3.5 Aerosol optical depth (550nm extinction) – ALL-SKY

Region	aerosol type	Model	2000	2030	2050	2100
Global	BC	GFDL	.0076	.0096	.0105	.0138
		GISS	.0045	.0034	.0028	NA
	Sulfate	GFDL	.1018	.1227	.0906	.0591
		GISS	.0250	.0312	.0278	NA
		NCAR	.048	.062	.052	NA
	Sea-salt	GFDL	.0236	.0236	.0236	.0236
		GISS	.1065	.1080	.1050	
		NCAR	.018	.018	.018	NA
	Dust	GFDL	.0281	.0281	.0281	.0281
		GISS	.0372	.0389	.0387	
		NCAR	.0275	.0275	.0275	NA
	OC	GFDL	.0104	.0122	.0131	.0166
		GISS	.0166	.0135	.0130	
	Nitrate	GISS	.0054	.0057	.0060	
	Total	GFDL	.1715	.1964	.1660	.1411
GISS		.1959	.2007	.1934	NA	
NCAR		.116	.1392	.1206	NA	
Northern Hemisphere	BC	GFDL	.0109	.0147	.0161	.0209
		GISS	.0062	.0043	.0032	NA
	Sulfate	GFDL	.1509	.1766	.1038	.0694
		GISS	.0352	.0449	.0388	NA
		NCAR	.078**	.097**	.073**	NA
	Dust	GISS	.0600	.0642	.0615	
		GFDL	.0491	.0491	.0491	.0491
	Sea-salt	GISS	.0630	.0619	.0647	
		GFDL	.0181	.0181	.0181	.0181
	Total	GFDL	.2430	.2756	.2056	.1807
GISS		.1910	.1985	.1907	NA	
NCAR		.1538	.1827	.1502	NA	
Southern Hemisphere	BC	GFDL	.0042	.0046	.0049	.0066
		GISS	.0029	.0026	.0023	NA
	Sulfate	GFDL	.0526	.0689	.0774	.0487
		GISS	.0148	.0175	.0170	NA
		NCAR	0.052**	.062**	.075**	
	Dust	GISS	.0144	.0137	.0159	
		GFDL	.0071	.0071	.0071	.0071
	Sea-salt	GISS	.1502	.1541	.1453	
		GFDL	.0291	.0291	.0291	.0291
	Total	GFDL	.1000	.1171	.1263	.1015
GISS		.1997	.2030	.1962	NA	
NCAR		.0779	.0957	.0910	NA	

** Total for sulfate + sea salt.

2049
2050

2051

2052 **3.3 Climate Studies**2053 **3.3.1 Experimental Design**

2054 The climate studies discussed here consisted of transient climate simulations that were
2055 designed to isolate the climate effects of projected changes in the short-lived species and
2056 calculate their importance relative to that of the long-lived well-mixed greenhouse gases.
2057 The simulations from the GFDL, GISS, and NCAR groups each employed ensembles
2058 (multiple simulations differing only in their initial conditions) in order to reduce the
2059 unforced variability in the chaotic climate system. One three-member ensemble included
2060 the evolution of short- and long-lived species following the A1B scenario, while the
2061 second ensemble included only the evolution of long-lived species with the short-lived
2062 species fixed at present values. While all three groups used the same values for the long-
2063 lived species, each had its own version of an A1B scenario for short-lived species, as
2064 discussed previously in Section 3.2.

2065

2066 The global three-dimensional distributions of short-lived gases and aerosols were
2067 modeled using each group's chemistry-aerosol composition model. For the first
2068 ensemble, the GFDL simulations used aerosol and ozone distributions computed each
2069 decade out to 2100, while the GISS and NCAR simulations employed values computed
2070 for 2000, 2030, and 2050. Either seasonally varying or monthly-average three-
2071 dimensional distributions were saved. Short-lived species concentrations for intermediate
2072 years were linearly interpolated between the values for computed years. In both sets of
2073 simulations, the concentrations of long-lived species varied with time. In practice, NCAR

2074 performed only a single pair of simulations out to 2050, while GISS performed all three
2075 pairs out to 2050, and GFDL extended all three pairs out to 2100.

2076

2077 **3.3.2 Climate Models**

2078 **3.3.2.1 Geophysical Fluid Dynamics Laboratory (GFDL)**

2079 Climate simulations at GFDL used the comprehensive climate model (Atmosphere-
2080 Ocean General Circulation Model (AOGCM); see Box 1.1) recently developed at
2081 NOAA's Geophysical Fluid Dynamics Laboratory, which has described in detail in
2082 (Delworth *et al.*, 2006). The control simulation of this AOGCM (using present-day
2083 values of radiatively active species) has a stable, realistic climate when integrated over
2084 multiple centuries. The model is able to capture the main features of the global evolution
2085 of observed surface temperature for the 20th century as well as many continental-scale
2086 features (Knutson *et al.*, 2006). Its equilibrium climate sensitivity to a doubling of CO₂ is
2087 3.4°C³⁷ (Stouffer *et al.*, 2006). The model includes the radiative effects of well-mixed
2088 gases and ozone on the climate as well as the direct effects of aerosols, but does not
2089 include the indirect aerosol effects (see Box 3.1). Further details on the model resolution,
2090 model physics, and model performance are included in Appendix 3.2 (Climate Models) in
2091 the section on Geophysical Fluid Dynamics Laboratory.

2092

2093 **3.3.2.2 Goddard Institute for Space Studies (GISS)**

2094 The GISS climate simulations were performed using GISS ModelE (Schmidt *et al.*,
2095 2006). This model has been extensively evaluated against observations (Schmidt *et al.*,

³⁷ Equilibrium climate sensitivity is defined here as the global -mean annual- mean surface temperature change of a climate model in response to a doubling of atmospheric carbon dioxide from preindustrial levels, when the model has fully adjusted to the change in carbon dioxide.

2096 2006), and has a climate sensitivity in accord with values inferred from paleoclimate data
2097 and similar to that of mainstream General Circulation Models.; the equilibrium climate
2098 sensitivity for doubled CO₂ is 2.6°C. The radiatively active species in the model include
2099 well-mixed gases, ozone, and aerosols. The model includes a simple parameterization for
2100 the aerosol indirect effect (Menon *et al.*, 2002) (see box on aerosol indirect effect).
2101 Further details on the model resolution and model physics are included in Appendix 3.2
2102 (Climate Models) in the section on Goddard Institute for Space Studies.

2103

2104 **3.3.2.3 National Center for Atmospheric Research (NCAR)**

2105 The transient climate simulations use the NCAR Community Climate System Model
2106 CCSM3 (Collins *et al.*, 2006). The equilibrium climate sensitivity of this model to
2107 doubled CO₂ is 2.7°C. Further details on the model resolution and construction are found
2108 in Appendix 3.2 (Climate Models) in the section on National Center for Atmospheric
2109 Research.

2110

Box 3.1: Radiative Effects of Aerosols

The direct effects of aerosols refer to their scattering and absorption of both incoming solar and outgoing terrestrial radiation. By reflecting incoming radiation back to space, most aerosols have a negative radiative forcing (cooling effect). For reflective aerosols (sulfate, organic carbon, nitrate, dust and sea-salt), this effect dominates over their absorption of outgoing radiation (the greenhouse effect) on the global scale. The balance varies both geographically and seasonally as a function of solar radiation and the ground temperature. In contrast, absorbing aerosols such as black carbon have a positive radiative forcing (warming effect) as they absorb incoming and outgoing radiation, reducing the overall fraction of the sun's irradiance that it reflected back to space. They can also absorb outgoing radiation from the Earth (the greenhouse effect).

In addition to their direct radiative effects, aerosols may also lead to an indirect radiative forcing of the climate system through their effect on clouds. Two aerosol indirect effects are identified: The first indirect effect (also known as the cloud albedo effect) occurs when an increase in aerosols causes an increase in cloud droplet concentration and a decrease in droplet size for fixed liquid water content (Twomey, 1974). Having more, smaller drops increases the cloud albedo (reflectivity). The second indirect effect (also known as the cloud lifetime effect) occurs when the reduction in cloud droplet size affects the precipitation efficiency, tending to increase the liquid water content, the cloud lifetime (Albrecht, 1989), and the cloud thickness (Pincus and Baker, 1994). As the clouds last longer, this leads to an increase in cloud cover. It has been argued that empirical data suggest that the second indirect effect is the dominant process (Hansen *et al.*, 2005).

The direct effects of aerosols are relatively well-represented in climate models such as those described in Section 3.3.2 and used in this study, though substantial uncertainties exist regarding the optical properties of some aerosol types and especially of aerosol mixtures. Because of the inherent complexity of the aerosol indirect effect, climate model studies dealing with its quantification necessarily include an important level of simplification. While this represents a legitimate approach, it should be clear that the climate model estimates of the aerosol indirect effect are very uncertain.

The studies discussed in chapter 3 of this report include the direct effects of aerosols in all three models (though nitrate is only included in the GISS model). The indirect effect is only included in the GISS model, which uses a highly simplified representation of the second indirect effect.

2111

2112 **3.3.3 Radiative Forcing Calculations**

2113 The radiative forcing at the tropopause provides a useful, though limited, indicator of the
2114 climate response to perturbations (Hansen *et al.*, 2005) (see Box 3.2).

2115

2116

Box 3.2: Radiative Forcing

Radiative forcing is defined as the change in net (down minus up) irradiance (solar plus longwave, in W m^{-2}) at the tropopause due to a perturbation after allowing for stratospheric temperatures to adjust to radiative equilibrium, but with surface and tropospheric temperatures and state held fixed at the unperturbed values (IPCC, 2007; Ramaswamy et al, 2001). This quantity is also sometimes termed adjusted radiative forcing. If the stratospheric temperatures are not allowed to adjust, the irradiance change is termed instantaneous radiative forcing.

The utility of the radiative forcing concept is that, to first order, the equilibrium global-mean, annual-mean surface temperature change is proportional to the radiative forcing, for a wide range of radiative perturbations (WMO, 1986). The proportionality constant (often denoted as the climate sensitivity parameter, λ) is approximately the same (to within 25%) for most drivers of climate change (IPCC, 2007), with a typical value of $\sim 0.5\text{-}0.7$ for most models. This enables a readily calculable and comparable measure of the climate response to radiative perturbations, such as those discussed in this Chapter.

2117

2118 **3.3.3.1 Global and Hemispheric Average Values: GFDL and GISS**

2119 Radiative forcing calculations were performed by GFDL (adjusted forcing) and GISS
2120 (instantaneous forcing), but were not performed for the NCAR model. The annual-
2121 average global-mean radiative forcing (RF) from short-lived species at 2030 relative to
2122 2000 is small in both the GFDL and GISS models (Figure 3.3; Table 3.6). However, this
2123 is for quite different reasons. In the GFDL model, a large increase in sulfate optical depth
2124 leads to a negative forcing that is largely balanced by positive forcings from increased
2125 black carbon aerosol and ozone. In the GISS model, increased sulfate and reduced black
2126 carbon both lead to relatively small negative forcings that largely offset a substantial
2127 positive forcing from increased ozone. Moving to 2050, the models now diverge in their
2128 net values as well as the individual contributions. The GFDL model finds a positive
2129 radiative forcing due in nearly equal parts to increased black carbon and ozone. In
2130 contrast, 2050 radiative forcing in the GISS model again reflects an offset between
2131 positive forcing from ozone and negative aerosol forcing, with the largest contribution to

2132 the latter from reduced levels of black carbon. Both models show a partial cancellation of
 2133 the black carbon forcing by an opposing forcing from organic carbon. Thus, the two
 2134 models show somewhat consistent results for ozone, but differ dramatically for black
 2135 carbon and sulfate aerosol. By 2100, the GFDL model has a large positive radiative
 2136 forcing relative to 2000, due to the continued increase in black carbon as well as the
 2137 decrease in sulfate.

2138
 2139

Table 3.6 Global mean radiative forcing for short-lived species ($W m^{-2}$)

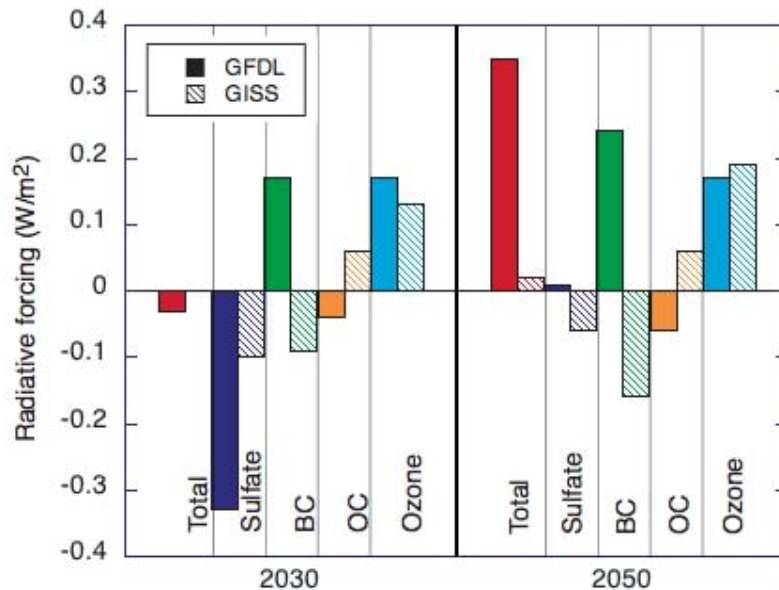
	Model	2030	2050	2100
Total	GFDL	.04	.48	1.17
	GISS	.00	.02	NA
Aerosols	GFDL	-.15	.24	.98
	GISS	-.13	-.17	NA
Sulfate	GFDL	-.32	.01	.51
	GISS	-.10	-.06	NA
BC	GFDL	.21	.30	.63
	GISS	-.09	-.16	NA
OC	GFDL	-.04	-.06	-.15
	GISS	.06	.06	NA
Ozone	GFDL	.19	.23	.19
	GISS	.13	.19	NA

2140 Values are annual average radiative forcings at the tropopause (meteorological tropopause in the GISS
 2141 model, 'linear' tropopause in the GFDL model). 'Aerosols' is the total of sulfate, black carbon (BC), and
 2142 organic carbon (OC) (plus nitrate for GISS). GISS values do not include aerosol indirect effects that were
 2143 present in that model.
 2144 GFDL values are for adjusted radiative forcing; GISS values are for instantaneous radiative forcing (see
 2145 Box 3.2). The GFDL values are from (Levy *et al.*, 2007).
 2146

2147 Inter-model differences in radiative forcing are predominantly due to differences in
 2148 modeled burdens rather than to differences in the calculation of radiative properties in the
 2149 models. This can be seen clearly by examining the RF-to-burden ratio, which we term the
 2150 radiative efficiency (Table 3.7). This shows fairly similar values for GFDL and GISS.
 2151 The largest differences are seen for black carbon, which may reflect differences in the
 2152 geographic location of projected black carbon changes as well as differing treatments of

2153 the radiative properties of black carbon. Additionally, the vertical distribution of the
2154 black carbon changes will affect the radiative forcing, as will their location relative to
2155 clouds. Variations in modeling the aerosol uptake of water, which can have a substantial
2156 impact on the aerosol optical depth, do not seem to play a very large role in the global
2157 mean radiative forcing judging from the fairly close agreement in the two models' sulfate
2158 radiative efficiencies (Table 3.7). They may contribute to the ~20% difference in the RF-
2159 to-burden ratios for sulfate, however. Examination of the RF-to-aerosol optical depth
2160 change (Table 3.7) shows that given a particular aerosol optical depth change, the models
2161 are in good agreement as to the resulting radiative forcing. We caution that this result
2162 contrasts with a wider model study that found larger differences in this ratio (Schulz *et*
2163 *al.*, 2006), though the variation in RF-to-aerosol optical depth across models was still
2164 less than the variation in aerosol optical depth itself. This suggests a possible further
2165 source of model differences that could exist were different models to be used in a study
2166 such as this.

2167



2168

2169

2170

2171

2172

2173

2174

Figure 3.3 Global mean annual average radiative forcing (in W m^{-2}) from short-lived species at 2030 and 2050 relative to 2000. Values from the GFDL model are shown as solid bars; values from the GISS model have diagonal hatching. (Note that instantaneous forcing values from the GFDL model are shown in this figure, not the adjusted forcings shown in Table 3.6.)

2175

2176

2177

2178

2179

2180

2181

2182

2183

2184

Both the GFDL and GISS models show a positive forcing from ozone that stems partially from increased tropospheric ozone concentrations (Table 3.2) due to increased NO_x emissions (Table 3.1) and partially from the recovery of stratospheric ozone due to reductions in emissions of ozone-depleting substances (primarily halogens). The forcing from the tropospheric portion of the ozone changes is substantially more important, however (Shindell *et al.*, 2007). (The NCAR group did not calculate the radiative forcing, but forcing in their model is likely to have been similar, as they found an increase in the tropospheric ozone burden from 2000 to 2050 of 15.0 Dobson Units (DU), very close to the GISS value of 16.2 DU (Table 3.2).) As shown previously, however, the apparent sensitivity of ozone burden to changes in NO_x emissions differs substantially between the GISS and GFDL models. Thus the similarity in the radiative forcing may be largely

2185 fortuitous, resulting from a cancellation of changes in emissions and of sensitivities of
 2186 ozone to NO_x emissions.
 2187
 2188 Thus, at 2030, differences in the physical processes in the two models dominate the
 2189 differences in radiative forcing between the two models. The large divergence in
 2190 radiative forcing from sulfate stems from both the chemical conversion efficiency of SO₂
 2191 to sulfate being more than a factor of two larger in the GFDL model than in the GISS
 2192 model, and the greater role of sulfate in producing aerosol optical depth in the GFDL
 2193 model. In addition, the GISS model includes a substantial absorption of sulfate onto dust,
 2194 a process that is highly uncertain. Such a process would reduce the radiative forcing due
 2195 to sulfate. At 2050, emissions and concentrations of sulfur dioxide have returned to near
 2196 their 2000 level, so that these differences are not so important at this time. Hence, the
 2197 2050 differences between the two models are dominated by differences in black carbon
 2198 emissions projections and not by differences in physical processes. Differences in the
 2199 residence times and radiative efficiencies for black carbon are substantial but tend to
 2200 offset.

2201
 2202

Table 3.7 Radiative efficiency.

Species	Model	(W m ⁻²)/Tg	(W m ⁻²)/AOD
BC	GFDL	2.8	104
	GISS	1.5	94
OC	GFDL	-0.18	NA
	GISS	-0.16	NA
Sulfate	GFDL	-.47	-16
	GISS	-.59	-16

2203 Values are given for the radiative efficiency in terms of the RF-to-burden ratio and the RF-to-aerosol
 2204 optical depth (AOD) ratio. All values are global-mean, annual-mean averages. Values for radiative forcing
 2205 and burden or aerosol optical depth changes are for 2050 versus 2000 for black carbon (BC) and organic
 2206 carbon (OC), and 2030 versus 2000 for sulfate in order to analyze the largest changes for each species.
 2207 GISS values for the sulfate burden changes include only the portion of sulfate not absorbed onto dust, as
 2208 this portion alone is radiatively important.

2209

2210 On a hemispheric scale, the GISS and GFDL models again differ greatly (Table 3.8). The
 2211 GFDL model shows a very large positive forcing in the Northern Hemisphere in 2050
 2212 due primarily to reductions in emissions of sulfate precursors and increased emissions of
 2213 black carbon. Increases in sulfate precursor emissions from developing countries lead to a
 2214 negative forcing in the Southern Hemisphere in the GFDL model. In the GISS model, the
 2215 sign of the total net forcings are reversed, with negative values in the Northern
 2216 Hemisphere and positive in the Southern Hemisphere (Table 3.8). The GISS results are
 2217 primarily due to the reduction in BC in the Northern Hemisphere and the influence of
 2218 increased ozone and reduced OC in the Southern Hemisphere (where sea-salt dominates
 2219 the aerosol optical depth, so that anthropogenic aerosol emissions changes are relatively
 2220 less important).

2221

2222

Table 3.8 Hemispheric radiative forcing ($W m^{-2}$).

	Model	2030	2050	2100
Northern Hemisphere	GFDL	.15	1.09	1.91
	GISS	-.15	-.14	NA
Southern Hemisphere	GFDL	-.09	-.14	.42
	GISS	.16	.18	NA

2223

2224

2225

Values are the net annual average forcings at the tropopause in each hemisphere from aerosols and ozone. GISS forcing values do not include aerosol indirect effects that were present in that model.

2226

3.3.3.2 Regional Forcing Patterns

2227

2228

2229

2230

2231

The differences in hemispheric and global forcings can be attributed to strong forcing changes in particular regions, and hence to regional emissions as the radiative forcing is typically localized relatively close to the region of emissions. Comparison of the spatial patterns of radiative forcing in the GISS and GFDL models reveals that the starkest discrepancies occur in the developing nations of South and East Asia (Figure 3.4). The

2232 emissions scenario used by the GISS model projects strong increases in SO₂ emissions
2233 from India, with little change over China. In contrast, the scenario used by the GFDL
2234 model has large decreases in sulfate emissions in both regions, especially China.

2235

2236 The scenarios are much more similar for the developed world, with both projecting
2237 reductions in sulfate precursor emissions for North America and Europe, for example,
2238 leading to a positive radiative forcing in both cases. Differences between the scenarios
2239 are even larger for black carbon, which increases throughout most of the Northern
2240 Hemisphere in the GFDL model but decreases in the GISS model. Again, however, the
2241 divergence is especially large over South and East Asia, where the GISS model has large
2242 reductions while the GFDL model has large increases (Figure 3.4). Thus the differences
2243 in the global total emissions discussed previously (Figure 3.1; Table 3.1) and in the
2244 global radiative forcing (Figure 3.2; Table 3.6) arise primarily from differences in
2245 projected emissions from developing countries in Asia.

2246

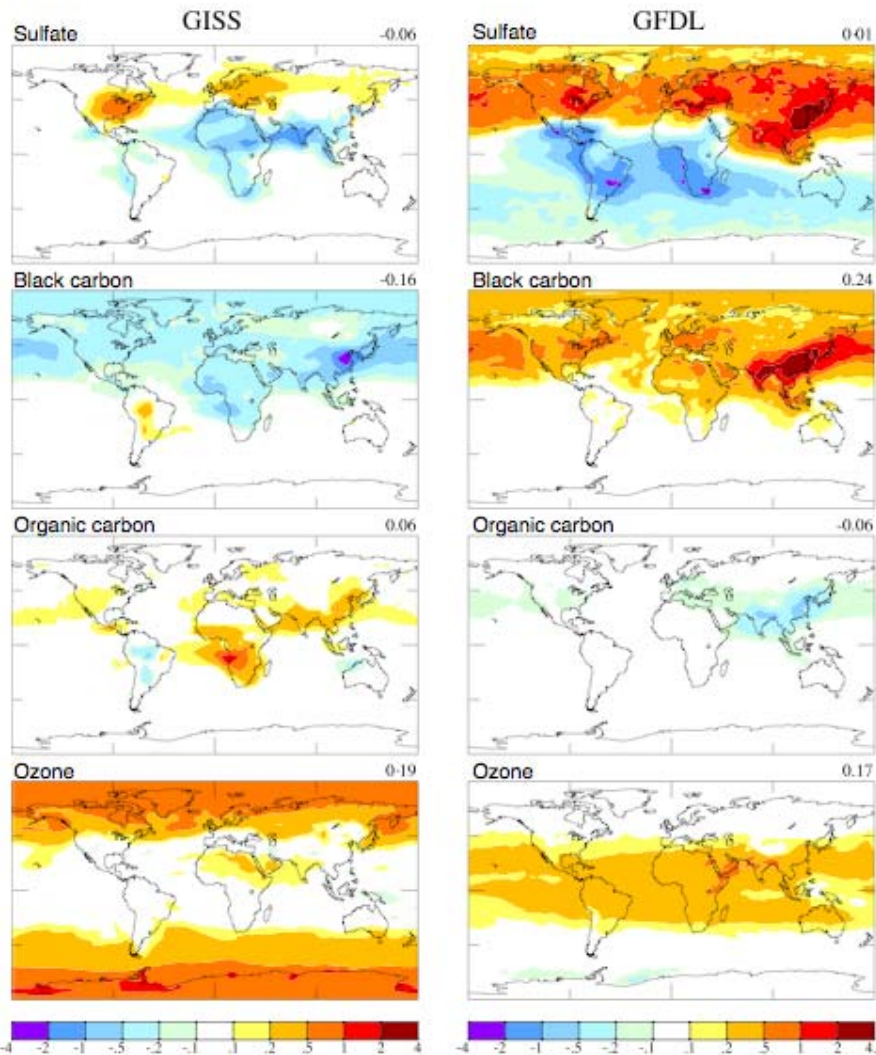
2247 The radiative forcing from organic carbon is generally similar in its spatial pattern to
2248 black carbon, but of opposite sign and substantially reduced magnitude (25-40% of the
2249 black carbon radiative forcing). Substantial differences again occur between the
2250 emissions scenarios of the two models, this time primarily over African biomass burning
2251 regions. As discussed previously, the GFDL model assumed that biomass burning
2252 emissions would scale with ½ the factor used for purely anthropogenic emissions, while
2253 the GISS model instead used regional biomass burning emissions projections from
2254 (Streets *et al.*, 2004), with substantial reductions in African biomass burning.

2255

2256 The spatial pattern of radiative forcing from ozone is also very different in the two
2257 models (Figure 3.4). However, this forcing is not so closely tied to the region of precursor
2258 emissions in the GISS model where much of the forcing is related to an increased flux of
2259 ozone into the troposphere owing to the recovery of lower stratospheric ozone. This leads
2260 to substantial positive forcing in that model at high latitudes, even without including the
2261 effects of climate change on circulation (see section 3.3.3.4). At low latitudes, GISS
2262 shows little forcing as the modeled increase in upper stratospheric ozone causes cooling
2263 which offsets part of the warming caused by lower stratospheric ozone increases.

2264 Additionally, the overall increase in overhead stratospheric ozone reduces the
2265 photochemical formation of ozone in the troposphere, offsetting some of the
2266 enhancement there due to increased precursor emissions. The GFDL model does not
2267 show a similar high latitude enhancement, however, but instead shows maximum ozone
2268 forcing in the tropics. This may reflect a greater geographic shift in emissions to lower
2269 latitudes, a greater efficiency in transporting ozone and its precursors to the upper
2270 troposphere, where ozone has the greatest positive forcing efficiency, and differences in
2271 the relative importance of change in the overlying stratospheric ozone column. The
2272 GFDL radiative forcing is similar to results from models with tropospheric ozone only
2273 (Gauss *et al.*, 2003).

2274



2275
 2276 **Figure 3.4** Annual average instantaneous radiative forcing ($W m^{-2}$) near 2050 relative to 2000 for the
 2277 indicated individual short-lived species in the GISS (left) and GFDL (right) models. Radiative forcing from
 2278 long-lived species is largely spatially uniform over the globe. (Note that the instantaneous forcings shown
 2279 here for the GFDL model differ from the adjusted forcings show in Table 3.6.).
 2280

2281 **3.3.3.3 Effects of uncertainties in methane concentrations on radiative forcing**

2282 The SAP 3.2 simulations included methane concentrations prescribed to A1B values from
 2283 the AIM integrated assessment model, for consistency with the long-lived species runs.

2284 To investigate the potential uncertainty in the methane value derived by that integrated
 2285 assessment model , the GISS model performed an additional 2050 simulation using its

2286 internal methane cycle model (Shindell *et al.*, 2007). The simulation included prescribed
2287 anthropogenic emissions increases from the AIM model to allow comparisons with the
2288 AIM results used in the results in this report (SAP 3.2). Natural spatially and seasonally
2289 varying emissions and soil adsorption were the standard amounts described in (Shindell
2290 *et al.*, 2003). Both the methane emissions from wetlands and the biogenic isoprene
2291 emissions were interactive with the climate in this run (Guenther *et al.*, 1995; Shindell *et*
2292 *al.*, 2004), though the distribution of vegetation did not respond to climate change.
2293
2294 Methane's oxidation rate is calculated by the model's chemistry scheme in both the
2295 troposphere and stratosphere. Thus methane can affect its own lifetime (which is
2296 primarily governed by tropospheric oxidation rates), as can other molecules that compete
2297 with methane for hydroxyl radicals (the main oxidizing agent), such as isoprene. The
2298 simulations included 2050 surface climate (sea-surface temperatures and sea ice, taken
2299 from an earlier climate model run). Changes in water vapor induced by the altered
2300 climate affect methane oxidation in those runs. Methane was initialized with estimated
2301 2050 abundances and the simulations were run for 3 years. We note that the IMAGE
2302 integrated assessment model projected a continuous increase in methane emissions, rather
2303 different from the increase through 2030 and slow decrease thereafter in the AIM
2304 integrated assessment model. At 2050, for example, this led to projected anthropogenic
2305 methane emissions of 512 Tg/yr in the IMAGE model, substantially greater than the 452
2306 Tg/yr from the AIM model used here (compared with 323 Tg/yr for 2000).
2307

2308 We find that methane emissions from wetlands increase from 195 to 241 Tg/yr while
2309 emissions of isoprene increase from 356 to 555 Tg/yr. Additionally, even in the absence
2310 of changes in emissions from natural sources, the projected anthropogenic emissions of
2311 ozone precursors (including methane itself) increase the lifetime of methane while
2312 climate change reduces it via increased temperature and water vapor (Table 3.9). These
2313 responses to anthropogenic emissions and to climate change without interactive
2314 emissions are qualitatively consistent with those reported from a range of models (using
2315 different emissions projections) in (Stevenson *et al.*, 2006). The effect of precursor
2316 emissions is stronger in our scenario, so that the net effect of anthropogenic emissions
2317 and climate changes is to increase methane's lifetime. When natural emissions are also
2318 allowed to respond to climate change, increased competition from isoprene and increased
2319 methane emissions from wetlands lead to further increases in methane's lifetime (Table
2320 3.9) and enhanced methane abundance.

2321

2322 The 2050 simulation with the model's internal methane cycle had a global mean surface
2323 methane value of 2.86 ppmv in year 3, with sources exceeding sinks by 80 Tg/yr (a
2324 growth rate that may reflect an overestimate of the loss rate in the AIM model used in the
2325 initial guess). Extrapolating the change in methane out to equilibrium using an
2326 exponential fit to the three years of model results yields a 2050 value of 3.21 ppmv.

2327

2328 We have calculated radiative forcings using the standard calculation (Table 6.2 in
2329 (Ramaswamy *et al.*, 2001)) assuming an increase in N₂O from 316 to 350 ppb in 2050,
2330 following the A1B 'marker' scenario (using the AIM integrated assessment model). The

2331 2050 methane forcing using the methane concentration specified in the A1B ‘marker’
2332 scenario would be 0.22 W m^{-2} while using the larger methane concentrations of 2.86 or
2333 3.21 ppmv calculated with our model gives 0.36 or 0.46 W m^{-2} , respectively. Of course, it
2334 is difficult to estimate methane’s abundance at a particular time without performing a full
2335 transient methane simulation. However, uncertainty in the forcing from methane appears
2336 to be at least $0.1\text{-}0.2 \text{ W m}^{-2}$. Note that use of the 40% larger anthropogenic methane
2337 emission increase from the IMAGE integrated assessment model would have led to a
2338 substantially larger forcing. Should the results of our modeling of the methane cycle
2339 prove to be fairly robust, this would imply that future positive forcing from methane
2340 might be substantially larger than current estimates based on integrated assessment model
2341 projections.

2342

2343 We note that while the A1B projections assume a substantial increase in atmospheric
2344 methane in the future, the growth rate of methane has in fact decreased markedly since
2345 the early 1990s and leveled off since ~1999 (Dlugokencky *et al.*, 2003). Hence, the
2346 projections may overestimate future atmospheric concentrations. However, there are
2347 indications that the growth rate decrease was primarily due to reduced anthropogenic
2348 emissions, and that these have been increasing again since 1999 (though masked by a
2349 coincident decrease in natural methane emissions) (Bousquet *et al.*, 2006). All of this
2350 suggests that atmospheric methane may in fact increase substantially again in the future,
2351 as assumed by the integrated assessment models, although other methane studies have
2352 argued for an increase in its principle loss path as the explanation, rather than changes in
2353 emissions (*e.g.* Fiore *et al.*, 2006). Other emissions, such as NO_x from lightning and from

2354 soil and dimethyl-sulfide from the oceans, are also expected to respond to climate
 2355 change. Changes in land cover would also affect both emissions and removal of trace
 2356 species. Further work is required to gauge the importance of these and other climate-
 2357 chemistry feedbacks.

2358 **Table 3.9** Methane lifetime in GISS simulations. Includes calculated photochemical loss (in troposphere
 2359 and stratosphere) and prescribed 30 Tg/yr loss to soils.

Run	Lifetime (years)
2000	9.01
2030	9.96
2050	10.39
2030 with climate change	9.72
2050 with climate change	10.01
2050 with methane cycle	10.42

2360

2361 **3.3.3.4 Effects of Climate Change on Radiative Forcing**

2362 The chemical composition simulations (Section 3.2) did not include the effects of climate
 2363 change on the short-lived species, only the effects of projected changes in anthropogenic
 2364 emissions. Separate sets of simulations with the GISS model included climate change via
 2365 prescribed sea-surface temperatures and sea-ice cover taken from prior runs. Climate
 2366 change increased the radiative forcing from ozone by increasing stratosphere-troposphere
 2367 exchange (STE) and hence ozone near the tropopause where it is most important
 2368 radiatively (Hansen *et al.*, 1997). This effect outweighed increased reaction of excited
 2369 atomic oxygen with the enhanced tropospheric water vapor found in a warmer climate,
 2370 which led to ozone reductions in the tropical lower troposphere. The overall impact was
 2371 to increase radiative forcing by $.07 \text{ W m}^{-2}$ in 2050. Climate change slightly increased the
 2372 negative forcing from sulfate (by $.01 \text{ W m}^{-2}$), consistent with an increase in tropospheric
 2373 ozone in these runs (as ozone aids in sulfur dioxide oxidation both directly and via
 2374 hydroxyl formation).

2375

2376 Dust emissions decreased slightly (~5% at 2050) in these climate runs, but there was
2377 more sulfate on dust, suggesting that this played only a minor role in the sulfate forcing
2378 response to climate change. The reduction in dust would itself lead to a slight negative
2379 forcing ($\sim 0.02 \text{ W m}^{-2}$). However, emissions in the model respond only to changes in
2380 surface wind speeds, and not to changes in sources due to either CO₂ fertilization or
2381 climate-induced vegetation changes which have a very uncertain effect on future dust
2382 emissions (Mahowald and Luo, 2003; Woodward *et al.*, 2005).

2383

2384 Much of the increase in ozone forcing results from an increase in stratosphere-
2385 troposphere exchange in the GISS model of 134 Tg/yr (~27% of its present-day value) as
2386 climate warms. An increase in transport rates between the stratosphere and the
2387 troposphere is a robust projection of climate models (Butchart *et al.*, 2006). Combined
2388 with the expected recovery of stratospheric ozone, this should enhance the influx of
2389 stratospheric ozone into the lower atmosphere. However, the net effect of climate change
2390 on ozone is more difficult to determine as it results from the difference between enhanced
2391 stratosphere-troposphere exchange and enhanced chemical loss in the troposphere in a
2392 more humid environment, which is not consistent among climate models (Stevenson *et*
2393 *al.*, 2006).

2394

2395 3.3.4 Climate Model Simulations 2000 – 2050

2396 As discussed in Section 3.3.1, the experimental design consists of two sets of simulations:
2397 1) the effects of changes in short-lived and long-lived species in the 21st century

2398 (employing the A1B scenario for the evolution of the long-lived species and the output
2399 from the composition models discussed on Section 3.2 for the short-lived species); 2) the
2400 effects of changes in the long-lived species only, with the short-lived species
2401 concentrations held at 2000 values. The effects of short-lived species changes are
2402 determined by subtracting the climate responses of the runs with changes in long-lived
2403 species only from those with changes in long-lived and short-lived species. Simulations
2404 where only the short-lived species change were not included in the experimental design,
2405 because such a scenarios are neither realistic nor policy relevant

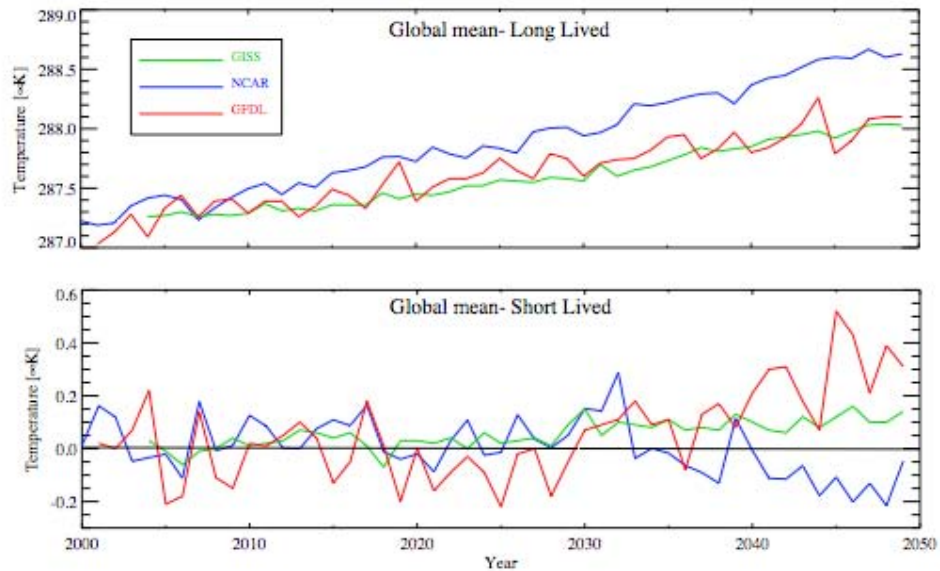
2406

2407 **3.3.4.1 Surface Temperature Changes**

2408 The global-mean annual-mean surface temperature responses to short-lived species are
2409 not as dissimilar as one might have expected, given the different emissions used and the
2410 different physical processes included. The NCAR model ran only a single simulation,
2411 which showed little or no statistically significant³⁸ effects of the short-lived species on
2412 global mean surface temperatures. The GFDL and GISS models both ran 3-member
2413 ensemble simulations, and both show a statistically significant warming effect from
2414 short-lived species from around 2030 to the end of the runs (Figure 3.5). The GFDL
2415 model shows a warming of 0.28 K (ensemble mean 2046-2050). This value is
2416 commensurate with the adjusted radiative forcing of $\sim 0.48 \text{ W m}^{-2}$. computed for 2050.
2417 The GISS model shows substantially more warming, $\sim 0.13 \text{ K}$ near 2050, than would be
2418 expected from the direct radiative forcing in that model and its climate sensitivity ($\lambda =$
2419 $\sim 0.6 \text{ K (W m}^{-2}\text{)}^{-1}$) owing to the presence of the aerosol indirect effect, which contributes
2420 additional warming as aerosol loading decreases in the future (Shindell *et al.*, 2007).

³⁸ The statistical methods used to assess significance are discussed in Box 3.3.

2421



2422
 2423
 2424
 2425
 2426
 2427

Figure 3.5 Global mean annual average temperature in the simulations with time-varying long-lived (top) and short-lived (bottom) species. Results are 3-member ensemble means for GFDL and GISS and single-member simulations for NCAR. Results for the short-lived species are obtained by subtraction of the (long-lived) species calculations from the (short + long-lived) species calculations.

2428 The overall global annual average influence of short-lived species is to augment the
 2429 warming from well-mixed greenhouse gases by ~20-25% in these two models (17% for
 2430 GISS and 27% for GFDL based on 2046-2050 vs. the first 5 years of the run). It is
 2431 important to note, however, that these models responded as they did for different reasons.

Box 3.3: Statistical Methods

A result is deemed to be statistically significant if it is unlikely to have occurred by chance (*i.e.*, the probability that it occurred by chance is less than some specified threshold). A 95% confidence level means that the odds are 20:1 against the result having occurred by chance..

Statistical significance in the GFDL climate model results was evaluated using two approaches. For global-mean, or hemispheric-mean results involving a temperature departure from the initial (2000) value, the range (highest to lowest temperature change) of the three ensemble members used to obtain the ensemble-mean result was computed. The ensemble-mean result was deemed significant if that range was entirely different from zero. For regional (latitude-longitude) results comprising the difference of two time series, as in the evolution of temperature change due to short-lived species, the student-t test for significance was applied at each model grid point, with the result deemed significant if the statistical test showed significance at the 95% confidence level.

2432

2433

In the GFDL simulations, reduced sulfate and increased black carbon and ozone all

2434

combined to cause warming. In contrast, in the GISS model, the warming resulted from

2435

increased ozone and a reduced aerosol indirect effect, with a substantial offset (cooling)

2436

from reduced black carbon. The lack of a substantial effect from short-lived species in the

2437

NCAR simulations is attributable to the emissions used, which produced small increases

2438

in sulfate (cooling) and small increases in black carbon (warming) that largely offset one

2439

another (thus their aerosol optical depth changed little from 2000 to 2050).

2440

2441

Hemispheric temperatures show trends largely consistent with the radiative forcings

2442

(Table 3.8), namely substantial warming in the Northern Hemisphere in the GFDL model

2443

and in the Southern Hemisphere in the GISS model (Figure 3.6). The Northern

2444

Hemisphere warming in the GFDL model is driven primarily by the large decreases

2445

projected for sulfate and the large increase projected for black carbon in that model for

2446

the industrialized areas of the Northern Hemisphere (Levy *et al.*, 2007). This causes the

2447

aerosol optical depth from sulfate to drop by 1/3 in the Northern Hemisphere by 2050

2448

while the aerosol optical depth from black carbon increases by 50%. The large change in

2449 sulfate dominates the overall aerosol optical depth change in that model (Table 3.5). The
2450 magnitude of the Northern Hemisphere warming is ~0.5 K by 2050, consistent with the
2451 ~1.1 W m⁻² radiative forcing in that model, when one accounts for the fact that the
2452 warming has not been fully realized due to the lag-time for oceanic heat adjustment.
2453 There is an overall negative forcing in the Southern Hemisphere in the GFDL model, as
2454 sulfate precursor emissions increase in the developing world while black carbon changes
2455 little. Some of the negative forcing from aerosols in the Southern Hemisphere is offset by
2456 positive forcing from ozone, which increases rather uniformly over much of the world in
2457 that model (Levy *et al.*, 2007), leading to a small net effect and minimal temperature
2458 change from short-lived species (Figure 3.6).

2459

2460 The change in the forcing due to the aerosol indirect effect in the GISS model was argued
2461 to be on the order of 0.1 W m⁻² in 2050 (Shindell *et al.*, 2007). Combining this with the
2462 GISS hemispheric radiative forcings (excluding the indirect effect) in Table 3.8 yields a
2463 Northern Hemisphere radiative forcing near zero and a Southern Hemisphere forcing of
2464 ~0.3 W m⁻². These forcings are consistent with the warming of ~0.15 K seen in that
2465 model in the Southern Hemisphere and the lack of response in the Northern Hemisphere.
2466 Northern Hemisphere aerosol optical depth changes are dominated by a substantial
2467 reduction in black and organic carbon (the black carbon aerosol optical depth in the
2468 Northern Hemisphere falls by nearly 50%), which more than offsets a slight increase in
2469 sulfate (particularly as this model is less sensitive to sulfate). These aerosol changes lead
2470 to negative Northern Hemisphere forcing. In the Southern Hemisphere, the GISS model
2471 shows only small changes in aerosols, so that positive forcing from ozone dominates the

2472 net radiative forcing. The aerosol indirect effect further accentuates the positive forcing
2473 owing to reductions in black carbon and organic carbon. The signs of the temperature
2474 response in the two hemispheres are thus opposite in the GISS model to what they are in
2475 the GFDL model.

2476

2477 As for the global case, trends in the NCAR model are not significantly different in the
2478 runs with and without short-lived species. This is the result of only a miniscule change in
2479 aerosol optical depth in the Northern Hemisphere (-2%), as sulfate and carbonaceous
2480 aerosol precursor emissions are both near their present-day values by 2050 in that model.
2481 In the Southern Hemisphere, there is an increase in aerosol optical depth from 2000 to
2482 2050, which seems to be primarily due to sulfate, but this is largely offset by increased
2483 ozone in the Southern Hemisphere as stratospheric ozone recovers.

2484

2485 Thus it is clear that at global and especially at hemispheric scales, the three climate
2486 models are being driven by substantially different trends in their aerosol species. These
2487 differences in aerosols are largely related to the differences in the projected emissions of
2488 aerosol precursors, though there is some contribution from differences in aerosol
2489 modeling as discussed previously. Additionally, the climate response of each model is
2490 different to some extent owing to the inclusion of different physical processes in the
2491 models, especially the inclusion of the aerosol indirect effect in the GISS model.

2492 However, the above analysis strongly suggests that the largest contributor to the inter-
2493 model variations in projected warming arise from different assumptions about emissions
2494 trends.

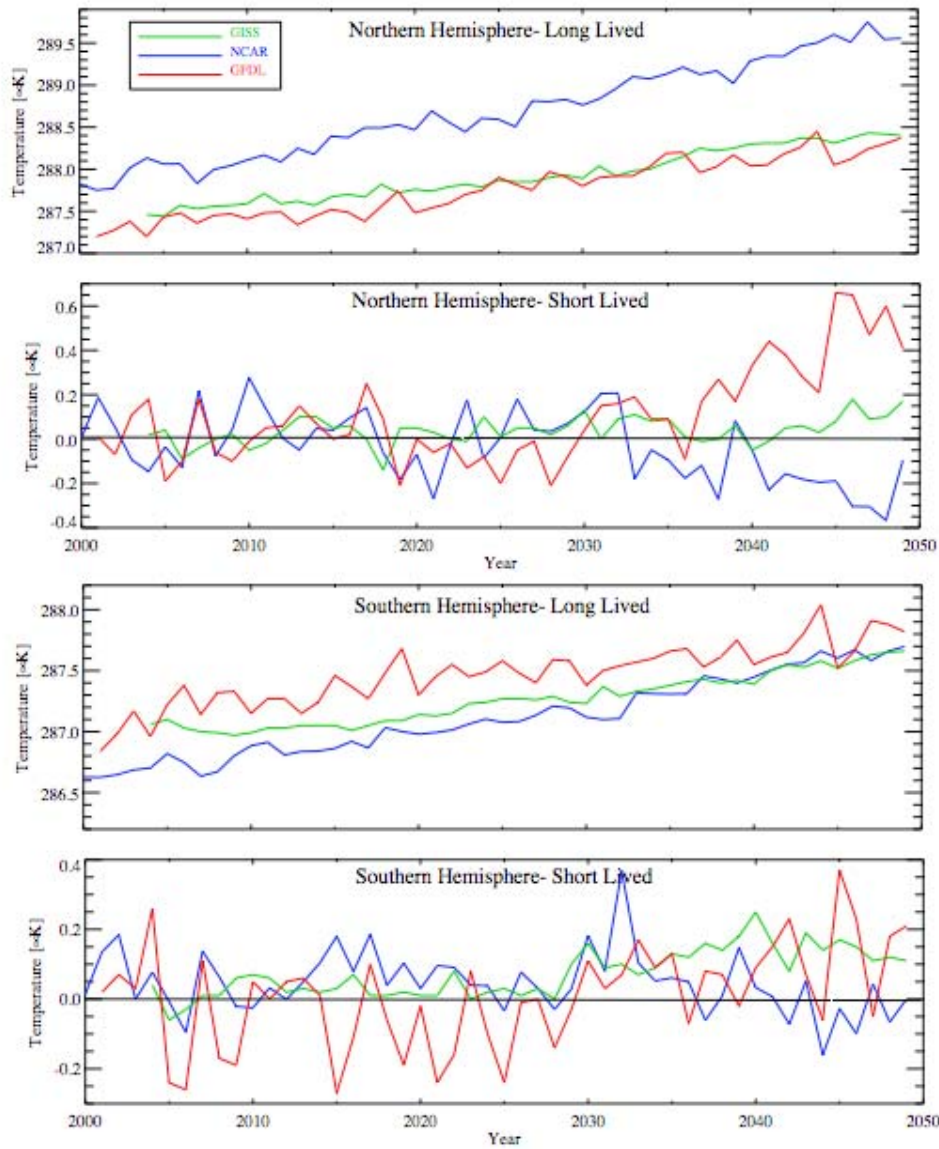
2495

2496 At smaller spatial scales, the annual average patterns of surface temperature changes
2497 induced by the short-lived species show even larger divergences (Figure 3.7). Around
2498 2030, the largest responses are seen at Northern middle and high latitudes. These show
2499 large regions of both cooling and warming that are characteristic of the response to
2500 dynamic variations. Surprisingly, all three models show cooling near Alaska and a region
2501 of warming over Siberia. However, most of the response at these latitudes is not
2502 statistically significant in the models owing to large natural variability. Other regions,
2503 such as the Labrador Sea/Baffin Island area or Scandinavia, show substantial variations
2504 between models, again suggesting these middle and high latitude dynamic responses are
2505 not robust.

2506

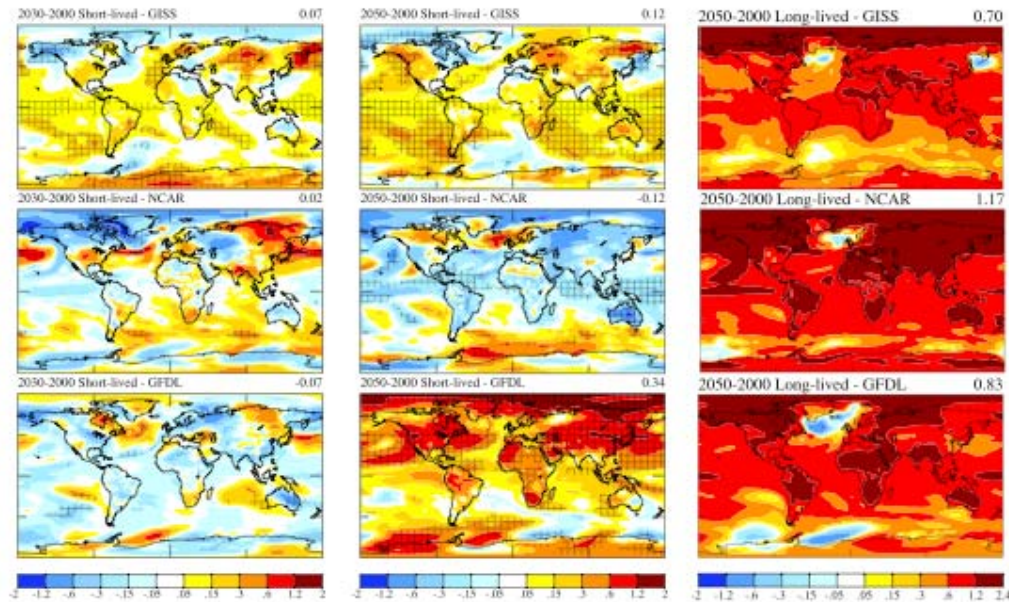
2507 In the tropics, where dynamic variability is much smaller, the models find much greater
2508 areas with statistically significant responses, especially by 2050. The NCAR model finds
2509 a small but significant cooling over tropical oceans, while the other models find warming.
2510 As in the global-mean case, this appears to arise from differences in aerosol burdens and
2511 optical depths.

2512



2513
 2514
 2515
 2516
 2517
 2518

Figure 3.6 Hemispheric mean annual average temperature in the simulations with time-varying long-lived and short-lived species. Results are ensemble means for GFDL and GISS.



2519
2520
2521
2522
2523
2524
2525
2526
2527

Figure 3.7 Annual average surface temperature response (K) in the climate models to short-lived species (left and center columns) and long-lived species (right column) changes for the indicated times. The changes at 2030 are 2020-2029 in the NCAR and GFDL models and 2028-2033 in the GISS model. At 2050, they are 2040-2049 in the NCAR model, 2046-2055 in the GFDL model, and 2040-2050 in the GISS model. Hatching indicates statistical significance (95%) for the response to short-lived species. Virtually all colored values are statistically significant in the response to long-lived species. Values in the upper right corners give the global mean.

2528 In the Arctic, the GISS and NCAR models find primarily a cooling effect from projected
2529 changes in short-lived species (especially near 2030 for GISS, and 2050 for NCAR). In
2530 contrast, the GFDL model finds a substantial warming there. This may be due in part to
2531 the increasing trend in black carbon in that model.

2532

2533 In the Antarctic, the GISS model shows warming related primarily to stratospheric ozone
2534 recovery. The GFDL model shows a similar result by 2050 (after which stratospheric
2535 ozone was unchanged in that model). NCAR does not show as clear an Antarctic
2536 warming, however, even though this model also included recovery of ozone in the
2537 Antarctic lower stratosphere. This is surprising given that the NCAR model appeared to

2538 show a substantial response to ozone depletion in analyses of the Southern Hemisphere
2539 circulation in IPCC AR4 simulations (Miller *et al.*, 2006b). That analysis showed that
2540 most climate models found a general strengthening of the westerly flow in the Southern
2541 Hemisphere in response to stratospheric ozone depletion. A stronger flow isolates the
2542 polar region from lower latitude air, leading to cooling over the Antarctic interior and
2543 warming at the peninsula. Conversely, recovery should lead to warming of the interior
2544 (enhanced by the direct positive radiative forcing from increased ozone), as in the GISS
2545 and GFDL simulations. However, in the GISS model the effect diminishes with time,
2546 suggesting that other aspects of the response to short-lived species become more
2547 important in these scenarios over time, presumably as projected aerosol changes grow
2548 ever larger.

2549

2550 Warming over the central United States is present in the GISS model at all times (but is
2551 not statistically significant), in the GFDL model from about the 2040s on, and in the
2552 NCAR model around 2030, but not at 2050. The United States and other Northern
2553 Hemisphere industrialized regions might be especially sensitive due to the projected
2554 reduction in sulfate precursor emissions in the Northern Hemisphere. This effect is
2555 especially large in the GFDL model, where forcings from sulfate decreases and black
2556 carbon increases both contribute to warming, though it should be noted that the largest
2557 radiative forcing is over Asia, not over the US and Europe (Fig. 3.4). In the NCAR
2558 model, the warming effect vanishes by 2050 as both sulfate and black carbon decrease,
2559 producing temperature responses of opposite sign. In the GISS model, reductions in

2560 sulfate and increases in ozone both contribute to warming; however, these are partially
2561 offset by cooling from reduced black carbon.

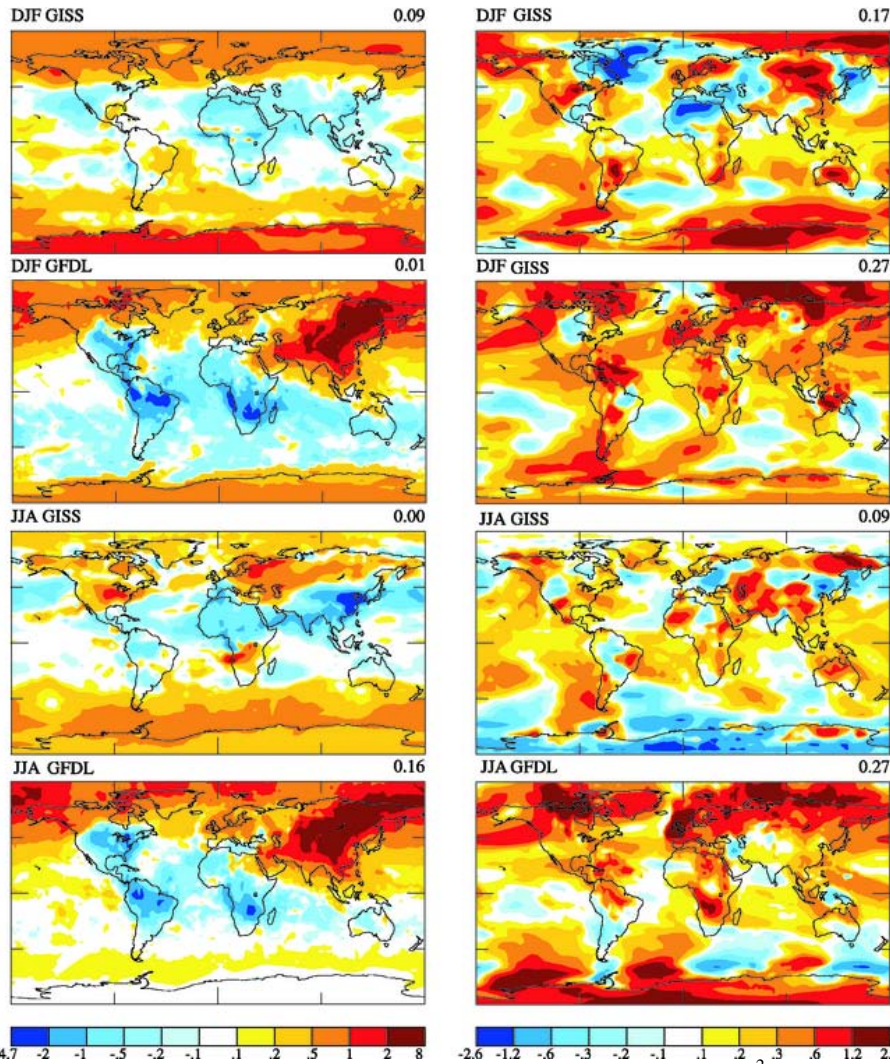
2562

2563 The surface temperature changes induced by the long-lived species are clearly much
2564 larger than those induced by short-lived species over most of the Earth by 2050 (Figure
2565 3.7). In some regions, however, the two are of comparable magnitude (*e.g.* the polar
2566 regions and parts of the Northern mid-latitude continents in the GFDL model, parts of the
2567 Southern Ocean in the GISS model). Consistency between the models is also clearly
2568 greater in their response to long-lived than to short-lived species.

2569

2570 Overall, it is clear that the regional surface temperature response does not closely follow
2571 the regional radiative forcing patterns based on either GISS or GFDL results. Both
2572 models show very large forcings over East Asia, for example, yet have minimal response
2573 there. This is especially clear when comparing the seasonal radiative forcings and climate
2574 response (Figure 3.8). Though some of the spatial mismatches could result from a lag in
2575 the climate response to seasonally varying forcings, the divergence between the patterns
2576 of forcing and response is large even for areas with minimal seasonality in the forcing
2577 (*e.g.* Africa, subtropical Asia).

2578



2579
2580
2581
2582
2583
2584
2585
2586
2587

Figure 3.8 Seasonal average net tropopause instantaneous radiative forcing ($W m^{-2}$) in 2050 versus 2000 from short-lived species (left column) and surface temperature (K) response (right column) in the GISS and GFDL models. Boreal winter (December-February) is shown in the top two rows, while boreal summer (June-August) is shown in the bottom two rows. The temperature changes at 2050 are 2046-2055 in the GFDL model and 2041-2050 in the GISS model. Values in the upper right corners give the global mean. (Note that the instantaneous forcings shown here for the GFDL model differ from the adjusted forcings show in Table 3.6.).

2588

3.3.4.2 Precipitation, Sea-level Rise, Soil Moisture, etc.

2589
2590
2591
2592

Changes in other climate parameters such as precipitation or sea level due to short-lived species are typically too small to isolate statistically. These would generally be expected to follow the global mean surface temperature change, however, for many of the most important features. For example, the portion of sea-level rise attributable to thermal

2593 expansion of the oceans would be enhanced by ~20-25% due to short-lived species in the
2594 GISS and GFDL models. Similarly, the enhancement of precipitation along the equator
2595 and drying of the subtropics that is a robust feature of climate models under a warming
2596 climate (Held and Soden, 2006) would also be accentuated under the GFDL and GISS
2597 models with their significant tropical warming, though probably not under the NCAR
2598 scenario. Such a feature can indeed be seen in the GISS response in the Atlantic and
2599 Indian Oceans.

2600

2601 On a regional scale, there are some suggestions of trends but statistical significance is
2602 marginal for either annual or seasonal changes. The NCAR model shows reductions in
2603 winter precipitation due to short-lived species across most of the United States in the
2604 2040s, and reductions in summer precipitation in the southeastern part of the United
2605 States. That model also suggests an increase in summer monsoon rainfall over South
2606 Asia. In contrast, the GISS model shows slight increases in winter precipitation over the
2607 central United States, and a mixed signal in summer (and spring) with increased
2608 precipitation over the Southeast and Southwest United States but decreases over the
2609 Northeast United States. During fall, precipitation decreases over most of the country. As
2610 in the NCAR model, there is an increase in summer (and fall) precipitation over South
2611 Asia. In the annual average, the GFDL model shows no statistically significant trend over
2612 the United States. Given that significant trends are hard to identify in any of the models,
2613 and that the models do not agree on the trends themselves, we believe that it is not
2614 possible to reliably estimate precipitation trends owing to short-lived species changes
2615 under the A1B storyline.

2616

2617 **3.3.4.3 Discussion**

2618 In the transient climate simulations, three climate models examined the response to
2619 projected changes in short-lived species. The results differed substantially among the
2620 models. Comparison has shown that the differences in the underlying emissions
2621 projections, due to differences between the various Integrated Assessment Models that
2622 provided those projections and to assumptions made about emissions not provided by the
2623 Integrated Assessment Models, were the dominant source of inter-model differences in
2624 projected aerosol trends. These were not the only source of differences, however. For
2625 example, the GFDL model's aerosol optical depth is substantially more sensitive to
2626 sulfate than the GISS model, with the NCAR model in between. This is partially due to
2627 the inclusion of sulfate absorption onto dust being present only in the GISS model.
2628 Additionally, the indirect effect of aerosols was included only in the GISS model. Thus,
2629 the inclusion of different physical processes played a role in the inter-model differences,
2630 and was especially important near 2030, when sulfur dioxide (SO₂) emissions were near
2631 their peak. With the inclusion of the aerosol indirect effect, the GFDL model might yield
2632 a substantially larger warming, given that sulfate is the largest contributor to aerosol mass
2633 globally and that the GFDL sulfate concentrations decreased beyond 2030.

2634

2635 Differences were also created by the models' differing simulations of the hydrologic
2636 cycle, which removes soluble species, and oxidation. Inter-model differences between the
2637 GFDL and GISS models in the residence times of aerosols were substantial for sulfate,
2638 and differences in the radiative effect of black carbon were also potentially sizeable. In

2639 nearly all cases, however, these were outweighed by emissions differences. This was not
2640 the case for sulfate at 2030, nor for tropospheric ozone; differences in the modeled
2641 conversion of SO₂ to sulfate and the sensitivity of ozone to NO_x emissions were larger
2642 than differences in projected precursor emissions. Hence, in these cases uncertainties in
2643 physical processes, including chemistry, dominate over uncertainties in emissions.

2644

2645 We also reiterate that uncertainties in the aerosol indirect effect and in internal mixing
2646 between aerosol types are either not included at all or only partially in these simulations.
2647 Sensitivity studies and analysis of the GISS model results indicates that the forcing from
2648 reductions in the aerosol indirect effect was roughly 0.1-0.2 W m⁻², while the inclusion of
2649 sulfate absorption onto dust reduced the negative forcing from sulfate at 2030 or 2050 by
2650 up to 0.2 W m⁻² (Shindell *et al.*, 2007). These sensitivities suggest that uncertainties in
2651 these processes could alter the global mean projected temperature trends by up to 0.1 K at
2652 2030 or 2050, a value comparable to the total temperature trend in that model. Hence
2653 without the aerosol indirect effect, the GISS model would likely have shown minimal
2654 warming, while without sulfate absorption onto dust surface it would like have shown a
2655 substantially greater warming trend (at least at 2030).

2656

2657 The responses of methane (and other hydrocarbon) emissions and of stratosphere-
2658 troposphere exchange to climate change can also potentially have significant impacts on
2659 radiative forcing, and these processes were not included in these simulations. As
2660 discussed in sections 3.3.3.3 and 3.3.3.4, the resulting changes to radiative forcing could
2661 again substantially alter the projected temperature trends. Additionally, given the large

2662 influence of uncertainties in emissions projections, we stress that the magnitude and even
2663 the sign of the effects of short-lived species on climate might be different were alternative
2664 emissions projections used in these same models. Thus, the response of short-lived
2665 species and methane has been only partially characterized by the present study, and
2666 substantial work remains to reduce uncertainties and further clarify the potential role of
2667 short-lived species in future climate change.

2668

2669 The results clearly indicate that the spatial distribution of radiative forcing is generally
2670 less important than the spatial distribution of climate sensitivity in predicting climate
2671 impact. Thus, both short-lived and long-lived species appear to cause enhanced climate
2672 responses in the same regions of high sensitivity rather than short-lived species having an
2673 enhanced effect primarily in or near polluted areas. This result is supported by analysis of
2674 the response to larger radiative perturbations in these models for the future (Levy *et al.*,
2675 2007) and the past (Shindell *et al.*, 2007). It is also consistent with earlier modeling
2676 studies examining the response to different inhomogeneous forcings than those
2677 investigated here (Mitchell *et al.*, 1995; Boer and Yu, 2003; Berntsen *et al.*, 2005;
2678 Hansen *et al.*, 2005). This suggests that the mismatch between model simulations of the
2679 regional patterns of 20th century climate trends and observations is likely not attributable
2680 to unrealistic spatially inhomogeneous forcings imposed in those models. Instead, the
2681 models may exhibit regional climate sensitivities that do not match the real world, and/or
2682 some of the observed regional changes may have been unforced.

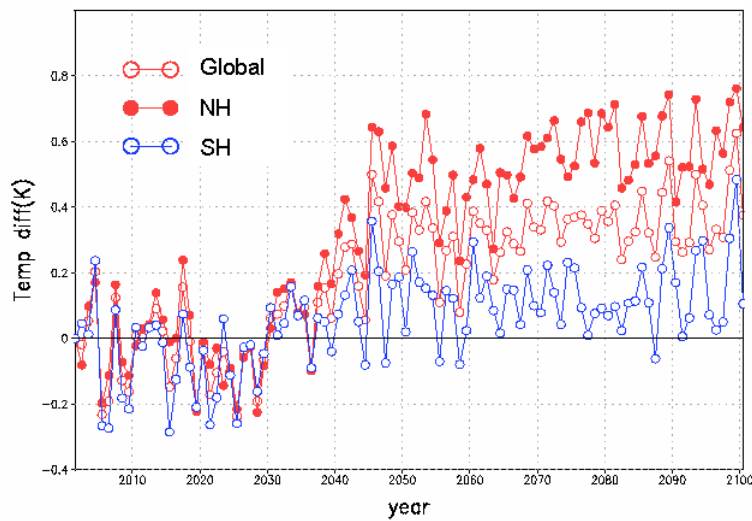
2683

2684

2685 **3.3.5 Climate Simulations Extended to 2100**

2686 Following the A1B “marker” scenario into the second half of the 21st century for both
 2687 three-member ensembles, the GFDL simulations (Levy *et al.*, 2007) find significant
 2688 climate impacts due to emissions of sulfur dioxide (SO₂), the precursor of sulfate aerosol,
 2689 (which decrease to ~35% of 2000 levels by year 2100) and of black carbon (scaled to
 2690 carbon monoxide emissions in the GFDL model) which continue to increase. This is
 2691 confirmed by their respective radiative forcing values for 2100 in Table 3.6. By 2080 –
 2692 2100, these projected changes in emission levels of short-lived species contribute a
 2693 significant portion of the total predicted surface temperature warming for the full A1B
 2694 scenario; 0.2°C in the Southern Hemisphere, 0.4°C globally, and 0.6°C in the Northern
 2695 Hemisphere as shown in the time series of yearly average surface temperature change in
 2696 Figure 3.9.

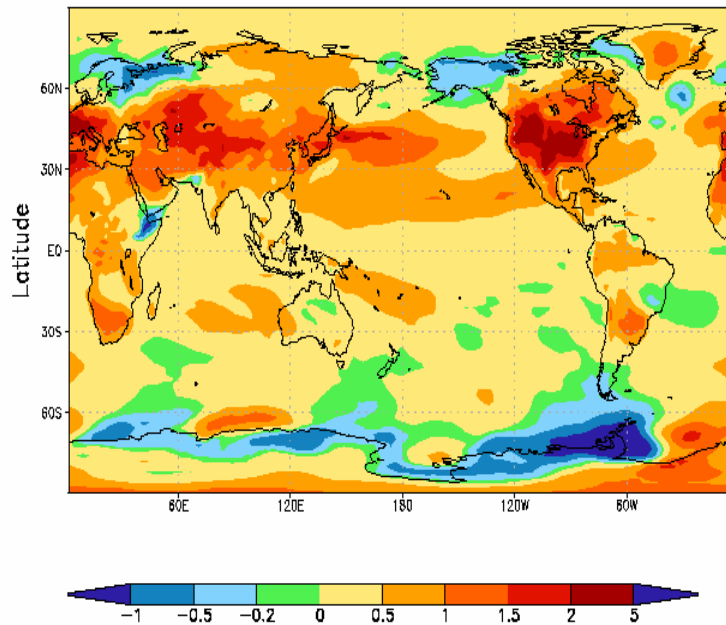
2697



2698 **Figure 3.9** Surface temperature change (2000 to 2100) due to short-lived species in the GFDL model.
 2699
 2700

2701 In Figure 3.10 we examine Northern Hemisphere summer surface temperature change
 2702 between the 2090s (average over 2091-2100) and the 2000s (average over 2001-2010)
 2703 due to the changes in emissions of short-lived species between the first decade and the

2704 last decade of the 21st Century. Note the large warming in the Northern Hemisphere mid
 2705 latitudes with the major hot spots over the continental United States, Southern Europe
 2706 and the Mediterranean. Eastern Asia, the region with the strongest radiative forcing due
 2707 to changes in emissions and loading of short-lived species, is not one of the hot spots.
 2708 The mid latitude warm belt is statistically significant to the 95th percentile and the hottest
 2709 spots are significant to the 99th percentile. By contrast, the annual-average and seasonal
 2710 patterns of change in precipitation due to changes in emissions of short-lived species
 2711 between the first and last decades of the 21st Century (not shown) are, in general, not
 2712 statistically significant.
 2713

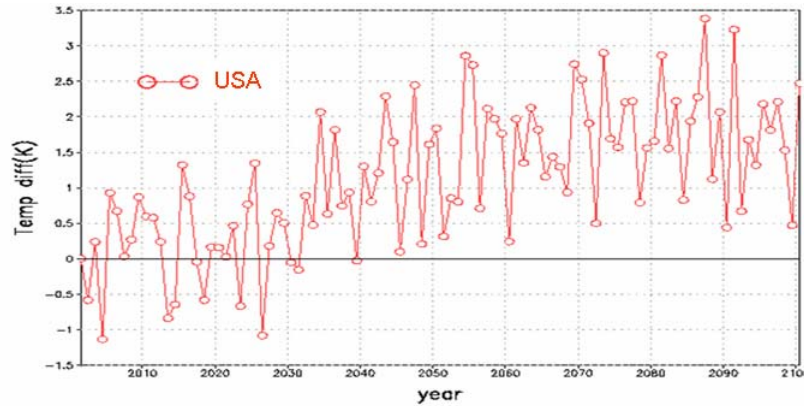


2714 **Figure 3.10** Surface temperature change due to short-lived species during Northern Hemisphere summer
 2715 for 2100-2091 vs. 2010-2001 in the GFDL model.
 2716
 2717

2718 We now focus on the large summertime warming over the United States and consider the
 2719 21st Century time series shown in Figure 3.11. By 2100, the change in short-lived species,
 2720 primarily the decrease in sulfate and increase in black carbon over Asia, contribute

2721 ~1.5°C of the ~4°C temperature warming predicted for the continental United States with
 2722 the effects of changes in both short-lived and long-lived species included.

2723



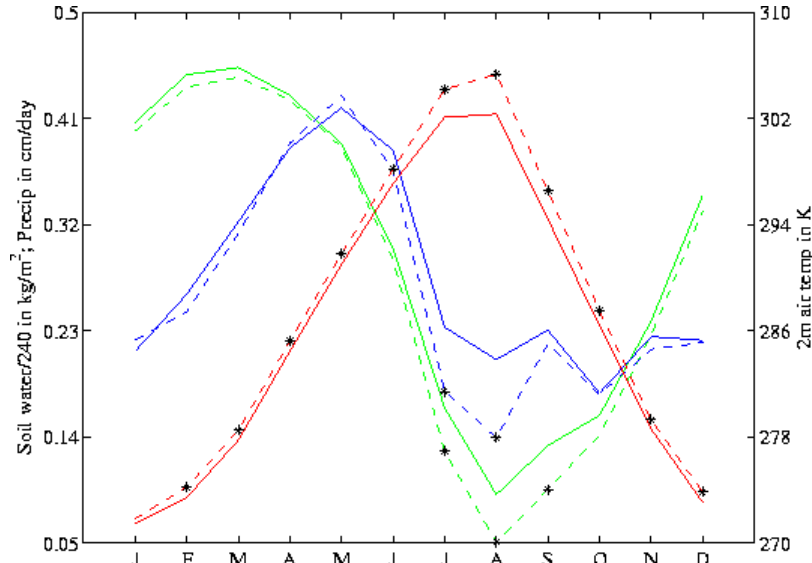
2724
 2725
 2726
 2727

Figure 3.11 Surface temperature change (K) due to short-lived species over the continental United States during Northern Hemisphere summer in the GFDL model.

2728 In Figure 3.12, we focus more narrowly on the central United States where the strong
 2729 summertime warming was predicted for 2100. Monthly-mean area-averaged values of
 2730 temperature, precipitation, and available root-zone soil water are shown for both the full
 2731 A1B emission scenario (dashed lines) and the emission scenario with short-lived species
 2732 levels fixed at 2001 values (solid lines). The values are ensemble averages over the last
 2733 40 years (2061-2100) for each simulation. Here the climate model does predict a
 2734 statistically significant (at the 95% confidence level) decrease in precipitation due to the
 2735 change in short-lived species (blue curves in Figure 3.12). We next consider root-zone
 2736 soil water, a quantity that integrates and responds to both temperature and precipitation.
 2737 There is a statistically significant (at the 95% confidence level) decrease of up to 50% in
 2738 available root-zone soil water in the Central United States during late summer (July
 2739 through September), which could have important consequences for United States grain
 2740 production, and merits future attention. This is the result of a global increase in short-
 2741 lived species forcing, located primarily over Asia, which in turn results from the large

2742 changes projected by the A1B “marker” scenario for Asian emissions of SO₂ and black
 2743 carbon.

2744



2745 **Figure 3.12** Monthly-mean time-series of available root-zone soil water (green lines, scaled by a factor of
 2746 1/240 for plotting purposes), precipitation (blue lines), and 2-meter air temperature (red lines), averaged
 2747 over the Central United States (105 to 82.5°W longitude; 32.5 to 45°N latitude). Dashed lines are for the
 2748 ensemble mean of the A1B experiments, averaged over the years 2061-2100; solid lines are for the
 2749 ensemble mean of the A1B* experiments, also averaged over the years 2061-2100. The asterisks represent
 2750 those A1B monthly average values that are different from their companion A1B* values at the 95%
 2751 confidence level.
 2752
 2753

2754 We also find, as already discussed for year 2050 in Section 3.3.4, that the regional
 2755 patterns of climate change in 2100 due to changes in emissions of short-lived species are
 2756 the result of regional patterns in the climate system’s response, rather than regional
 2757 patterns in radiative forcing. The global patterns of surface temperature change in 2100
 2758 are similar for the short-lived species and the well-mixed greenhouse gases with the
 2759 strongest surface temperature warming occurring over the summer continental US and
 2760 Mediterranean and the winter Arctic, while the major change in radiative forcing is over
 2761 Asia (Levy *et al.*, 2007). The predicted summertime warming over the US is greatly
 2762 enhanced by projected reductions in SO₂ emissions and increased black carbon emissions

2763 and the resulting positive radiative forcings over Asia. In the A1B scenario, this is
2764 assumed to be the result of Asian decisions addressing their local and regional air quality.
2765 The integrated assessment model projections for A1B assume that SO₂ emissions will be
2766 reduced in the future in order to improve air quality, but did not explicitly project
2767 carbonaceous aerosol emissions. Scaling future carbonaceous emissions according to
2768 carbon monoxide emissions projections does not lead to similar reductions in emissions
2769 of these particulates, so that there is an issue of consistency in projecting the influence of
2770 future air quality decisions that deserves further study.

2771

2772 **3.4 Regional Emission Sector Perturbations and Regional Models**

2773 **3.4.1 Introduction to Regional Emission Sector Studies**

2774 An additional set of simulations used global models to examine the impact of individual
2775 emission sectors in specific regions on short-lived species. This study, in which the GISS
2776 and NCAR groups participated, was designed to examine the climate effects of short-
2777 lived species in a more policy-relevant way by focusing on the economic activities that
2778 could potentially be subject to regulation or reduction in usage (*e.g.* by improved
2779 efficiency). We look at reductions in total emissions from a given sector in particular
2780 regions (North America and Asia), and do not consider any changes in technology or the
2781 relative contributions within a sector. As such, these are more useful for assessing the
2782 potential impacts of reductions in total power/fuel usage rather than changes in the mix of
2783 power generation/transportation types or in emissions control technologies targeted at
2784 specific pollutants.

2785

2786 3.4.2 Global Models

2787 The GISS model setup for the regional emission sector perturbation experiments was the
2788 same as that used in the transient climate studies (section 3.2 and 3.3; see Appendix 3.1
2789 and 3.2, sections on Goddard Institute for Space Studies). The NCAR regional/sector
2790 perturbation simulations used the CAM-chem model (Lamarque *et al.*, 2005b), in which a
2791 updated version of the MOZART chemical transport model (Horowitz *et al.*, 2003) is
2792 embedded within the Community Atmosphere Model (CAM3, Collins *et al.*, 2006).
2793 CAM-chem has a representation of tropospheric chemistry with non-methane
2794 hydrocarbons (NMHCs) treated up to isoprene, toluene and monoterpenes. The aerosol
2795 simulation in CAM-chem includes the bulk aerosol mass of black carbon (BC,
2796 hydrophobic and hydrophilic), primary organic carbon (POA, hydrophobic and
2797 hydrophilic), secondary organic carbon (SOA), ammonium and ammonium nitrate, and
2798 sulfate aerosols. Further details on the CAM-chem model are found in Appendix 3.2 in
2799 the section on National Center for Atmospheric Research.

2800

2801 3.4.3 Impact of Emission Sectors on Short-Lived Species

2802 This set of experiments consisted of six simulations each reducing the present-day
2803 emissions by 30% in one sector for one region. By using present-day emissions, the
2804 results are not tied to any particular scenario. For present-day emissions, the IIASA 2000
2805 inventory, based on the 1995 EDGAR3.2 inventory extrapolated to 2000 using national
2806 and sector economic development data, was used (Dentener *et al.*, 2005), as in the GISS
2807 simulations described above. The exception to this is biomass burning emissions, which
2808 are taken from the Global Fire Emission Database (GFED) averaged over 1997-2002

2809 (Van der Werf *et al.*, 2003) with emission factors from (Andreae and Merlet, 2001) for
2810 aerosols. The regions were defined as North America (60-130°W, 25-60°N) and Asia
2811 (60-130°E, 0-50°N) and the economic sectors defined according to the IIASA inventory
2812 as the domestic sector, the surface transportation sector, and a combined industry and
2813 power sector (the NCAR model did not perform the transportation sector simulations).

2814

2815 A control run with no perturbations was also performed to allow comparison. The goal of
2816 these simulations was to calculate the radiative forcing from all the short-lived species to
2817 identify the relative contribution of the given economic sectors in these two regions. This
2818 complements prior work examining the response to a subset of the species included here
2819 (*e.g.*, Koch *et al.*, 2007; Unger *et al.*, 2007). As the forcings were expected to be small,
2820 we concentrate on simple metrics rather than the climate response. NCAR did not
2821 calculate radiative forcing, so we also use aerosol optical depth, which is a good indicator
2822 of the radiative forcing from aerosols. All simulations were 11-year runs, with analysis
2823 performed over the last 10 years.

2824

2825 The simulations were not performed using a full methane cycle, but the methane response
2826 to the imposed perturbations can be estimated by examining the changes in methane's
2827 oxidation rate. In these simulations, methane was prescribed at present-day values. Thus
2828 any change in methane oxidation is due solely to changes in the abundance of oxidizing
2829 agents. The difference in the steady-state abundance of methane that would occur as a
2830 result of this oxidation change is a simple calculation ($[\text{CH}_4]'/[\text{CH}_4] = L/L'$ for the global
2831 mean where L is the methane loss rate and the 'prime' notation indicates the adjusted

2832 amounts). Use of the model's oxidation rate in the perturbation runs fully captures spatial
2833 and seasonal variations, and thus provides an accurate estimate of the equilibrium
2834 response of methane to the emissions changes. Finally, the radiative forcing resulting
2835 from these indirect methane changes is calculated using the standard formulation
2836 (Ramaswamy *et al.*, 2001).

2837

2838 We first examine the global mean annual average radiative forcing in the GISS model
2839 from the regional perturbations and those by economic sectors (Table 3.10). The effect of
2840 the perturbations is generally larger for Asian than in North American emissions. The
2841 only radiative forcing from an individual species to exceed 10mW m^{-2} from a North
2842 American perturbation is the sulfate forcing from a reduction in industrial/power
2843 emissions. In contrast, forcings from sulfate, black carbon, organic carbon and ozone all
2844 exceed 10 mW m^{-2} in response to perturbations in developing Asia, with the largest
2845 response for reductions in black carbon when domestic emissions are reduced (-42 mW
2846 m^{-2}). The spatial pattern of the radiative forcing is also shown (Figure 3.13). The two
2847 largest net forcings are in response to changes in North American industrial/power
2848 emissions, whose forcing is positive and is dominated by reductions in forcing from
2849 sulfate, and the Asia domestic sector, whose forcing is negative and dominated by
2850 reductions in black carbon and ozone. The spatial pattern of the aerosol optical depth
2851 changes capture the bulk of the radiative forcing in these two cases (Figure 3.14 versus
2852 Figure 3.13). The sign is opposite, however, in the case of industrial/power emissions as
2853 these dominated by reflective sulfate aerosols, so decreased aerosol optical depth causes
2854 positive radiative forcing.

2855

2856 The GISS and NCAR models show very similar patterns of aerosol optical depth changes
2857 for these two perturbation experiments. For emissions reduction in the Asia domestic
2858 sector, the global mean aerosol optical depth decreases by 0.15 in the GISS model and
2859 0.13 in the NCAR model, while for the North American industrial/power sector the
2860 decreases are 0.09 and 0.13, respectively. Hence the aerosol response appears to be fairly
2861 robust across these two models. Results suggest that the calculation of radiative forcing
2862 from aerosol optical depth introduces an additional inter-model difference that is less than
2863 that from the aerosol optical depth calculation (Schulz *et al.*, 2006), so that the total inter-
2864 model variation in RF from aerosols is probably on order of 50%. Results for ozone show
2865 marked differences, however, with the response of the tropospheric ozone column in the
2866 GISS model nearly always a factor of 2-3 greater than in the NCAR model. We believe
2867 that these differences primarily reflect the inclusion of the stratosphere in the GISS
2868 model, which leads to enhanced forcing as ozone near the tropopause has a particularly
2869 large radiative impact. Hence, the ozone radiative forcing is not yet robust to inter-model
2870 differences. However, aerosols typically have a larger influence on climate than ozone, so
2871 that the net radiative forcing remains a relatively more robust quantity.

2872

2873 We also examine changes in surface pollution levels in these simulations. Changes in
2874 surface ozone are typically small, with annual average local reductions of up to about 1-
2875 1.5 ppbv in both the NCAR and GISS models in response to reduction in transportation
2876 or industrial/power emissions. These increase to levels of 1-3 ppbv during boreal
2877 summer. Both these annual and summer increases are statistically significant. Changes in

2878 particulate are larger. In most cases, substantial reduction in surface particulate
2879 concentrations result from the regional economic sector emissions reductions. This is
2880 especially so in the Asia domestic analysis, where summer sulfate concentrations are
2881 lowered by 100-250 pptv locally, and black carbon concentrations drop by 1800-2000
2882 pptv for both summer and annual averages. Smaller air quality improvements are also
2883 clear in the response to industrial/power and transportation emissions reductions in both
2884 regions. These reductions in particulate are generally quite similar in the two models,
2885 with differences of only 5-20% in most cases.

2886

2887 The analysis shows that reductions in surface transportation emissions have a net
2888 negative forcing from short-lived species in both regions, primarily due to reductions in
2889 black carbon and ozone. As these are both pollutants at the surface, reducing emissions
2890 transport offers a way to simultaneously improve human health and mitigate climate
2891 warming (though the climate impact is quite small for Asia). The total climate mitigation
2892 would of course be larger adding in the effect of reduced emissions of long-lived
2893 greenhouse gases. In contrast, industrial/power sector emissions have their largest effect
2894 on climate via short-lived species through sulfate, and hence yield a positive forcing.
2895 Thus, the net effect of changes in short-lived species to industrial/power emissions
2896 reductions will offset a portion of any climate benefit from reduced emissions of long-
2897 lived species. The domestic sector presents a more similar picture to that seen for surface
2898 transportation. The effects are substantially larger in Asia, however. Hence, reductions in
2899 domestic emissions from Asia offer another means to improve human health and mitigate
2900 warming. Note that the effects become particularly strong in Northern Hemisphere

2901 summer (Table 3.12), offering a potential path to help mitigating increased summer heat
2902 over the Northern Hemisphere continents.

2903

2904 Overall, the Asia domestic emissions offer the strongest leverage on climate via short-
2905 lived species. This is partially a result of their magnitude, and partially their occurrence at
2906 lower latitudes than North American (or European) emissions. This enhances their impact
2907 as photochemistry is faster and incoming radiation is more abundant at lower latitudes.

2908 Perturbing the Asia domestic sector in the IIASA 2000 emissions inventory used here
2909 yields a much greater effect via black carbon changes than via sulfate changes. This
2910 reflects the influence of domestic fuel usage, for which black carbon is the dominant
2911 emitted species, and hence reductions from emissions in this sector in particular seem
2912 attractive for warming mitigation. As domestic usage and emissions are extremely
2913 difficult to quantify in the developing world, further studies of this sector are especially
2914 needed to characterize the uncertainty in these emissions. The GISS and NCAR results
2915 differ in the magnitude of the aerosol optical depth change resulting from the Asia
2916 domestic sector perturbations by only 13%, and this sector/region has the largest
2917 influence in both models for both radiative forcing and surface pollution. The stronger
2918 aerosol optical depth response in the NCAR model suggests that the RF in that model
2919 might be even larger than the 50 mW m^{-2} global mean annual average seen in the GISS
2920 results.

2921

2922 Further work is required to more thoroughly characterize the robustness of these
2923 conclusions across a larger number of models, to explore the impact of aerosol indirect

2924 effects on clouds, and to examine alternative emissions scenarios considering changes in
 2925 the mix of sources constituting a given sector and the influence of potential technological
 2926 changes. The latter could be designed to reduce emissions of particular pollutants, while
 2927 not affecting others. Our results for the radiative forcing from individual species give an
 2928 idea of the potential impact of such technologies. However, we note that these
 2929 technologies could also have effects on overall fuel consumption by altering the
 2930 efficiency of a particular process.

2931

2932 Interestingly, both the transient climate projections and the present-day perturbations find
 2933 that emissions from Asia are the most important controllers of climate trends or
 2934 mitigation. Given that the RF reduction from decreases in Asia domestic emissions
 2935 extends over much of the Northern Hemisphere (Figure 3.13), and the conclusion from
 2936 the transient climate simulations that the climate response to short-lived species changes
 2937 is not closely localized near their emissions, it seems plausible that emissions from this
 2938 region may have as larger or larger an effect on other parts of the Northern Hemisphere
 2939 as changes in local emissions.

2940 **Table 3.10** Radiative forcing (in mW m^{-2}) from regional emission sector perturbations in the GISS model.

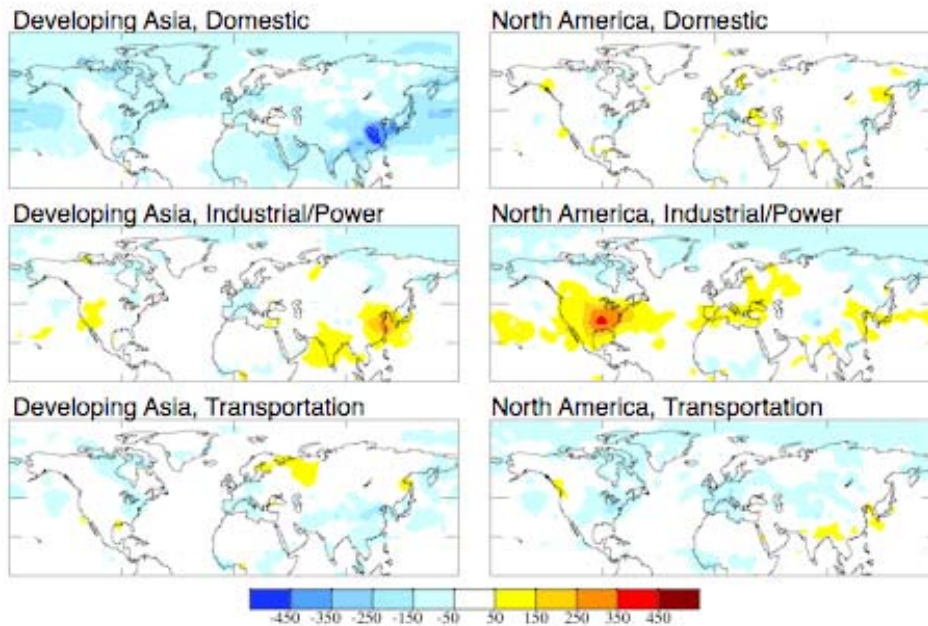
Region	Sector	Sulfate	BC	OC	Nitrate	Ozone	Methane (indirect)	All
North America	domestic	0	-3	2	1	2	1	4
	surface transportation	-3	-5	0	1	-5	4	-9
	industry/power	14	-2	-1	0	5	2	18
Asia	domestic	0	-42	13	1	-12	-2	-41
	surface transportation	2	-8	1	2	-5	7	-2
	industry/power	13	-4	0	-1	-1	5	12

2941 Perturbations are 30% reduction in emissions of all species from the indicated economic sector in the given
 2942 region. Direct forcings are shown for sulfate, black carbon (BC), organic carbon (OC), nitrate, and ozone.
 2943 The effect of ozone precursor species on methane is included as methane "indirect". Note that aerosol
 2944 indirect effects are not included.
 2945

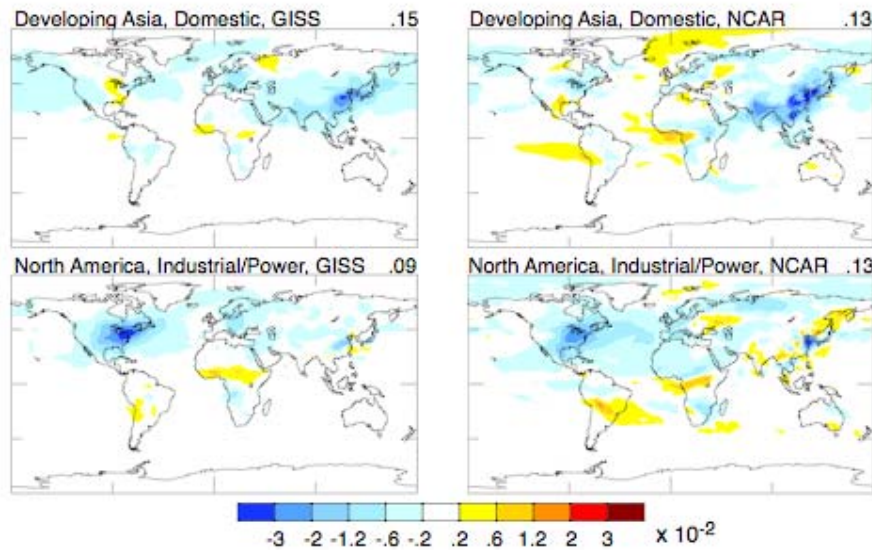
2946 **Table 3.11** Total short-lived species radiative forcing (in mW m^{-2}) as in Table 3.10 but for summer (June-
 2947 August).

Region	Sector	Total forcing
North America	domestic	6
	surface transportation	-10
	industry/power	34
Asia	domestic	-69
	surface transportation	-3
	industry/power	10

2948



2949 **Figure 3.13** Short-lived species annual average radiative forcing (mW m^{-2}) due to 30% reductions in
 2950 emissions from the given region and economic sector in the GISS model.
 2951
 2952
 2953



2954
 2955 **Figure 3.14** Annual average aerosol optical depth change due to 30% reductions in emissions from the
 2956 given region and economic sector in the GISS (left column) and NCAR (right column) models. Values in
 2957 the upper right give the global mean.
 2958

2959 **3.4.4 Regional Downscaling Climate Simulations**

2960 The sector-based simulations presented in Section 3.4.3 suggest that reductions in surface
 2961 level short-lived species ozone or BC would have a negative RF, while reductions in
 2962 sulfate aerosols from the utility sector would have a positive RF effect. If concentration
 2963 levels for these short-lived species (ozone and components of PM_{2.5}) exceed threshold
 2964 standards under the U.S. Clean Air Act, emission control strategies must be developed.
 2965 Since these short-lived species vary spatially and are affected by local emissions, regional
 2966 scale models are needed to develop the emission control strategies that meet these
 2967 standards at county and state levels. To achieve reductions in PM_{2.5}, emission scenarios
 2968 often include utility sector emission reductions to lower sulfate aerosol levels. As shown
 2969 in the previous section, lowering sulfate aerosol concentrations could actually have
 2970 negative implications for RF and climate temperature increases. Regional downscaling

2971 studies shown in this section suggest that future changes in regional climate could reduce
2972 the benefits from anticipated emission reductions on lowering ozone.

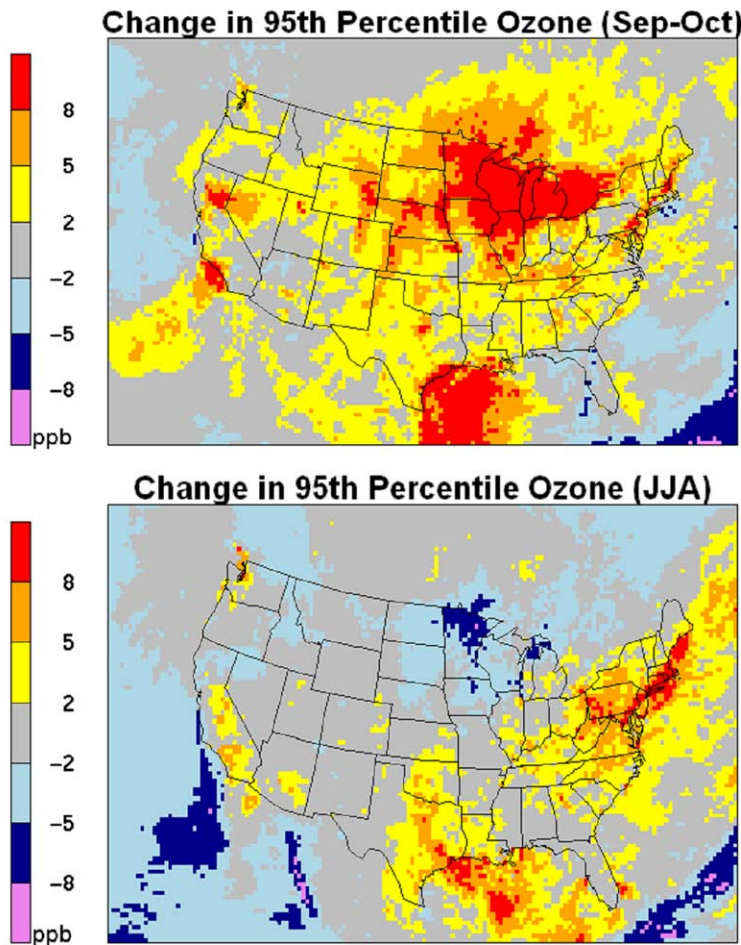
2973

2974 Downscaled regional scale climate (RCM) simulations (*e.g.*, Leung and Gustafson, 2005;
2975 Liang *et al.*, 2006, Liang *et al.*, 2004) rely on a global climate model to provide boundary
2976 conditions for the regional domain as well as the radiative effect of well-mixed GHGs
2977 within the domain for the radiation calculations. Regionally downscaled climate
2978 simulations are needed by a number of applications that must consider local changes in
2979 future climate. Since ozone and PM_{2.5} exceedances of regulatory thresholds are
2980 substantially affected by local scale changes in emissions and meteorology, several recent
2981 studies have used regionally downscaled climate scenarios have been used to study the
2982 sensitivity of air quality to potential changes in future climate. The primary purpose of
2983 these studies was to study how increases in temperature and other future climate changes
2984 could affect ozone and PM_{2.5} and potentially decrease the effectiveness of anticipated
2985 emission reductions.

2986

2987 Using downscaled RCM simulations from and Gustafson (2005), Nolte *et al.* (2007) have
2988 used the EPA/NOAA CMAQ model to test the impact of future (ca. 2050) climate on
2989 ozone and aerosols with current emission scenarios. Biogenic emissions, which are
2990 meteorologically dependent, were re-calculated under the future climate scenario. Results
2991 suggest that future climate changes could increase maximum ozone levels by
2992 approximately 10% in some regions (see Figure 3.15). With anticipated emission
2993 reductions under U.S. Clean Air Act requirements, these results suggest that future

2994 climate could dampen the effectiveness of these emission controls. Evaluation of
 2995 ensemble RCM results are essential for this application before quantitative conclusions
 2996 can be made about the impact of future climate on specific emission control strategies;
 2997 however, these results suggest that climate change is a factor that needs to be considered
 2998 in air quality management.
 2999



3000
 3001 **Figure 3.15** From Nolte *et al.* (2007), the change in ozone at the upper end of the ozone distribution
 3002 (average of the $\geq 95^{\text{th}}$ values for each grid) for (2050 - Present) years of simulation under A1B RCM
 3003 simulations.
 3004

3005 These regional downscaling climate studies discussed rely on climate forcing linkages
 3006 from global climate simulations with future trends for long-lived species including CO₂,

3007 CH₄, N₂O, and chlorofluorocarbon. The influence of short-lived species on future climate
3008 has not been included in those studies to date; however, more recent developments are
3009 underway to include direct and indirect radiative effects in the regional chemistry model.
3010 Based on the known positive radiative forcing effect of ozone, the increases in ozone in
3011 response to future climate in Figure 3.15 should have a positive RF effect that could
3012 dampen the net negative radiative forcing anticipated from future emission reductions for
3013 ozone (see Section 3.4.3).

3014

3015 While regional downscaling climate impacts from short-lived species cannot be directly
3016 reported on, future emission scenarios for short-lived species were considered by several
3017 regional downscaling studies for the purpose of air quality impacts under future climate.
3018 The impact of climate only and then an emission change scenario were tested by (Nolte *et*
3019 *al.*, 2007) and (Hogrefe *et al.*, 2004). As presented in Figure 3.15, results looking only at
3020 the climate sensitivity without future changes in emissions suggest that future climate
3021 changes could increase maximum ozone levels by approximately 8ppb or 10% in some
3022 regions of North America. Looking at future emission scenarios for NO_x and SO₂
3023 reductions demonstrates that the uncertainty in the future emission scenarios introduces a
3024 much larger variation in the air quality conclusions depending on the scenario (Hogrefe *et*
3025 *al.*, 2004; Nolte *et al.*, 2007). Similar to the findings here about short-lived species'
3026 impact on climate, the range of plausible air quality impacts from future short-lived
3027 emission scenarios suggest very different outcomes, and the future scenarios of emissions
3028 for short-lived species have a great deal of obvious, inherent uncertainty.

3029 **CHAPTER 3 REFERENCES**

3030

3031 **Albrecht**, B. A. (1989), Aerosols, cloud microphysics, and fractional cloudiness,
3032 *Science*, 245, 1227-1230.

3033

3034 **Andreae**, M. O., and P. Merlet (2001), Emission of trace gases and aerosols from
3035 biomass burning, *Global Biogeochem. Cycles*, 15, 955-966.

3036

3037 **Bauer**, S. E., M. I. Mishchenko, A. Lacis, S. Zhang, J. Perlwitz, and S. M. Metzger
3038 (2006), Do sulfate and nitrate coatings on mineral dust have important effects on
3039 radiative properties and climate modeling?, *J. Geophys. Res.*, 112, D06307, doi:
3040 10.1029/2005JD006977.

3041

3042 **Berntsen**, T. K., J. S. Fuglestvedt, M. M. Joshi, K. P. Shine, N. Stuber, M. Ponater, R.
3043 Sausen, D. A. Hauglustaine, and L. Li (2005), Response of climate to regional
3044 emissions of ozone precursors: sensitivities and warming potentials, *Tellus B*, 57,
3045 283–304.

3046

3047 **Boer**, G., and B. Yu (2003), Climate sensitivity and response, *Clim. Dyn.*, 20, 415-429.

3048

3049 **Bousquet**, P., *et al.* (2006), Contribution of anthropogenic and natural sources to
3050 atmospheric methane variability, *Nature*, 443, 439-442.

3051

3052 **Butchart**, N., *et al.* (2006), A multi-model study of climate change in the Brewer-
3053 Dobson circulation, *Clim. Dyn.*, 10.1007/s00382-006-0162-4.

3054

3055 **Collins**, W. D., P. J. Rasch, B. E. Eaton, B. Khattatov, J.-F. Lamarque, and C. S. Zender
3056 (2001), Simulating aerosols using a chemical transport model with assimilation of
3057 satellite aerosol retrievals: Methodology for INDOEX, *J. Geophys. Res.*, 106,
3058 7313–7336.

3059

3060 **Collins**, W. D., *et al.* (2006), The formulation and atmospheric simulation of the
3061 Community Atmosphere Model: CAM3, *J. Clim.*, 19, 2144-2161.

3062

3063 **Delworth**, T. L., *et al.* (2006), GFDL's CM2 Global Coupled Climate Models. Part I:
3064 Formulation and simulation characteristics, *J. Clim.*, 19, 643-674.

3065

3066 **Dentener**, F. D., D. S. Stevenson, J. Cofala, R. Mechler, M. Amann, P. Bergamaschi, F.
3067 Raes, and R. G. Derwent (2005), Tropospheric methane and ozone in the period
3068 1990-2030: CTM calculations on the role of air pollutant and methane emissions
3069 controls, *Atmos. Chem. Phys.*, 5, 1731-1755.

3070

3071 **Dlugokencky**, E. J., S. Houweling, L. Bruhwiler, K. A. Masarie, P. M. Lang, J. B. Miller,
3072 and P. P. Tans (2003), Atmospheric methane levels off: Temporary pause or a
3073 new steady-state?, *Geophys. Res. Lett.*, 30, 1992, doi:10.1029/2003GL018126.

- 3074 **Fiore, A.M., L.W. Horowitz, E.J. Dlugokencky, and J. Jason West, Impact of**
3075 **Meteorology and Emissions on Methane Trends, 1990-2004 , Geophys. Res. Lett.,**
3076 **33, L12809, doi:10.1029/2006GL026199, 2006.**
3077
- 3078 **Gauss, M., et al. (2003), Radiative forcing in the 21st century due to ozone changes in**
3079 **the troposphere and the lower stratosphere, J. Geophys. Res., 108, 4292,**
3080 **doi:10.1029/2002JD002624.**
3081
- 3082 **Ginoux, P., L. W. Horowitz, V. Ramaswamy, I. V. Geogdzhayev, B. N. Holben, G.**
3083 **Stenchikov, and X. Tie (2006), Evaluation of aerosol distribution and optical**
3084 **depth in the Geophysical Fluid Dynamics Laboratory coupled model CM2.1 for**
3085 **present climate, J. Geophys. Res., 111, D22210, doi:10.1029/2005JD006707.**
3086
- 3087 **Guenther, A., et al. (1995), A global model of natural volatile organic compound**
3088 **emissions, J. Geophys. Res., 100, 8873-8892.**
3089
- 3090 **Gustafson, W. I., and L. R. Leung, 2007: Regional downscaling for air quality**
3091 **assessment: A reasonable proposition? Bulletin of the American Meteorological**
3092 **Society, in press.**
- 3093 **Hansen, J., et al. (2005), Efficacy of Climate Forcings, J. Geophys. Res., 110, D18104,**
3094 **doi:10.1029/2005JD005776.**
3095
- 3096 **Hansen, J., et al. (2007), Dangerous human-made interference with climate: A GISS**
3097 **modelE study, Atmos. Chem. Phys., 7, 2287-2312.**
3098
- 3099 **Hansen, J. E., M. Sato, and R. Reudy (1997), Radiative forcing and climate response, J.**
3100 **Geophys. Res., 102, 6831-6864.**
3101
- 3102 **Held, I. M., and B. J. Soden (2006), Robust responses of the hydrological cycle to global**
3103 **warming, J. Clim., in press.**
3104
- 3105 **Hogrefe, C., et al. (2004), Simulating changes in regional air pollution over the eastern**
3106 **United States due to changes in global and regional climate and emissions, J.**
3107 **Geophys. Res., 109(D22), D22301, doi:10.1029/2004JD004690.**
3108
- 3109 **Horowitz, L. W. (2006), Past, present, and future concentrations of tropospheric ozone**
3110 **and aerosols: Methodology, ozone evaluation, and sensitivity to aerosol wet**
3111 **removal, J. Geophys. Res., 111, D22211, doi:10.1029/2005JD006937.**
3112
- 3113 **Horowitz, L. W., et al. (2003), A global simulation of tropospheric ozone and related**
3114 **tracers: Description and evaluation of MOZART, version 2, J. Geophys. Res.,**
3115 **108(D24), 4784, doi:10.1029/2002JD002853.**
3116
- 3117 **Kiehl, J. T., J. J. Hack, G. B. Bonan, B. A. Boville, D. L. Williamson, and P. J. Rasch**
3118 **(1998), The National Center for Atmospheric Research Community Climate**
3119 **Model: CCM3, J. Clim., 11, 1131-1149.**

- 3120
3121 **Kiehl, J. T., T. L. Schneider, R. W. Portmann, and S. Solomon (1999),** Climate forcing
3122 due to tropospheric and stratospheric ozone, *J. Geophys. Res.*, 104, 31,239-
3123 231,254.
3124
- 3125 **Kinne, S., et al. (2006),** An AeroCom initial assessment – optical properties in aerosol
3126 component modules of global models, *Atmos. Chem. Phys.*, 6, 1815-1834.
3127
- 3128 **Koch, D., T. Bond, D. Streets, N. Bell, and G. R. van der Werf (2007),** Global impacts of
3129 aerosols from particular source regions and sectors, *J. Geophys. Res.*, 112,
3130 D02205, doi:10.1029/2005JD007024.
3131
- 3132 **Koch, D., G. Schmidt, and C. Field (2006),** Sulfur, sea salt and radionuclide aerosols in
3133 GISS ModelE, *J. Geophys. Res.*, 111, D06206, doi:10.1029/2004JD005550.
3134
- 3135 **Lamarque, J.-F., P. Hess, L. Emmons, L. Buja, W. M. Washington, and C. Granier**
3136 **(2005a),** Tropospheric ozone evolution between 1890 and 1990, *J. Geophys. Res.*,
3137 110, D08304, doi:10.1029/2004JD005537.
3138
- 3139 **Lamarque, J.-F., J. T. Kiehl, P. G. Hess, W. D. Collins, L. K. Emmons, P. Ginoux, C.**
3140 **Luo, and T. X. X. (2005b),** Response of a coupled chemistry-climate model to
3141 changes in aerosol emissions: Global impact on the hydrological cycle and the
3142 tropospheric burdens of OH, ozone and NO_x, *Geophys. Res. Lett.*, 16, L16809,
3143 doi:10.1029/2005GL023419.
3144
- 3145 **Leung, L. R., and W. I. Gustafson, 2005:** Potential regional climate change and
3146 implications to US air quality. *Geophysical Research Letters*, 32, L16711,
3147 doi:10.1029/2005GL022911.
3148
- 3149 **Levy, H., M. D. Schwarzkopf, L. Horowitz, and V. Ramaswamy (2007),** Anthropogenic
3150 Short-lived Radiative Species at the Intersection of Climate and Air Quality,
3151 submitted.
3152
- 3153 **Liang, X.Z. et al., 2006:** Regional climate model downscaling of the U.S. summer
3154 climate and future change. *Journal Geophysical Research*, in press.
3155
- 3156 **Liang, X. Z., L. Li, K. E. Kunkel, M. Ting, and J. X. L. Wang, 2004:** Regional climate
3157 model simulation of U.S. precipitation during 1982–2002. Part I: Annual cycle.
3158 *Journal of Climate*, 17(18), 3510-3529.
3159
- 3160 **Mahowald, N. M., and C. Luo (2003),** A less dusty future?, *Geophys. Res. Lett.*, 30,
3161 1903, doi:10.1029/2003GL017880.
3162
- 3163 **Menon, S., A. , D. Del Genio, D. Koch, and G. Tselioudis (2002),** GCM Simulations of
3164 the Aerosol Indirect Effect: Sensitivity to Cloud Parameterization and Aerosol
3165 Burden, *J. Atmos. Sci.*, 59, 692-713.

- 3166
3167 **Metzger, S., F. Dentener, S. Pandis, and J. Lelieveld (2002),** Gas/aerosol partitioning: 1.
3168 A computationally efficient model, *J. Geophys. Res.*, 107,
3169 doi:10.1029/2001JD001102.
- 3170 **Miller, R. L., et al. (2006a),** Mineral Dust Aerosols in the NASA Goddard Institute for
3171 Space Studies ModelE AGCM, *J. Geophys. Res.*, 111, D0208,
3172 doi:10.1029/2005JD005796.
- 3173 **Miller, R. L., G. A. Schmidt, and D. T. Shindell (2006b),** Forced variations of annular
3174 modes in the 20th century Intergovernmental Panel on Climate Change Fourth
3175 Assessment Report models, *J. Geophys. Res.*, 111, D18101,
3176 doi:10.1029/2005JD006323.
- 3177
- 3178 **Mitchell, J. F. B., R. A. Davis, W. J. Ingram, and C. A. Senior (1995),** On Surface
3179 Temperature, Greenhouse Gases, and Aerosols: Models and Observations, *J.*
3180 *Clim.*, 8, 2364–2386.
- 3181
- 3182 **Nakicenovic, N., et al. (2000),** IPCC Special Report on Emissions Scenarios, 570 pp.,
3183 Cambridge University Press, Cambridge, UK.
- 3184
- 3185 **Nolte, C., A. B. Gilliland, and C. Hogrefe (2007),** Linking global to regional models to
3186 investigate future climate impacts on U.S. regional air quality 1. Surface ozone
3187 concentrations, submitted.
- 3188
- 3189 **Olivier, J. G. J., and J. J. M. Berdowski (2001),** Global emissions sources and sinks, in
3190 *The Climate System*, edited by J. Berdowski, et al., pp. 33-78, A.A. Balkema
3191 Publishers/Swets & Zeitlinger Publishers, Lisse, The Netherlands.
- 3192
- 3193 **Penner, J. E., J. Quaas, T. Storelvmo, T. Takemura, O. Boucher, H. Guo, A. Kirkevåg, J.**
3194 **E. Kristjánsson, and Ø. Seland (2006),** Model intercomparison of indirect aerosol
3195 effects, *Atmos. Chem. Phys. Discuss.*, 6, 1579-1617.
- 3196
- 3197 **Pincus, R., and M. Baker (1994),** Precipitation, solar absorption, and albedo
3198 susceptibility in marine boundary layer clouds, *Nature*, 372, 250-252.
- 3199
- 3200 **Ramaswamy, V., et al. (2001),** Radiative forcing of climate change, in *Climate Change*
3201 2001, edited by J. T. Houghton, pp. 349-416, Cambridge Univ. Press, Cambridge.
- 3202
- 3203 **Schmidt, G. A., et al. (2006),** Present day atmospheric simulations using GISS ModelE:
3204 Comparison to in-situ, satellite and reanalysis data, *J. Clim.*, 19, 153-192.
- 3205
- 3206 **Schulz, M., et al. (2006),** Radiative forcing by aerosols as derived from the AeroCom
3207 present-day and pre-industrial simulations, *Atmos. Chem. Phys.*, 6, 5225-5246.
- 3208
- 3209 **Shindell, D. T., G. Faluvegi, S. E. Bauer, D. M. Koch, N. Unger, S. Menon, A., R. L.**
3210 **Miller, G. A. Schmidt, and D. G. Streets (2007),** Climate response to projected

- 3211 changes in short-lived species under an A1B scenario from 2000-2050 in the
3212 GISS climate model, *J. Geophys. Res.*, 112, D20103, doi:10.1029/2007JD008753.
3213
- 3214 **Shindell, D. T., G. Faluvegi, and N. Bell (2003)**, Preindustrial-to-present-day radiative
3215 forcing by tropospheric ozone from improved simulations with the GISS
3216 chemistry-climate GCM, *Atmos. Chem. Phys.*, 3, 1675-1702.
3217
- 3218 **Shindell, D. T., G. Faluvegi, A. Lacis, J. E. Hansen, R. Ruedy, and E. Aguilar (2006a)**,
3219 The role of tropospheric ozone increases in 20th century climate change, *J.*
3220 *Geophys. Res.*, 111, D08302, , doi:10.1029/2005JD006348.
3221
- 3222 **Shindell, D. T., G. Faluvegi, N. Unger, E. Aguilar, G. A. Schmidt, D. Koch, S. E. Bauer,**
3223 **and R. L. Miller (2006b)**, Simulations of preindustrial, present-day, and 2100
3224 conditions in the NASA GISS composition and climate model G-PUCCINI,
3225 *Atmos. Chem. Phys.*, 6, 4427-4459.
3226
- 3227 **Shindell, D. T., B. P. Walter, and G. Faluvegi (2004)**, Impacts of climate change on
3228 methane emissions from wetlands, *Geophys. Res. Lett.*, 31, L21202,
3229 doi:10.1029/2004GL021009.
3230
- 3231 **Stevenson, D. S., et al. (2006)**, Multi-model ensemble simulations of present-day and
3232 near-future tropospheric ozone, *J. Geophys. Res.*, 111, D08301,
3233 doi:10.1029/2005JD006338.
3234
- 3235 **Stewart, R. W., S. Hameed, and J. P. Pinto (1977)**, Photochemistry of the tropospheric
3236 ozone, *J. Geophys. Res.*, 82, 3134-3140.
3237
- 3238 **Streets, D., T. C. Bond, T. Lee, and C. Jang (2004)**, On the future of carbonaceous
3239 aerosol emissions, *J. Geophys. Res.*, 109, doi:10.1029/2004JD004902.
3240
- 3241 **Tie, X., G. Brasseur, L. Emmons, L. Horowitz, and D. Kinnison (2001)**, Effects of
3242 aerosols on tropospheric oxidants: A global model study, *J. Geophys. Res.*, 106,
3243 22931-22964.
3244
- 3245 **Tie, X., S. Madronich, S. Walters, D. P. Edwards, P. Ginoux, N. Mahowald, R. Zhang, C.**
3246 **Lou, and G. Brasseur (2005)**, Assessment of the global impact of aerosols on
3247 tropospheric oxidants, *J. Geophys. Res.*, 110, D03204,
3248 doi:10.1029/2004JD005359.
3249
- 3250 **Twomey, S. (1974)**, Pollution and the planetary albedo, *Atmos. Env.*, 8, 1251-1256.
3251
- 3252 **Unger, N., D. T. Shindell, D. M. Koch, and D. G. Streets (2007)**, Air pollution radiative
3253 forcing from specific emissions sectors at 2030, *J. Geophys. Res.*, in press.
3254

3255 **Van der Werf**, G. R., J. T. Randerson, G. J. Collatz, and G. L. (2003), Carbon emissions
3256 from fires in tropical and subtropical ecosystems, *Global Change Biology*, 9, 547-
3257 562.
3258
3259 **Woodward**, S., D. L. Roberts, and R. A. Betts (2005), A simulation of the effect of
3260 climate change-induced desertification on mineral dust aerosol, *Geophys. Res.*
3261 *Lett.*, 32, L18810, doi:10.1029/2005GL023482.
3262

3263 **Appendix 3.1 Composition Models**

3264

3265 **A.3.1.1 Geophysical Fluid Dynamics Laboratory**

3266 Composition changes for the short-lived species from 2000 to 2100 in the GFDL
3267 experiments were calculated using the global chemical transport model MOZART-2
3268 (Model for Ozone And Related chemical Tracers, version 2.4), which has been described
3269 in detail previously (Horowitz *et al.*, 2003; Horowitz, 2006; and references therein. This
3270 model was used to generate distributions of ozone, sulfate, black and organic carbon, and
3271 dust for the emission scenarios discussed in Section 3.2.1. Emissions and initial
3272 conditions for methane were scaled each decade to match the global average methane
3273 abundances specified in the A1B “marker” scenario. The model includes 63 gas-phase
3274 species, 11 aerosol and precursor species to simulate sulfate, nitrate, ammonium, and
3275 black and organic carbon and five size bins for mineral dust (diameter size bins of 0.2-2.0
3276 μm , 2.0-3.6 μm , 3.6-6.0 μm , 6.0-12.0 μm , and 12.0-20.0 μm). Hydrophobic black and
3277 organic carbon are chemically transformed into hydrophilic forms with a lifetime of 1.63
3278 days (Tie *et al.*, 2005). Different aerosol types are assumed to be externally mixed and do
3279 not interact with one another. Sulfur oxidation in the gas phase and within clouds is fully
3280 interactive with the gas-phase oxidant chemistry.

3281

3282 The transport in MOZART-2 is driven with meteorological inputs provided every three
3283 hours by the middle-atmosphere version of the NCAR Community Climate Model (Kiehl
3284 *et al.*, 1998). The meteorology was the same for each decade, thus excluding any
3285 feedbacks from climate change on natural emissions and rates of chemical reactions and
3286 removal. Thus, natural emissions, such as those of isoprene, dust, and NO_x from

3287 lightning, are held constant at present-day levels. Convective mass fluxes are re-
3288 diagnosed from the large-scale meteorology using the Hack (1994) and Zhang and
3289 McFarlane (1995) schemes. Vertical diffusion within the boundary layer is diagnosed
3290 using the scheme of Holtslag and Boville (1993). Tracer advection is performed using a
3291 flux-form semi-Lagrangian scheme (Lin and Rood, 1996).

3292

3293 The horizontal resolution is 2.8° latitude x 2.8° longitude, with 34 hybrid sigma-pressure
3294 levels extending up to 4 hPa. Photolysis frequencies for clear-sky are interpolated from a
3295 pre-calculated lookup table, based on a standard radiative transfer calculation (TUV
3296 version 3.0; (Madronich and Flocke, 1998). The values are modified to account for
3297 cloudiness (Brasseur *et al.*, 1998), but do not account for effects of the simulated
3298 aerosols. Heterogeneous hydrolysis of N_2O_5 and NO_3 on aerosol surfaces occurs at a rate
3299 based on the simulated sulfate surface area, with a reaction probability = 0.04 (Tie *et*
3300 *al.*, 2005). Stratospheric concentrations of ozone and several other long-lived gases are
3301 relaxed to present-day climatological values.

3302

3303 Dry deposition velocities for gas-phase species are calculated off-line using a resistance-
3304 in-series scheme (Wesely, 1989). Deposition velocities for aerosol species are prescribed
3305 as by Tie *et al.* (2005). Wet removal of soluble species in and below clouds is included as
3306 a first-order loss process, based on the large-scale and convective precipitation rates, as
3307 described by Horowitz *et al.* (2003). In-cloud scavenging is based on the
3308 parameterization of Giorgi and Chameides (1985), while below-cloud washout of highly
3309 soluble species follows Brasseur *et al.* (1998). For gas-phase species, the removal rate

3310 depends strongly on the temperature-dependent effective Henry's law constant. Wet
3311 deposition of soluble aerosols (sulfate, hydrophilic BC, hydrophilic OC, ammonium, and
3312 nitrate) is calculated by scaling the removal rate to that of highly-soluble HNO₃,
3313 assuming the aerosols have a first-order loss rate constant equal to 20% of that of HNO₃
3314 (Tie *et al.*, 2005). This scaling introduces a large uncertainty into the calculation of
3315 aerosol burdens. The sensitivity of model results to this scale factor is discussed below
3316 (Section 5). Wet removal of dust is calculated using the formulation of Zender *et al.*
3317 (2003), with below-cloud scavenging efficiencies of 0.02 m² kg⁻¹ for convective and 0.04
3318 m² kg⁻¹ for stratiform precipitation.

3319

3320 The ozone and aerosol distributions from these simulations have been evaluated by
3321 Horowitz (2006) and Ginoux *et al.* (2006), respectively. Simulated ozone concentrations
3322 agree well with present-day observations and recent trends (Horowitz, 2006). Overall, the
3323 predicted concentrations of aerosol are within a factor 2 of the observed values and have
3324 a tendency to be overestimated (Ginoux *et al.*, 2006). The annual mean surface sulfate
3325 concentrations match observed values within a factor 2 with values ranging from 0.05 µg
3326 m⁻³ in the remote marine atmosphere to 13 µg m⁻³ in polluted regions. In general, the
3327 simulated concentrations are over-predicted in summer and under-predicted in winter.
3328 Sulfate mass column and zonal mean profiles are comparable to previous studies,
3329 although the global mean burden is about 15% higher. The annual mean concentration of
3330 carbonaceous aerosols is generally overestimated in polluted regions by up to a factor of
3331 2. An exception is West Africa where other models show significant loadings of
3332 carbonaceous aerosols associated with biomass burning activities during the dry season

3333 while our results do not show any perturbation arising from such activities. The source of
3334 this discrepancy seems to be caused in part by the emission inventory in West Africa. The
3335 annual mean dust concentration at the surface agrees with the observations to within a
3336 factor 2, except over Antarctica where it is underestimated by a factor of 5.

3337

3338 The three-dimensional monthly mean distributions of ozone, black and organic carbon
3339 aerosol, and sulfate aerosol from MOZART-2 were archived from simulations for each
3340 decade from 2000 to 2100. The results from these simulations were then interpolated to
3341 intermediate years and used in the transient climate simulations. The distribution of dust
3342 from a present-day simulation in MOZART-2 was used in all years of the climate
3343 simulations.

3344

3345 **A.3.1.2 Goddard Institute for Space Studies**

3346 The configuration of the GISS composition model used here has been described in detail
3347 in (Shindell *et al.*, 2007). The composition model PUCCINI (Physical Understanding of
3348 Composition-Climate INteractions and Impacts) includes ozone and oxidant
3349 photochemistry in both the troposphere and stratosphere (Shindell *et al.*, 2006).

3350 Photochemistry includes 155 reactions. The model calculates the abundances of 51
3351 chemical species, 26 of which are transported by the model's advection scheme. It uses
3352 'lumped families' for hydrocarbons and PANs. Chemical reactions involving these
3353 surrogates are based on the similarity between the molecular bond structures within each
3354 family using the reduced chemical mechanism of (Houweling *et al.*, 1998). This
3355 mechanism is based on the Carbon Bond Mechanism-4 (CBM-4) (Gery *et al.*, 1989),

3356 modified to better represent the globally important range of conditions. The CBM-4
3357 scheme has been
3358
3359 validated extensively against smog chamber experiments and more detailed chemical
3360 schemes. This scheme was modified for use in global models by removing aromatic
3361 compounds and adding in reactions important in background conditions, including
3362 organic nitrate and organic peroxide reactions, and extending the methane oxidation
3363 chemistry. The revised scheme was then readjusted based on the more extensive Regional
3364 Atmospheric Chemistry Model (RACM) (Stockwell *et al.*, 1997), and the modified
3365 scheme includes several surrogate species designed to compensate for biases relative to
3366 the RACM mechanism. The modified scheme was shown to agree well with the detailed
3367 RACM reference mechanism over a wide range of chemical conditions including
3368 relatively pristine environments (Houweling *et al.*, 1998).
3369
3370 Rate coefficients are taken from the NASA JPL 2000 handbook (Sander *et al.*, 2000).
3371 Photolysis rates are calculated using the Fast-J2 scheme (Bian and Prather, 2002), except
3372 for the photolysis of water and nitric oxide (NO) in the Schumann-Runge bands, which
3373 are parameterized according to (Nicolet, 1984; Nicolet and Cieslik, 1980). The aerosols
3374 component simulates sulfate, carbonaceous and sea-salt aerosols (Koch *et al.*, 2007; Koch
3375 *et al.*, 2006) and nitrate aerosols (Bauer *et al.*, 2006). It includes prognostic simulations
3376 of DMS, MSA, SO₂ and sulfate mass distributions. The mineral dust aerosol model
3377 transports four different sizes classes of dust particles with radii between 0.1-1, 1-2, 2-4,
3378 and 4-8 microns (Miller *et al.*, 2006). Most importantly, these components interact with

3379 one another, with linkages including oxidants affecting sulfate, gas-phase nitrogen
3380 species affecting nitrate, sulfate affecting nitrogen heterogeneous chemistry via reaction
3381 of N_2O_5 to HNO_3 , and sulfate and nitrate being absorbed onto mineral dust surfaces (*i.e.*,
3382 the aerosols are internally mixed as coatings form on dust surfaces (Bauer *et al.*, 2006).
3383 The latter is described by a pseudo first-order rate coefficient which gives the net
3384 irreversible removal rate of gas-phase species to an aerosol surface. We use the uptake
3385 coefficient of 0.1 recommended from laboratory measurements (Hanisch and Crowley,
3386 2001), though this value is fairly uncertain.

3387

3388 Phase transformation and removal of soluble species is calculated using a wet deposition
3389 scheme in which soluble gases can be removed into either moist convective plumes or
3390 large-scale clouds as derived from the GCM's internal cloud scheme (Del Genio and
3391 Yao, 1993). During convection, all chemical species are transported along with the
3392 convective plumes, with scavenging of soluble species within and below cloud updrafts.
3393 In large-scale stratiform clouds, soluble gases are removed based on the fraction of the
3394 grid box over which precipitation is taking place. Washout of soluble species is
3395 calculated below precipitating clouds. In the case of either evaporation of precipitation
3396 before reaching the ground, or detrainment or evaporation from a convective updraft, the
3397 dissolved species are returned to the air. Wet chemistry calculations take place in each
3398 grid box at each time step, including the coupling with the convection scheme's
3399 entraining and nonentraining plumes (which are based on the convective instability in the
3400 particular grid box at that time), so are entirely consistent with the contemporaneous
3401 model physics. The solubility of each gas is determined by an effective Henry's Law

3402 coefficient, assuming a pH of 4.5. Surface dry deposition is calculated using a resistance-
3403 in-series model (Wesely and Hicks, 1977) coupled to a global, seasonally varying
3404 vegetation data set as given by (Chin *et al.*, 1996).

3405

3406 The 2000 simulation uses the 2000 emission inventory of the International Institute for
3407 Applied Systems Analysis (IIASA), except for biomass burning which is taken from the
3408 Global Fire Emission Database (GFED) averaged over 1997-2002 (Van der Werf *et al.*,
3409 2003) with emission factors from (Andrae and Merlet, 2001) for aerosols. The IIASA
3410 inventory is based on the 1995 EDGAR3.2 inventory (Olivier and Berdowski, 2001),
3411 extrapolated to 2000 using national and sector economic development data (Dentener *et*
3412 *al.*, 2005). Lightning NO_x emissions are calculated internally in the GCM (5.6 Tg/yr for
3413 present-day), and other natural sources are prescribed according to conventional
3414 estimates. Dust emissions are constant at 1580 Tg/yr, while isoprene emissions are 356
3415 Tg/yr. Emissions of DMS are 41 Tg/yr.

3416

3417 The simulations described here were run with this composition model included within a
3418 23-layer (up to 0.01 hPa), 4° x 5° horizontal resolution version of the ModelE climate
3419 model (Schmidt *et al.*, 2006). This composition model was used for both the transient
3420 climate and regional/sector emissions perturbation simulations.

3421

3422 Present-day composition results in the model are generally similar to those in the
3423 underlying chemistry and aerosol models documented previously. The model used here
3424 does not include the enhanced convective scavenging of insoluble species prescribed in

3425 (Koch *et al.*, 2007). Therefore our carbonaceous aerosol burden, especially in the free
3426 troposphere, is nearly double that of (Koch *et al.*, 2007). Comparison with the limited
3427 available observations is comparable between the two simulations (a positive bias
3428 replaces a negative bias).

3429

3430 **A.3.1.3 National Center for Atmospheric Research**

3431 Various methods were used at NCAR to estimate future composition. Present-day
3432 tropospheric ozone was taken from calculations performed by Lamarque *et al.* (2005)
3433 using the MOZART-2 model; beyond 2000, tropospheric ozone was calculated by T.
3434 Wigley using the MAGICC model
3435 (<http://www.cru.uea.ac.uk/~mikeh/software/magicc.htm>) forced by the time-varying
3436 emissions of NO_x, methane and VOCs and these average global values were used to scale
3437 the present-day distribution. Future carbonaceous aerosols were scaled from their
3438 present-day distribution (Collins *et al.*, 2001) by a globally uniform factor whose time
3439 evolution follows the global evolution of SO₂ emissions. Future levels of sulfate aerosols
3440 were calculated using the MOZART model. Stratospheric ozone changes are prescribed
3441 following the study by (Kiehl *et al.*, 1999).

3442

3443 The Model for Ozone and Related chemical Tracers version 2 (MOZART-2) is
3444 described by Horowitz *et al.* (2003) and references therein. The model provides the
3445 distribution of 80 chemical constituents (including nonmethane hydrocarbons) between
3446 the surface and the stratosphere. The model was run at a uniform horizontal resolution
3447 of ~2.8° in both latitude and longitude. The vertical discretization of the

3448 meteorological data (described below) and hence of the model consists of 18 hybrid
3449 levels from the ground to ~4 hPa. The evolution of species is calculated with a time
3450 step of 20 min.

3451 The tropospheric photolysis rates use a vertical distribution of ozone based on the
3452 simulated ozone in the troposphere and on the climatology from Kiehl *et al.* (1999)
3453 above. For each simulation, this latter distribution is updated to reflect the changes in the
3454 lower stratosphere during the 20th century, affecting only the photolysis rates and not the
3455 amount of ozone transported from the stratosphere.

3456

3457 The NCAR regional/sector perturbation simulations (Section 3.4) used a version of
3458 MOZART chemical transport model (Horowitz *et al.*, 2003) embedded within the
3459 Community Atmosphere Model (CAM3, Collins *et al.*, 2006). This model, known as
3460 CAM-chem, includes an extension of the chemical mechanism presented by Horowitz *et*
3461 *al.* (2003) to include an updated terpene oxidation scheme and a better treatment of
3462 anthropogenic non-methane hydrocarbons (NMHCs). The MOZART aerosols have been
3463 extended by Tie *et al.* (2001, 2005) to include a representation of ammonium nitrate that
3464 is dependent on the amount of sulfate and ammonia present in the air mass following the
3465 parameterization of gas/aerosol partitioning by Metzger *et al.* (2002). In brief, CAM-
3466 chem simulates the evolution of the bulk aerosol mass of black carbon (BC, hydrophobic
3467 and hydrophilic), primary organic (POA, hydrophobic and hydrophilic), second organic
3468 (SOA, linked to the gas-phase chemistry through the oxidation of atmospheric NMHCs
3469 as in (Chung and Seinfeld, 2002), ammonium and ammonium nitrate (from NH₃
3470 emissions), and sulfate aerosols (from SO₂ and DMS emissions). It also considers the

3471 uptake of N₂O₅, HO₂, NO₂, and NO₃ on aerosols. Results from the CAM-chem model are
3472 discussed by Lamarque *et al.* (2005b). A description of sea-salt, updated from Tie *et al.*
3473 (2005), is also included. Finally, a monthly-varying climatology of dust is used only for
3474 radiative calculations. The CAM-chem model considers only the direct effect of aerosols
3475 and the atmospheric model is coupled with the chemistry solely through the radiative
3476 fluxes, taking into account all radiatively active gases and aerosols. The horizontal
3477 resolution is 2° latitude x 2.5° longitude, with 26 levels ranging from the surface to ~4
3478 hPa.

3479 **Appendix 3.2 Climate Models**

3480 **A.3.2.1 Geophysical Fluid Dynamics Laboratory**

3481 Climate simulations at GFDL used the coupled climate model recently developed at
3482 NOAA's Geophysical Fluid Dynamics Laboratory, which has been previously described
3483 in detail (Delworth *et al.*, 2006). We will summarize here. The model simulates
3484 atmospheric and oceanic climate and variability from the diurnal time-scale through
3485 multi-century climate change without employing flux adjustment. The control simulation
3486 has a stable, realistic climate when integrated over multiple centuries and a realistic
3487 ENSO (Wittenberg *et al.*, 2006). Its equilibrium climate response to a doubling of CO₂ is
3488 3.4C¹ (Stouffer *et al.*, 2006). There are no indirect aerosol effects included in any of the
3489 simulations. The resolution of the land and atmospheric components is 2.5° longitude x
3490 2° latitude and the atmospheric model has 24 vertical levels. The ocean resolution is 1°
3491 latitude x 1° longitude, with meridional resolution equatorward of 30° becoming
3492 progressively finer, such that the meridional resolution is 1/3° at the Equator. There are
3493 50 vertical levels in the ocean, with 22 evenly spaced levels within the top 220 m. The
3494 ocean component has poles over North America and Eurasia to avoid polar filtering.
3495
3496 Using a five member ensemble simulation of the historical climate (1861-2003) including
3497 the evolution of natural and anthropogenic forcing agents, the GFDL climate model is
3498 able to capture the global historical trend in observed surface temperature for the 20th
3499 century as well as many continental-scale features (Knutson *et al.*, 2006). However, the
3500 model shows some tendency for too much twentieth-century warming in lower latitudes
3501 and too little warming in higher latitudes. Differences in Arctic Oscillation behavior

3502 between models and observations contribute substantially to an underprediction of the
3503 observed warming over northern Asia. El Niño interactions complicate comparisons of
3504 observed and simulated temperature records for the El Chichón and Mt. Pinatubo
3505 eruptions during the early 1980s and early 1990s (Knutson *et al.*, 2006). In Figure 7d of
3506 Knutson *et al.* (2006), where the model ensemble and observations are compared grid
3507 box by grid box, ~ 60% of those grid boxes with sufficient observational data have 20th
3508 Century surface temperature trends that agree quantitatively with the model ensemble. In
3509 general, many observed continental-scale features, including a 20th century cooling over
3510 the North Atlantic, are captured by the model ensemble, as Figures 7a and 7c in Knutson
3511 *et al.* (2006) show. However, the model ensemble does not capture the observed cooling
3512 over the southeastern US and it produces a 20th century cooling over the North Pacific
3513 that is not observed.

3514

3515 **A.3.2.2 Goddard Institute for Space Studies**

3516 The GISS climate simulations were performed using GISS ModelE (Schmidt *et al.*,
3517 2006). We use a 20-layer version of the atmospheric model (up to 0.1 hPa) coupled to a
3518 dynamic ocean without flux adjustment, both run at 4 by 5 degree horizontal resolution,
3519 as in the GISS-ER IPCC AR4 simulations (Hansen *et al.*, 2007). This model has been
3520 extensively evaluated against observations (Schmidt *et al.*, 2006), and has a climate
3521 sensitivity in accord with values inferred from paleoclimate data and similar to that of
3522 mainstream GCMs; an equilibrium climate sensitivity of 2.6°C for doubled CO₂.

3523 The modeled radiatively active species influence the climate in the GCM. Ozone and
3524 aerosols can affect both the short and long wavelength radiation flux. Water uptake on

3525 aerosol surfaces influences the aerosol effective radius, refractive index and extinction
3526 efficiency as a function of wavelength and the local relative humidity (Koch *et al.*, 2007),
3527 which in turn affects the GCM's radiation field.

3528

3529 The GISS model also includes a simple parameterization for the aerosol indirect effect
3530 (Menon *et al.*, 2002) (see box on aerosol indirect effect). For the present simulations, we
3531 use only cloud cover changes (the 2nd indirect effect), with empirical coefficients
3532 selected to give roughly -1 W m^{-2} forcing from the preindustrial to the present, a value
3533 chosen to match diurnal temperature and satellite polarization measurements, as
3534 described in (Hansen *et al.*, 2005). We note, however, that this forcing is roughly twice
3535 the value of many other model studies (Penner *et al.*, 2006). The aerosol indirect effect in
3536 the model takes place only from the surface through ~ 570 hPa, as we only let aerosols
3537 affect liquid-phase stratus clouds.

3538

3539 **A.3.2.3 National Center for Atmospheric Research**

3540 The transient climate simulations use the NCAR Community Climate System Model
3541 CCSM3 (Collins *et al.*, 2006). This model had been run previously with evolution of
3542 short-lived species in the future for the IPCC AR4. The model was run at T85 ($\sim 1.4^\circ \times$
3543 1.4° resolution). For this study, a new simulation was performed for 2000-2050 in which
3544 ozone and aerosols were kept at their 2000 levels. The equilibrium climate sensitivity of
3545 this model to doubled CO_2 is 2.7°C .

- 3546 **Appendix 3.2 References**
3547
- 3548 **Bauer, S. E., M. I. Mishchenko, A. Lacis, S. Zhang, J. Perlwitz, and S. M. Metzger**
3549 (2006), Do sulfate and nitrate coatings on mineral dust have important effects on
3550 radiative properties and climate modeling?, *J. Geophys. Res.*, 112, D06307, doi:
3551 10.1029/2005JD006977.
3552
- 3553 **Bian, H., and M. Prather (2002), Fast-J2: Accurate simulations of photolysis in global**
3554 **climate models, *J. Atmos. Chem.*, 41, 281-296.**
3555
- 3556 **Brasseur, G. P., D. A. Hauglustaine, S. Walters, P. J. Rasch, J.-F. Müller, C. Granier,**
3557 **and X. Tie (1998), MOZART, a global chemical transport model for ozone and**
3558 **related chemical tracers, 1, Model description, *J. Geophys. Res.*, 103, 28,265-**
3559 **228,289.**
3560
- 3561 **Chin, M., D. J. Jacob, G. M. Gardner, M. S. Forman-Fowler, P. A. Spiro, and D. L.**
3562 **Savoie (1996), A global three-dimensional model of tropospheric sulfate, *J. Geophys.***
3563 ***Res.*, 101, 18,667-618,690.**
3564
- 3565 **Collins, W. D., P. J. Rasch, B. E. Eaton, B. Khattatov, J.-F. Lamarque, and C. S. Zender**
3566 **(2001), Simulating aerosols using a chemical transport model with assimilation of**
3567 **satellite aerosol retrievals: Methodology for INDOEX, *J. Geophys. Res.*, 106, 7313–**
3568 **7336.**
3569
- 3570 **Collins, W. D., *et al.* (2006), The formulation and atmospheric simulation of the**
3571 **Community Atmosphere Model: CAM3, *J. Clim.*, 19, 2144-2161.**
3572
- 3573 **Del Genio, A. D., and M.-S. Yao (1993), Efficient cumulus parameterization for long-**
3574 **term climate studies: The GISS scheme, in *The Representation of Cumulus***
3575 **Convection in Numerical Models, AMS Meteor. Monograph, edited by K. A.**
3576 **Emanuel and D. A. Raymond, pp. 181-184, American Meteorological Society.**
3577
- 3578 **Delworth, T. L., *et al.* (2006), GFDL's CM2 Global Coupled Climate Models. Part I:**
3579 **Formulation and simulation characteristics, *J. Clim.*, 19, 643-674.**
3580
- 3581 **Gery, M. W., G. Z. Whitten, J. P. Killus, and M. C. Dodge (1989), A photochemical**
3582 **kinetics mechanism for urban and regional scale computer modeling, *J. Geophys.***
3583 ***Res.*, 94, 925-956.**
3584
- 3585 **Ginoux, P., L. W. Horowitz, V. Ramaswamy, I. V. Geogdzhayev, B. N. Holben, G.**
3586 **Stenchikov, and X. Tie (2006), Evaluation of aerosol distribution and optical depth in**
3587 **the Geophysical Fluid Dynamics Laboratory coupled model CM2.1 for present**
3588 **climate, *J. Geophys. Res.*, 111, D22210, doi:10.1029/2005JD006707.**
3589
- 3590 **Giorgi, F., and W.L. Chameides (1985), The rainout parameterization in a photochemical**
3591 **model, *J. Geophys. Res.*, 90, 7872-7880.**

- 3592
3593 **Hack, J. J.** (1994), Parameterization of moist convection in the NCAR community
3594 climate model (CCM2), *J. Geophys. Res.*, 99, 5551– 5568.
3595
- 3596 **Hanisch, F.,** and J. N. Crowley (2001), The heterogeneous reactivity of gaseous nitric
3597 acid on authentic mineral dust samples, and on individual mineral and clay mineral
3598 components, *Phys. Chem. Chem. Phys.*, 3, 2474-2482.
3599
- 3600 **Hansen, J., et al.** (2005), Efficacy of Climate Forcings, *J. Geophys. Res.*, 110, D18104,
3601 doi:10.1029/2005JD005776.
3602
- 3603 **Hansen, J., et al.** (2007), Dangerous human-made interference with climate: A GISS
3604 modelE study, *Atmos. Chem. Phys.*, 7, 2287-2312.
3605
- 3606 **Holtslag, A.,** and B. Boville (1993), Local versus nonlocal boundary-layer diffusion in a
3607 global climate model, *J. Clim.*, 6, 1825-1842.
3608
- 3609 **Horowitz, L. W.** (2006), Past, present, and future concentrations of tropospheric ozone
3610 and aerosols: Methodology, ozone evaluation, and sensitivity to aerosol wet removal,
3611 *J. Geophys. Res.*, 111, D22211, doi:10.1029/2005JD006937.
3612
- 3613 **Horowitz, L. W., et al.** (2003), A global simulation of tropospheric ozone and related
3614 tracers: Description and evaluation of MOZART, version 2, *J. Geophys. Res.*,
3615 108(D24), 4784, doi:10.1029/2002JD002853.
3616
- 3617 **Houweling, S.,** F. Dentener, and J. Lelieveld (1998), The impact of non-methane
3618 hydrocarbon compounds on tropospheric photochemistry, *J. Geophys. Res.*, 103,
3619 10,673-610,696.
3620
- 3621 **Kiehl, J. T.,** J. J. Hack, G. B. Bonan, B. A. Boville, D. L. Williamson, and P. J. Rasch
3622 (1998), The National Center for Atmospheric Research Community Climate Model:
3623 CCM3, *J. Clim.*, 11, 1131-1149.
3624
- 3625 **Kiehl, J. T.,** T. L. Schneider, R. W. Portmann, and S. Solomon (1999), Climate forcing
3626 due to tropospheric and stratospheric ozone, *J. Geophys. Res.*, 104, 31,239-231,254.
3627
- 3628 **Koch, D.,** T. Bond, D. Streets, N. Bell, and G. R. van der Werf (2007), Global impacts of
3629 aerosols from particular source regions and sectors, *J. Geophys. Res.*, 112, D02205,
3630 doi:10.1029/2005JD007024.
3631
- 3632 **Koch, D.,** G. Schmidt, and C. Field (2006), Sulfur, sea salt and radionuclide aerosols in
3633 GISS ModelE, *J. Geophys. Res.*, 111, D06206, doi:10.1029/2004JD005550.
3634
- 3635 **Lamarque, J.-F.,** P. Hess, L. Emmons, L. Buja, W. M. Washington, and C. Granier
3636 (2005), Tropospheric ozone evolution between 1890 and 1990, *J. Geophys. Res.*, 110,
3637 D08304, doi:10.1029/2004JD005537.

- 3638
3639 **Lin, S.-J., and R.B. Rood (1996)**, Multidimensional flux-form semi-lagrangian transport
3640 schemes, *Mon. Wea. Rev.*, 124, 2046-2070.
3641
- 3642 **Madronich, S., and S. Flocke (1998)**, The role of solar radiation in atmospheric
3643 chemistry, in *Handbook of Environmental Chemistry*, edited by P. Boule, pp. 1-26,
3644 Springer-Verlag, New York.
3645
- 3646 **Menon, S., A. , D. Del Genio, D. Koch, and G. Tselioudis (2002)**, GCM Simulations of
3647 the Aerosol Indirect Effect: Sensitivity to Cloud Parameterization and Aerosol
3648 Burden, *J. Atmos. Sci.*, 59, 692-713.
3649
- 3650 **Miller, R. L., et al. (2006)**, Mineral Dust Aerosols in the NASA Goddard Institute for
3651 Space Studies ModelE AGCM, *J. Geophys. Res.*, 111, D0208,
3652 doi:10.1029/2005JD005796.
3653
- 3654 **Nicolet, M. (1984)**, On the photodissociation of water vapour in the mesosphere, *Planet.*
3655 *Space Sci.*, 32, 871-880.
3656
- 3657 **Nicolet, M., and S. Cieslik (1980)**, The photodissociation of nitric oxide in the
3658 mesosphere and stratosphere, *Planet. Space Sci.*, 28, 105-115.
3659
- 3660 **Penner, J. E., J. Quaas, T. Storelvmo, T. Takemura, O. Boucher, H. Guo, A. Kirkevåg, J.**
3661 **E. Kristjansson, and Ø. Seland (2006)**, Model intercomparison of indirect aerosol
3662 effects, *Atmos. Chem. Phys. Discuss.*, 6, 1579-1617.
3663
- 3664 **Sander, S. P., et al. (2000)**, Chemical kinetics and photochemical data for use in
3665 stratospheric modeling, *Eval. 13*, JPL Publ. 00-003.
3666
- 3667 **Schmidt, G. A., et al. (2006)**, Present day atmospheric simulations using GISS ModelE:
3668 Comparison to in-situ, satellite and reanalysis data, *J. Clim.*, 19, 153-192.
3669
- 3670 **Shindell, D. T., G. Faluvegi, S. E. Bauer, D. M. Koch, N. Unger, S. Menon, A., R. L.**
3671 **Miller, G. A. Schmidt, and D. G. Streets (2007)**, Climate response to projected
3672 changes in short-lived species under an A1B scenario from 2000-2050 in the GISS
3673 climate model, *J. Geophys. Res.*, 112, D20103, doi:10.1029/2007JD008753.
3674
- 3675 **Shindell, D. T., G. Faluvegi, N. Unger, E. Aguilar, G. A. Schmidt, D. Koch, S. E. Bauer,**
3676 **and R. L. Miller (2006)**, Simulations of preindustrial, present-day, and 2100
3677 conditions in the NASA GISS composition and climate model G-PUCCINI, *Atmos.*
3678 *Chem. Phys.*, 6, 4427-4459.
3679
- 3680 **Stockwell, W. R., F. Kirchner, M. Kuhn, and S. Seefeld (1997)**, A new mechanism for
3681 regional atmospheric chemistry modeling, 102, 25,847-825,879.
3682

- 3683 **Tie, X.**, S. Madronich, S. Walters, D.P. Edwards, P. Ginoux, N. Mahowald, R. Zhang, C.
3684 Lou, and G. Brasseur (2005), Assessment of the global impact of aerosols on
3685 tropospheric oxidants, *J. Geophys. Res.*, 110, D03204, doi:10.1029/2004JD005359.
3686
- 3687 **Wesely, M.L.** (1989), Parameterization of surface resistance to gaseous dry deposition in
3688 regional-scale numerical models, *Atmos. Environ.*, 23, 1293-1304.
3689
- 3690 **Wesely, M. L.**, and B. B. Hicks (1977), Some factors that affect the deposition rates of
3691 sulfur dioxide and similar gases on vegetation, *J. Air Pollut. Control Assoc.*, 27,
3692 1110-1116.
3693
- 3694 **Zender, C. S.**, H. Bian, and D. Newman (2003), Mineral Dust Entrainment and
3695 Deposition (DEAD) model: Description and 1990s dust climatology, *J. Geophys.*
3696 *Res.*, 108(D14), 4416, doi:10.1029/2002JD002775.
3697
- 3698 **Zhang, G.J.**, and N.A. McFarlane (1995), Sensitivity of climate simulations to the
3699 parameterization of cumulus convection in the Canadian Climate Centre general
3700 circulation model, *Atmos. Ocean*, 33, 407-446.

3701 **Chapter 4 Findings, Issues, Opportunities, and** 3702 **Recommendations**

3703

3704 **Lead Author(s):** Hiram Levy II, GFDL/NOAA; Drew T. Shindell, GISS/NASA; Alice
3705 Gilliland, ARL/NOAA

3706

3707 **4.1 Introduction**

3708 This Chapter, which is intended for both technical and non-technical audiences, provides
3709 a summary of the major findings, presents a number of new questions that were revealed
3710 by our study, and identifies new opportunities for future research.

3711

3712 **4.2 Major Findings**

3713 The major Findings of Synthesis and Assessment Product 3.2 are summarized below:

3714

3715 1. The SAP 2.1a emission scenarios for long-lived³⁹ species produce climate projections
3716 that are within the IPCC range, although it should be noted that the most extreme
3717 stabilization scenario⁴⁰, which is equivalent to a carbon dioxide stabilization level of 450
3718 ppm, results in global surface temperatures below those calculated for the most moderate
3719 IPCC scenario, particularly beyond 2050.

3720

³⁹ Atmospheric lifetimes for the long-lived radiative species of interest range from 10 years for methane to more than 100 years for nitrous oxide. While carbon dioxide's lifetime is more complex, we can think of it as being more than 100 years in the climate system. As a result of their long atmospheric lifetime, they are well-mixed and evenly distributed throughout. Global atmospheric lifetime is the mass of a species in the atmosphere divided by the mass that is removed from the atmosphere each year.

⁴⁰ Stabilization scenarios are a representation of the future emissions of a substance based on a coherent and internally consistent set of assumptions about the driving forces (such as population, socio-economic development, technological change) and their key relationships. These emissions are constrained so that the resulting atmospheric concentrations of the substance level-off at a pre-determined value in the future.

3721 2. Our results suggest that the short-lived⁴¹ species do matter to the climate, even out to
3722 year 2100. The presence of radiatively active⁴² short-lived species can significantly
3723 change the regional surface temperature response (for example over the summertime
3724 continental US). It is noteworthy that the location of the simulated climate response is not
3725 local to the forcing.

3726

3727 3. We find that the geographic (spatial) distribution of radiative forcing⁴³ is less
3728 important than the spatial distribution of climate response. Thus, both short-lived and
3729 long-lived species appear to cause enhanced climate responses in the same regions rather
3730 than short-lived species having an enhanced effect primarily in or near polluted areas.
3731 This means that regional emission control strategies for short-lived pollutants will have
3732 large-scale climate impacts.

3733

3734 4. The three comprehensive climate models⁴⁴ and their associated chemical composition
3735 models⁴⁵ participating in this report produced differing outcomes. Each model represents

⁴¹ Atmospheric lifetimes for the short-lived radiative species of interest range in the lower atmosphere from a day for nitrogen oxides, from a day to a week for most particles, and from a week to a month for ozone. As a result of their short lifetime their concentrations are highly variable and concentrated in the lowest part of the atmosphere, primarily near their sources.

⁴² Radiatively active indicates the ability of a substance to absorb and re-emit radiation, thus changing the temperature of the lower atmosphere.

⁴³ Radiative forcing is a measure of how the energy balance of the Earth-atmosphere system is influenced when factors that affect climate, such as atmospheric composition or surface reflectivity, are altered. When radiative forcing is positive, the energy of the Earth-atmosphere system will ultimately increase, leading to a warming of the system. In contrast, for a negative radiative forcing, the energy will ultimately decrease, leading to a cooling of the system. For technical details see Box 3.2.

⁴⁴ Comprehensive climate models are state-of-the-art numerical representation of the climate based on the physical, chemical and biological properties of its components, their interactions and feedback processes that accounts for many of climate's known properties. Coupled atmosphere/ocean/sea-ice General Circulation Models (AOGCMs) provide a comprehensive representation of the physical climate system.

⁴⁵ Chemical composition models are state-of-the-art numerical models that use the emission of gases and particles as inputs and simulate their chemical interactions, global transport by the winds, and removal by rain, snow and deposition to the earth's surface. The resulting outputs are global three-dimensional distributions of the initial gases and particles and their products.

3736 a thoughtful, but incomplete characterization of the driving forces and processes that are
3737 believed to be important to the climate or to the global distributions of the short-lived
3738 species. This was only a beginning. Much work remains to be done regarding the climate
3739 response to short-lived species.

3740

3741 5. The two most important uncertainties in characterizing the potential climate impact of
3742 short-lived species are found to be the projection of their future emissions and the
3743 determination of the indirect effect⁴⁶ of particles on climate. See 4.3 for a discussion of
3744 the fundamental difference between uncertainties in future emissions and uncertainties in
3745 processes, such as the indirect effect of particles.

3746

3747 6. Natural particles such as dust and sea salt also play an important role and their
3748 emissions and interactions differed significantly among the models, with consequences to
3749 the role of short-lived pollutants. This inconsistency among models should be reconciled
3750 in future studies.

3751

3752 7. Emissions reductions of soot in the domestic energy/power sector in Asia appear to
3753 offer the greatest potential for substantial, simultaneous improvement in local air quality
3754 and reduction of global climate change.

3755

3756

3757

⁴⁶ Particles may have an indirect effect on the climate system by modifying the optical properties and lifetime of clouds. A detailed technical discussion is given in Box 3.1.

3758 **4.3 Issues Raised**

3759 It is important to recognize the difference between uncertainties in processes and
3760 uncertainties in future emissions. Uncertainties in chemical and physical processes, which
3761 are discussed in 4.3.2-3, represent the state of our current knowledge. The fact that one
3762 modeling group chooses to include a process such as indirect forcing of climate by
3763 particles, while another group chooses not to, shows that our knowledge about short-lived
3764 species and their interactions with climate is still evolving. Eventually, with further
3765 research, uncertainties in chemical and physical processes can be reduced if not
3766 completely removed. However, uncertainties in future emissions, which are discussed in
3767 4.3.1, will always be with us. What we can do is develop a set of internally consistent
3768 emission scenarios that include all of the important radiative species and bracket the full
3769 range of possible future outcomes.

3770

3771 **4.3.1 Emission Projections**

3772 The analysis presented in Chapter 3 showed that the main contributors to the divergence
3773 among model projections of future particle loading and climate forcing were the
3774 differences in the underlying emissions projections. Those differences arose from two
3775 primary factors. First, different integrated assessment models⁴⁷ interpret a common
3776 socio-economic ‘storyline’ in different ways, as demonstrated in Chapter 2. Second,
3777 emission scenarios were not produce for some short-lived species and had to be added in
3778 later by other emissions modeling groups or by the climate modeling groups themselves.
3779 These same issues were also encountered in Chapter 2 which focused on the SAP 2.1

⁴⁷ Integrated assessment models are a framework of models, currently quite simplified, from the physical, biological, economic and social sciences that interact among themselves in a consistent manner and can be used to evaluate the status and the consequences of environmental change and the policy responses to it.

3780 stabilization scenarios. While emission scenarios for short-lived species were outside of
3781 SAP 2.1's mandate, climate projections require them. Part of the reason for the different
3782 emission inventories used here and in the IPCC studies was that the integrated assessment
3783 models did not recognize that these species were necessarily important when the
3784 scenarios were first constructed.

3785

3786 Just consider two of the integrated assessment models used to generate the sulfur dioxide
3787 and nitrogen oxide emissions for the A1B scenario used in Chapter 3: The two models
3788 project different rates of growth; Total energy use is also different in the two models,
3789 with 3% greater use in one model by 2030, but 9% less usage at 2050; That same model
3790 is less optimistic about emissions controls.

3791

3792 None of the emission models predict elemental and organic carbon aerosol⁴⁸ emissions.
3793 The GFDL composition model followed the IPCC suggestion to scale future carbon
3794 aerosol emissions by the emissions for carbon monoxide, which are projected to increase
3795 throughout the 21st century. By 2050, the projected carbon monoxide emission increases
3796 range from 8 to 119% across the collection of integrated assessment models used for the
3797 last IPCC report. In contrast, the GISS global chemical composition model used recent
3798 estimates by Streets *et al.* (2004) that project a substantial decrease in future emissions of
3799 carbon aerosol (Figure 3.1; Table 3.1). Ammonia emissions present a similar problem.
3800 They are sometimes scaled by default to follow nitrous oxide, which is projected to
3801 increase significantly. Given the number of ammonia sources that are disconnected from

⁴⁸ Aerosols are very small airborne solid or liquid particles that reside in the atmosphere for at least several hours with the smallest remaining airborne for days.

3802 nitrous oxide production, this may be questionable. Moreover newer projections for
3803 ammonia emission have a much slower rate of increase.

3804

3805 Finally, the global chemical composition models all used their own natural emissions.
3806 Though these were held constant, they influence the response to anthropogenic emissions
3807 by determining the background abundance of short-lived species. The level of natural
3808 species, dust, can also directly affect the level of an anthropogenic species, as it does in
3809 the GISS model by removing sulfate particles.

3810

3811 We face very significant problems in projecting the future emissions for short-lived
3812 species. Future climates are only weakly dependent on the projected emissions of short
3813 lived species for the next 20 years when, due to the inertia in the major emitters of most
3814 short-lived species, we may have credibility in forecasting emission trends for a species
3815 such as sulfur dioxide or the nitrogen oxides. However, we have shown that plausible
3816 emission scenarios for the short-lived species have the potential for significant climate
3817 impacts through the rest of the 21st century.

3818

3819 Unlike the long-lived greenhouse gases, they do not accumulate, so the full impact of
3820 short-lived species at year 2100 depends on their end of the century emissions. At this
3821 time, there is no credible quantitative skill in forecasting short-lived emissions out to
3822 2100. As Chapter 3 demonstrates, it is not even clear that we can currently predict the
3823 sign of the change for elemental carbon emissions over the next decade. This is a problem
3824 that requires not just enhanced scientific knowledge, but also the ability to predict social,

3825 economic and technological developments as far as 100 years into the future. One needs
3826 only to think back to 1907 to realize how difficult that is and will be.

3827

3828 **4.3.2 Aerosols (Indirect Effect, Direct Effect, Mixing, Water Uptake)**

3829 We find that several aspects of aerosol modeling have large uncertainties, of which the
3830 aerosol indirect effect, which is very poorly known, is probably the most critical. Many
3831 aspects of the aerosol-cloud interaction are not well quantified, and hence the effect was
3832 left out entirely in the GFDL and NCAR simulations. The GISS model used a highly
3833 parameterized approach that is quite crude. The modeling community as a whole cannot
3834 yet produce a credible characterization of the climate response to aerosol/cloud
3835 interactions. All models (including those participating in this study) are currently either
3836 ignoring it, or strongly constraining the model response.

3837

3838 As discussed in Section 3.2.4, observations of aerosol optical depth⁴⁹ are best able to
3839 constrain the total extinction (absorption + scattering) of sunlight by all aerosols under
3840 clear-sky conditions, but not to identify the effect of individual species which may scatter
3841 [cool] or absorb [warm]. Improved measurements of extinction and absorption may allow
3842 those two classes of aerosols to be separated, but will not solve the fundamental problem
3843 of determining the relative importance of individual species. As seen in this and other
3844 studies, models exhibit a wide range of relative contributions to total aerosol optical
3845 depth from the various natural and anthropogenic aerosols (see Figure 3.2). Thus, the
3846 direct radiative effect of changes in a particular aerosol species can be substantially

⁴⁹Aerosol optical depth is a measure of the fraction of radiation at a given wavelength absorbed or scattered by aerosols while passing through the atmosphere.

3847 different among models depending upon the relative importance of that aerosol.

3848

3849 Additionally, aerosol species are not independent of one another. They mix together, a
3850 process that is only beginning to be incorporated in composition and climate models. In
3851 these studies, for example, the GISS model included the influence of sulfate particles
3852 sticking to dust, which can decrease the sulfate radiative forcing, by ~40% between 2000
3853 and 2030 (Bauer *et al.*, 2007), but the sticking rates are quite uncertain. Mixing of other
3854 aerosol types is also highly uncertain, but is known to occur in the atmosphere and would
3855 also affect the magnitude of aerosol radiative forcings.

3856

3857 Another process that influences the effect of aerosols on climate is their uptake of water
3858 vapor, which alters their size and optical properties. This process is now included in all
3859 state-of –the-art comprehensive climate models. As the uptake varies exponentially with
3860 relative humidity, small differences in treatment of this process have the potential to
3861 cause large discrepancies. However, our analysis in Chapter 3 (*e.g.* Table 3.7) suggests
3862 that the differences induced by this process may be small relative to the others we have
3863 just discussed.

3864

3865 **4.3.3 Climate and Air Quality Policy Interdependence**

3866 Chapter 3 exposes major uncertainties in the climate impacts of short-lived species that
3867 will have to be addressed in future research. We raise important issues linking air quality
3868 control and global warming, but are unable to provide conclusive answers. We are able,
3869 however, to identify key questions that must be addressed by future research.

3870

3871 Most future sources of these short-lived species result from the same combustion
3872 processes responsible for the increases in atmospheric carbon dioxide. However,
3873 reductions in their emissions will be driven by local and regional air pollution issues that
3874 can be addressed independently of any reductions in carbon dioxide emissions.

3875 Furthermore their climate responses to emission changes can be felt much more quickly
3876 because of shorter atmospheric lifetimes. The good news is that there is at least one clear
3877 win-win solution for climate and air quality, methane reduction. Elemental carbon (black
3878 carbon) particles and nitrogen oxide are potential win-win as well, but the climate impact
3879 of reductions in their emissions is uncertain. On the other hand, the reduction of sulfur
3880 and organic carbon aerosols results in the loss of cooling and increased global warming.

3881

3882 The cases of black or elemental carbon (soot) and nitrogen oxide gases are illustrative of
3883 the complexities of this issue. A major source of soot is the burning of biofuel, the
3884 sources of which are primarily animal and human waste as well as crop residue, all of
3885 which are considered carbon dioxide neutral. Current suggested replacements result in the
3886 release of fossil carbon dioxide. Therefore this reduction in biofuel burning, while
3887 reducing the emission of soot, will increase the emission of carbon dioxide. The actual
3888 net climate response from reduced use of biofuel is not clear. The case of nitrogen oxides
3889 appears to be approximately neutral for climate, though clearly a strong win for air
3890 quality. Reducing nitrogen oxides reduces ozone, which reduces warming. However,
3891 reductions in both lead to reduced hydroxyl radicals and therefore an increased level of

3892 methane, which increases warming. We must pay careful attention to the “Law of
3893 Unintended Consequences”.

3894

3895 There clearly are win-win, win-uncertain, and win-lose situations regarding climate and
3896 actions taken to improve air quality. We are not making any policy recommendations in
3897 Synthesis and Assessment Product 3.2, but we do identify the policy relevant scientific
3898 issues. At this time we can not provide any quantitatively definitive scientific answers
3899 beyond the well known facts that the decrease of sulfur and organic carbon particles, both
3900 of which cool the climate, will increase global warming, while decreased methane will
3901 decrease global mean warming. Decreases in the burning of biofuel, as well as decreased
3902 emissions of nitrogen oxides are more complex and the net result is not clear at this time.

3903

3904 **4.4 Research Opportunities and Recommendations**

3905 This last Section of the report is a call for focused scientific research in emission
3906 projections, radiative forcing⁵⁰, chemical composition modeling and regional
3907 downscaling. Particular emphasis needs to be paid to the future emission scenarios for
3908 sulfur dioxide, elemental carbon particles and nitrogen oxides, to the indirect radiative
3909 forcing by aerosols, and to a number of ambiguities in current treatments of transport,
3910 deposition, and chemistry.

3911

3912

⁵⁰ Radiative forcing is a measure of how the energy balance of the Earth-atmosphere system is influenced when factors that affect climate, such as atmospheric composition or surface reflectivity, are altered. When radiative forcing is positive, the energy of the Earth-atmosphere system will ultimately increase, leading to a warming of the system. In contrast, for a negative radiative forcing, the energy will ultimately decrease, leading to a cooling of the system. For technical details see Box 3.2

3913 **4.4.1 Emission Scenario Development**

3914 Future climate studies must seriously address the very difficult issue of producing
3915 realistic and consistent 100 year emission scenarios for short-lived species that include a
3916 wide range of socio-economic and development pathways and are driven by local and
3917 regional air quality actions taken around the globe.

3918

3919 The current best projections used in this report and in the 4th Assessment Report of the
3920 IPCC do not even agree on whether elemental carbon particle and nitrogen oxide
3921 emission trends continue to increase or decrease. While all sulfur dioxide emissions
3922 trends assume that emissions in 2100 will be less than present, how much less is quite
3923 uncertain, and all may well be wrong. Part of the reason for the different emission
3924 inventories for short-lived species used here and in the IPCC studies was that the
3925 integrated assessment models did not recognize that these species were necessarily
3926 important when the scenarios were first constructed. Clarification of the challenges
3927 associated with emissions projections (not a simple matter of improving quantitative skill,
3928 as these are a function of difficult-to-anticipate socioeconomic choices) is also necessary.

3929

3930 As the greatest divergences in our study came from the carbon aerosols that were not
3931 projected for the A1B scenario, we strongly recommend that future emission scenarios
3932 pay greater attention to the short-lived species and provide consistent emissions
3933 projections for carbon aerosols and ammonia along with the other short-lived and long-
3934 lived species. We are aware that many integrated assessment models are already capable

3935 of providing this information (*e.g.* two of the three discussed in Chapter 2 provide carbon
3936 aerosol emissions).

3937

3938 We also recommend that climate models make greater efforts to study the effects of
3939 short-lived emissions projections in a manner that isolates their effect from that of the
3940 long-lived greenhouse gases. In particular, we believe there is merit in continuing to use a
3941 broad distribution of integrated assessment models to realistically characterize the range
3942 of potential futures for a given socio-economic storyline. In order to understand the
3943 contribution to uncertainty by the composition and climate models, it would also be
3944 worthwhile to perform a controlled experiment with identical emissions projections using
3945 multiple composition and climate models.

3946

3947 **4.4.2 Aerosol Studies (Direct Effect, Indirect Effect, Mixing, Water Uptake)**

3948 Calculation of the indirect effect is potentially the single most important deficiency in
3949 this study that can be directly improved. None of the models in the latest IPCC study or
3950 in this report realistically accounted for the full aerosol indirect radiative forcing. Given
3951 that the inclusion of a crude treatment of the aerosol indirect effect played a substantial
3952 role in one model's response in this study, it is clear that better characterization of this
3953 effect is imperative.

3954

3955 It is also clear that other potential aerosol processes need to be examined. An example is
3956 interactive dust loading, which can influence the composition of other short-lived species
3957 and can also be influenced by those species (*e.g.* via changes in solubility due to acid

3958 uptake (Fan *et al.*, 2004; Bauer and Koch, 2005)). Dust emission will also respond to
3959 vegetation changes as the climate warms. It has been speculated that arid regions may
3960 contract as a result of fertilization of plants by increased CO₂, reducing emission
3961 (*Mahowald and Luo*, 2003), while source regions may expand as a result of global
3962 warming and reduced rainfall, and thus increase emission (*Woodward et al.*, 2005). Note
3963 that the actual trend will depend upon local changes in climate, especially rainfall, which
3964 is among the least robust aspect of current climate projections. Other processes of
3965 potential importance that were not were included in these transient climate simulations
3966 are changes in atmospheric levels of sea-salt aerosol and changes in darkening of snow
3967 and ice surfaces by soot deposition.

3968

3969 Additional observations are clearly needed to better constrain the optical properties of
3970 aerosols. Measurement by devices such as the aerosol polarimeter on the NASA satellite,
3971 Glory, should provide some of the needed information. We recommend emphasis on
3972 long-term aerosol monitoring from ground and space, and on better characterization of
3973 aerosol microphysics in the laboratory. We also recommend greater use of the distinction
3974 between scattering and absorbing aerosols to characterize their relative importance.

3975

3976 **4.4.3 Improvements in Transport, Deposition, and Chemistry**

3977 The emission issues become even more problematical when the future distributions
3978 employed in the comprehensive climate models are generated by multiple global
3979 composition models, all with differing treatments of mixing in the lowest layers of the
3980 atmosphere, different treatment of transport and mixing by turbulence and clouds,

3981 different treatments of the removal of gases and particles by rain, snow and contact with
3982 the earth's surface, and different approximate treatments of the very large collection of
3983 chemical reaction that we do not yet fully understand. There are research opportunities in
3984 all phases of the behavior of short-lived species from their emission through their
3985 removal from the atmosphere.

3986

3987 **4.4.4 Recommendations for Regional Downscaling**

3988 Regional downscaling, where global climate models introduce climate forcing into
3989 regional climate models, is a relatively new development. Current regional downscaling
3990 results have relied on older comprehensive climate model simulations. Data from the
3991 newer comprehensive global models is needed and coordination and planning are critical
3992 since downscaling require input data every 3 or 6 hours. Further, a carefully coordinated
3993 set of region climate model predictions using various global and regional scale models
3994 and future scenarios is needed to reduce the uncertainty and identify methodological
3995 improvements.

3996

3997 The North American Regional Climate Change Assessment Program (NARCCAP,
3998 www.narccap.ucar.edu) is an ongoing effort that is actively taking this approach of
3999 multiple regional climate model simulations and multiple future scenarios. Four different
4000 comprehensive global models and six different regional models are being used to
4001 intercompare and evaluate regional climate simulations for North America. This effort
4002 and others like it should greatly help to advance regional downscaling approaches and
4003 provide important model archives for environmental quality and resources applications.

4004

4005 It is important to also note that these studies do not currently include short-lived species
4006 in the global climate simulations. Further, many regional models do not include
4007 feedbacks between air quality, the radiation budget and climate. These feedbacks may be
4008 quite important. For example, The U.S. EPA Clean Air Interstate Rule requires almost a
4009 30% reduction in SO₂ emissions in the Eastern United States during the next two
4010 decades. This could have a significant impact on the climate projections, as was shown in
4011 Chapter 3. We also need to separate the regional climate impacts of the direct and
4012 indirect effects of particles from the regional climate impacts of local emission changes.

4013

4014 More research is clearly needed to determine if downscaled regional climate simulations
4015 actually provide more detailed and realistic results. The higher regional resolution is
4016 important for a wide range of environmental issues including water and air quality,
4017 agricultural productivity, and fresh water supplies. For example, highly resolved regional
4018 climate information is needed to predict ozone and small particle (PM_{2.5}) levels, which
4019 are strongly influenced by local changes in emissions and climate.

4020

4021 **4.4.5 Expanded Analysis and Sensitivity Studies**

4022 Analyses of surface temperature response to changes in short-lived species need to be
4023 strengthened by additional sensitivity studies that should help to clarify causes and
4024 mechanisms. For example, in the GISS model, how much warming did the declining
4025 trend in the indirect effect contribute to its climate response and where? How would the
4026 GISS results differ if dust had not been permitted to take up sulfate aerosol? Determining

4027 the relative importance of these and other processes to the climate response would help
4028 prioritize the gaps in our knowledge. There are also a wide range climate-chemistry
4029 feedbacks and controls that should be explored. Both the response of the climate system
4030 to controls on short-lived species and the possible feedbacks, and the possible impacts of
4031 climate changes on short-lived species are all fertile areas for future research. While it
4032 was not possible, both due to time and resource restraints, for this study to explore these
4033 additional analyses, we recommend their future study.

4034

4035 The major unfinished analysis question in our minds is the relative contributions to the
4036 observed regional response of surface seasonal temperature from a model's regional
4037 climate response as opposed to the contribution from the regional forcing pattern. Is there
4038 a model independent regional climate response? What are the actual physical
4039 mechanisms driving the region temperature patterns that we observe? These all would
4040 appear to be very important areas of study. If our results are realistic, it would appear that
4041 the summertime continental US is extremely sensitive to increased radiative forcing in
4042 the Northern Hemisphere. This could have very significant implications for the United
4043 States policies regarding global warming.

4044

4045 **4.5 In Conclusion**

4046 With all the issues discussed in Chapter 4, the net result is that at this time we can not
4047 find a consensus on the duration, magnitude or even sign (warming or cooling) of the
4048 climate change due to future levels of the short-lived species. However, we have
4049 presented a plausible case for enhanced climate warming due to air quality policies that

4050 focus primarily on sulfate aerosol reduction and permit the emission of soot to continue
4051 to increase as realized in a version of the IPCC's A1B scenario. Alternative versions of
4052 this scenario for short-lived species that follow different pollution control storylines
4053 could have less impact. While we do not have definitive answers to the second goal of
4054 this report "to assess the sign, magnitude and duration of future climate impacts due to
4055 changing levels of short-lived radiative species of anthropogenic origin", we do provide
4056 plausible estimates that begin to characterize the range of possibilities and we identify
4057 key areas of uncertainty and provide motivation for addressing them.

4058 **Chapter 4 References**

- 4059 **Bauer, S. E., and D. Koch (2005),** Impact of heterogeneous sulfate formation at mineral
4060 dust surfaces on aerosol loads and radiative forcing in the Goddard Institute for
4061 Space Studies general circulation model, *J. Geophys. Res.*, **110**, D17202,
4062 doi:10.1029/2005JD005870.
4063
- 4064 **Bauer, S. E., D. Koch, N. Unger, S. M. Metzger, D. T. Shindell, and D. Streets (2007),**
4065 Nitrate aerosols today and in 2030: importance relative to other aerosol species
4066 and tropospheric ozone, *Atmos. Chem. Phys.*, **7**, 5043-5059.
4067
- 4068 **Fan, S-M., L. W. Horowitz, H. Levy II, and W. J. Moxim, 2004:** Impact of air pollution
4069 on wet deposition of mineral dust aerosols. *Geophysical Research Letters*, 31,
4070 L02104, doi:10.1029/2003GL018501.
4071
- 4072 **Mahowald, N. M., and C. Luo, 2003:** A less dusty future?, *Geophys. Res. Lett.*, **30**, 1903,
4073 doi:10.1029/2003GL017880.
4074
- 4075 **Streets, D., T. C. Bond, T. Lee, and C. Jang, 2004:** On the future of carbonaceous aerosol
4076 emissions, *J. Geophys. Res.*, **109**, doi:10.1029/2004JD004902.
4077
- 4078 **Woodward, S., D. L. Roberts, and R. A. Betts, 2005:** A simulation of the effect of
4079 climate change-induced desertification on mineral dust aerosol, *Geophys. Res.*
4080 *Lett.*, **32**, L18810, doi:10.1029/2005GL023482.

4081
4082
4083
4084
4085
4086
4087
4088
4089
4090
4091
4092
4093
4094
4095
4096
4097
4098
4099
4100
4101
4102
4103
4104

Appendix A

A. The Emission Scenarios of the IPCC Special Report on Emission Scenarios (SRES)

A1. The A1 storyline and scenario family describes a future world of very rapid economic growth, global population that peaks in mid-century and declines thereafter, and the rapid introduction of new and more efficient technologies.

Major underlying themes are convergence among regions, capacity building and increased cultural and social interactions, with a substantial reduction in regional differences in per capita income. The A1 scenario family develops into three groups that describe alternative directions of technological change in the energy system. The three A1 groups are distinguished by their technological emphasis: fossil intensive (A1FI), non-fossil energy sources (A1T), or a balance across all sources (A1B) (where balanced is defined as not relying too heavily on one particular energy source, on the assumption that similar improvement rates apply to all energy supply and end use technologies).

A2. The A2 storyline and scenario family describes a very heterogeneous world. The underlying theme is self reliance and preservation of local identities. Fertility patterns across regions converge very slowly, which results in continuously increasing population. Economic development is primarily regionally oriented and per capita economic growth and technological change more fragmented and slower than other storylines.

4105 **B1.** The B1 storyline and scenario family describes a convergent world with the same
4106 global population, that peaks in mid-century and declines thereafter, as in the A1
4107 storyline, but with rapid change in economic structures toward a service and information
4108 economy, with reductions in material intensity and the introduction of clean and resource
4109 efficient technologies. The emphasis is on global solutions to economic, social and
4110 environmental sustainability, including improved equity, but without additional climate
4111 initiatives.

4112

4113 **B2.** The B2 storyline and scenario family describes a world in which the emphasis is on
4114 local solutions to economic, social and environmental sustainability. It is a world with
4115 continuously increasing global population, at a rate lower than A2, intermediate levels of
4116 economic development, and less rapid and more diverse technological change than in the
4117 B1 and A1 storylines. While the scenario is also oriented towards environmental
4118 protection and social equity, it focuses on local and regional levels.

4119

4120 An illustrative scenario was chosen for each of the six scenario groups A1B, A1FI, A1T,
4121 A2, B1 and B2. All should be considered equally sound.

4122

4123 The SRES scenarios do not include additional climate initiatives, which means that no
4124 scenarios are included that explicitly assume implementation of the United Nations
4125 Framework Convention on Climate Change or the emissions targets of the Kyoto
4126 Protocol.

4127

4128 **B. Radiative Forcing Stabilization Levels (Wm^{-2}) and Approximate CO₂**
 4129 **Concentrations (ppmv) from the CCSP SAP 2.1a scenarios (taken from SAP 2.1a,**
 4130 **table 1.2).**

4131 The stabilization levels were constructed so that the CO₂ concentrations resulting from
 4132 stabilization of total radiative forcing, after accounting for radiative forcing from the non-
 4133 CO₂ GHGs included in this research, would be roughly 450 ppmv, 550 ppmv, 650 ppmv,
 4134 and 750 ppmv.

4135

	Total Radiative Forcing from GHGs (Wm^{-2})	Approximate Contribution to Radiative Forcing from Non-CO ₂ GHGs (Wm^{-2})	Approximate Contribution to Radiative Forcing from CO ₂ (Wm^{-2})	Corresponding CO ₂ Concentration (ppmv)
Level 1	3.4	0.8	2.6	450
Level 2	4.7	1.0	3.7	550
Level 3	5.8	1.3	4.5	650
Level 4	6.7	1.4	5.3	750
Year 1998	2.11	0.65	1.46	365
Pre-industrial	0	0	0	275

4136

4137 **Acronyms**

4138	AERONET	Aerosol Robotic Network
4139	AIM	Asian-Pacific Integrated Model
4140	AOD	Aerosol Optical Depth
4141	AOGCM	Atmosphere-Ocean General Circulation Model
4142	AR4	IPCC Fourth Assessment Report
4143	ARL	Air Resources Laboratory
4144	AVHRR	Advanced Very High Resolution Radiometer
4145	BC	black carbon
4146	CaCO₃	calcium carbonate
4147	CAM3	Community Atmosphere Model
4148	CCSM	Community Climate System Model
4149	CCSP	Climate Change Science Program
4150	CH₄	methane
4151	CO₂	carbon dioxide
4152	DMS	dimethylsulfide
4153	DU	Dobson unit
4154	ENSO	El Niño-Southern Oscillation
4155	ESM	Earth System Model
4156	GCM	General Circulation Model\Global Climate Model
4157	GFDL	Geophysical Fluid Dynamics Laboratory
4158	GHG	greenhouse gas
4159	GISS	Goddard Institute for Space Studies

4160	hPa	hectopascal
4161	HNO₃	nitric acid
4162	HO₂	hydroperoxyl radical
4163	H₂O₂	hydrogen Peroxide
4164	IAM	Integrated Assessment Model
4165	IGSM	MIT Integrated Global System Model
4166	IMAGE	Integrated Model to Assess the Greenhouse Effect
4167	IPCC	Intergovernmental Panel on Climate Change
4168	LL	long-lived
4169	MACCM3	NCAR Middle Atmosphere Community Climate Model, version 3
4170	MAGICC	Model for the Assessment of Greenhouse-gas Induced Climate Change
4171	MODIS	Moderate Resolution Imaging Spectroradiometer
4172	MOZART	Model for Ozone and Related Chemical Tracers
4173	NASA	National Aeronautics and Space Administration
4174	NCAR	National Center for Atmospheric Research
4175	NCDC	National Climatic Data Center
4176	NH	Northern Hemisphere
4177	NH₃	ammonia
4178	NMHC	non-methane hydrocarbons
4179	N₂O	nitrous oxide
4180	N₂O₅	nitric pentoxide
4181	NOAA	National Oceanic and Atmospheric Administration
4182	NO₂	nitrogen dioxide

4183	NO₃	nitrate radical
4184	NO_x	reactive nitrogen oxides
4185	NRC	National Research Council
4186	NSF	National Science Foundation
4187	O₃	ozone
4188	OC	organic carbon
4189	PPM	parts per million
4190	PPMV	parts per million by volume
4191	RF	radiative forcing
4192	SAP	Synthesis and Assessment Product
4193	SAR	IPCC Second Assessment Report
4194	SH	Southern Hemisphere
4195	SL	short-lived
4196	SO₂	sulfur dioxide
4197	SO₄	sulfate
4198	SOA	secondary organic aerosol
4199	SRES	Special Report on Emission Scenarios
4200	SST	sea surface temperature
4201	TAR	Third IPCC Assessment Report
4202	TUV	Tropospheric Ultraviolet and Visible Radiation Model
4203	VOC	volatile organic compounds
4204	Wm⁻²	watts per meter squared

4205 **Glossary**

4206 **Aerosols**

4207 tiny particles suspended in the air

4208

4209 **Anthropogenic**

4210 human-induced

4211

4212 **Attribution**

4213 attribution of causes of climate change is the process of establishing the most likely

4214 causes for a detected change with some defined level of confidence

4215

4216 **Black carbon**

4217 soot particles primarily from fossil fuel burning

4218

4219 **Climate sensitivity**

4220 the equilibrium change in global-average surface air

4221 temperature following a change in radiative forcing; in

4222 current usage, this term generally refers to the warming

4223 that would result if atmospheric carbon dioxide

4224 concentrations were to double from their pre-industrial

4225 levels

4226

4227 **Cold wave**

4228 cold spells of 4 days in duration with mean temperature falling below the threshold for a

4229 1 in 10 year recurrence interval

4230

4231 **Cyclone**

4232 a storm system that rotates around a center of low atmospheric pressure

4233

4234 **Tropical cyclone**

4235 a cyclone usually originating in the tropics, with a warm central core

4236

4237 **Extratropical cyclone**

4238 a cyclone originating in the mid or high latitudes, with a cold central core. Larger

4239 in scale than a tropical cyclone and with less central intensity

4240

4241 **Diurnal temperature range**

4242 the difference between maximum and minimum temperature over a period of 24 hours

4243

4244 **El Nino-Southern Oscillation**

4245 the waxing and waning every 2-7 years of El Niño and La Niña ocean temperature cycles

4246 along with the related atmospheric pressure component of the Southern Oscillation. The

4247 primary centers of ENSO variability are in the tropical Pacific, but ENSO effects can be

4248 felt across much of the globe

4249

4250 Forcing

4251 a natural or human-induced factor that influences climate

4252

4253 Greenhouse gases

4254 gases including water vapor, carbon dioxide, methane,

4255 nitrous oxide, and halocarbons that trap infrared heat,

4256 warming the air near the surface and in the lower levels

4257 of the atmosphere

4258

4259 Heat wave

4260 warm spells of 4 days in duration with mean temperature exceeding the threshold for a 1

4261 in 10 year recurrence interval

4262

4263 Inhomogeneity

4264 a break or interruption in an otherwise homogeneous record. For example, moving a

4265 weather station from the center of a city to the suburbs will create an inhomogeneity in

4266 the climate record

4267

4268 Monsoon

4269 a seasonal change in wind direction (driven by changes in temperature), often

4270 accompanied by a seasonal precipitation maximum

4271

4272 Parameterization

4273 a mathematical representation of a process that cannot

4274 be explicitly resolved in a climate model

4275

4276 Stratosphere

4277 the highly stratified region of the atmosphere above the troposphere extending from about

4278 10 km (ranging from 9 km in high latitudes to 16 km in the tropics on average) to about

4279 50 km

4280

4281 Troposphere

4282 the lowest part of the atmosphere from the surface to about 10 km in altitude in mid-

4283 latitudes (ranging from 9 km in high latitudes to 16 km in the tropics on average) where

4284 clouds and “weather” phenomena occur, in the troposphere, temperatures generally

4285 decrease with height

4286